SIMULATION OF GROUND WATER FLOW IN THE LOWER BOISE RIVER BASIN

Prepared by

Christian R. Petrich

Idaho Water Resources Research Institute
University of Idaho – Boise

Prepared for and in cooperation with

Idaho Department of Water Resources
1301 North Orchard Street
Boise, ID

FEBRUARY 2004

IDAHO WATER RESOURCES RESEARCH INSTITUTE
RESEARCH REPORT

IWRRI-2004-02

Acknowledgements

The work described in this report was conducted as part of the Treasure Valley Hydrologic Project (TVHP). Participants in the TVHP include the Idaho Department of Water Resources (IDWR), the Idaho Water Resources Research Institute (IWRRI), University of Idaho (UI), United Water Idaho, Inc. (UWI), Boise State University (BSU), U.S. Geological Survey (USGS), U.S. Bureau of Reclamation (USBR), Idaho Water Resource Board (IWRB), Ada and Canyon Counties, and the cities of Boise, Nampa, Caldwell, Meridian, Kuna, and Eagle. The project was funded by the U.S. Environmental Protection Agency, the Idaho State Legislature, UWI, and the IWRB. In addition, in-kind services were provided by UWI, USGS, and the USBR.

The author wishes to acknowledge the following contributions to this report:

- Scott Urban (IDWR) provided initial model development assistance and prepared the recharge and withdrawal data for the base-case simulations.
- Dr. John Doherty (Watermark Computing, Brisbane, Australia) helped develop and apply PEST (parameter estimation code) for the model calibration and predictive analysis.
- Dayna Ball (IDWR) and Diana Hegland provided proofreading and editing assistance.

Technical reviewers included:

- Paul Castelin (IDWR)
- Dr. John Doherty (Watermark Computing)
- Ken Neely (IDWR)
- Garth Newton (IDWR)
- R. D. Schmidt (USBR)
- Scott Urban (IDWR)

Abstract

The lower Boise River basin (Treasure Valley) aquifer system consists of a series of shallow, relatively high-permeability aquifers and a deeper, regional flow system. A numerical model of regional ground water flow was developed to evaluate (1) the effects of large-scale increases in ground water withdrawals on regional ground water levels and (2) the potential effects of altered recharge rates (associated with conversion of agricultural to urban land use) on regional ground water levels.

The model was constructed using the three-dimensional, finite difference MODFLOW code (Harbaugh et al., 2000; McDonald and Harbaugh, 1988; McDonald and Harbaugh, 1996). The model was calibrated under steady-state hydraulic conditions using the automated parameter estimation code PEST (Doherty, 1998; Doherty, 2000). Horizontal and vertical hydraulic conductivity parameters were calibrated to 200 averaged water level observations and 6 actual and estimated vertical head differences.

The model calibrated with higher hydraulic conductivity values in the uppermost aquifer zones, corresponding with known areas of coarser-grained sediments. PEST-calibrated parameter values also indicated relatively high hydraulic conductivity values in areas of the eastern and central portion of the valley associated with fluvial/deltaic deposition. Simulated fluxes between model layers in the base calibration indicated a relatively small amount of water moves vertically between model layers, especially in the lower layers. Based on simulation results, most recharge that occurred in shallow aquifer zones did not reach deeper zones.

A 10% increase or decrease in recharge led to minimal changes in water levels or parameter value estimates because shallow ground water levels in central portions of the basin are controlled, in part, by elevations of surface water channels. Decreased or increased recharge resulted in changes in the rates of water discharging to model drain, general head boundary (Lake Lowell), constant head (Snake River), and river (Boise River) cells. Changes in land use that lead to decreases in shallow-aquifer recharge may not have a substantial effect on shallow ground water levels until the water table elevations remain below those of nearby surface channels.

Simulations indicated that some ground water level declines might occur with a 20% increase in ground water withdrawals over 1996 levels. Modest simulated declines were observed in the Boise area in layers 1 and 2. Greater simulated declines were observed in the central portion of the valley (especially in the Lake Lowell area) in layers 3 and 4. The simulated 20% increase in ground water withdrawals resulted in increased losses from the Boise River (23%), decreased discharge to agricultural drains (62%), and decreased discharge to the Snake River (9%). Simulated water level declines and/or changes in mass balance components reflected a combination of parameter uncertainty and response to a changed hydraulic stress.

Table of Contents

Simulation Files (CD-ROM)

List of Figures

List of Tables

1. INTRODUCTION

1.1. Project Background

The lower Boise River basin (Figure 1-1) of southwestern Idaho (commonly referred to as the "Treasure Valley") has experienced significant population growth, local ground water declines, and periodic drought conditions in the last two decades. This led to public concern about the status and future of water resources in the valley. The Treasure Valley Hydrologic Project (TVHP) was formed to address some of these issues and to provide a framework for future water management.

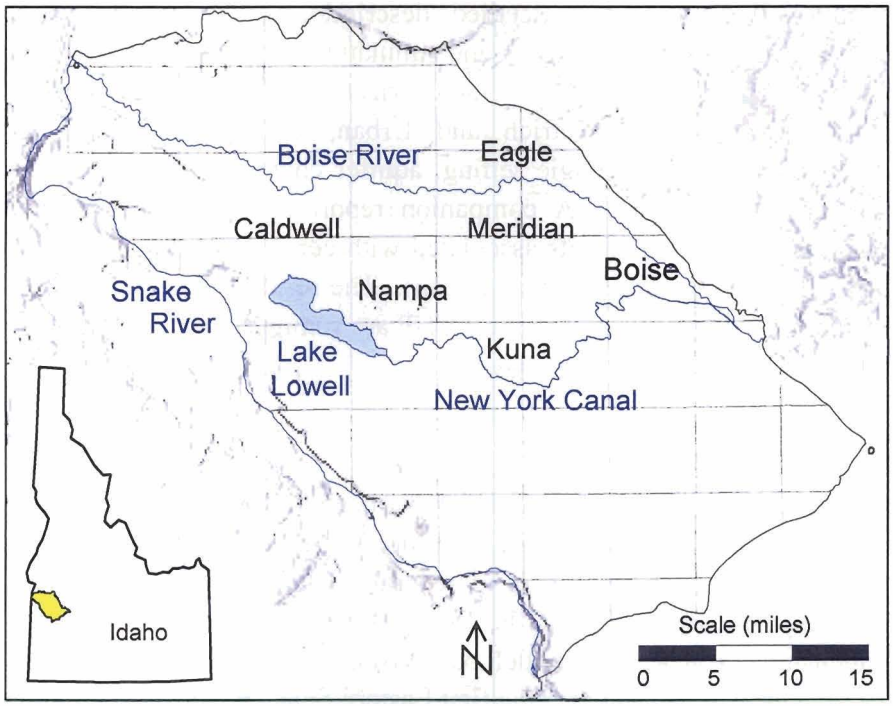

Figure 1-1: Treasure Valley area.

A numerical model of ground water flow was constructed as part of the TVHP. The purpose of the model was to develop an improved understanding of regional ground water flow in the Treasure Valley. General objectives of the model simulations were to evaluate (1) the effects of large-scale increases in ground water withdrawals on regional ground water levels and (2) the potential effects of altered recharge rates (associated with conversion of agricultural to urban land use) on regional ground water levels. Specific objectives included the following:

1. Construct a ground water flow model capable of simulating steady-state hydraulic conditions.

2. Use the modeling process as a framework for assembling hydrologic data.
3. Use the model to better define recharge processes and recharge rates to the regional aquifer system.
4. Evaluate potential changes in regional recharge rates associated with changes in land use.
5. Simulate the potential changes in ground water levels from increased ground water withdrawals associated with continued population growth.
6. Simulate the potential changes in ground water levels associated with processing currently unprocessed water right applications.

1.2. Report Scope

This report presents a summary of methods, data, and results of the ground water flow simulations, including a detailed description of the modeling approach, model construction, model calibration, and simulation results. The conceptual basis for model construction is described in "Characterization of Ground Water Flow in the Lower Boise River Basin" (Petrich and Urban, 2004), which also includes detailed descriptions of the geologic setting, aquifer characteristics, water levels, and aquifer inflows and outflows. A companion report describes simulations to evaluate the potential hydrologic effects associated with currently pending water right applications in the Treasure Valley (Petrich, 2004a). The results from these reports and from other research conducted as part of the TVHP are summarized in a project summary (Petrich, 2004b).

1.3. Previous Investigations

Several ground water flow models have been constructed to simulate regional ground water flow in all or parts of the Treasure Valley. Lindgren (1982) developed a model to evaluate the overall impact of federal irrigation and flood control projects on the economy and hydrology of the lower Boise River valley. This model was a two-dimensional (one-layer) model built using a finite difference code (de Sonneville, 1972) that was also used for the first Eastern Snake River Plain simulations.

Lindgren (1982) modeled the northern boundary of the lower Boise River system (along the northern highlands bounding the Boise River) as an impermeable, no-flow boundary. A southeast no-flow boundary extended from the Snake River south of Melba to a point 6 miles east of Kuna and from a point 11 miles east of Kuna to Diversion Dam on the Boise River. A constant head boundary was used between the latter no-flow segments because ground water contours and other information indicated ground water flow across the boundary in this area. Head-dependent boundaries were assigned to the remaining Snake River reaches, the Boise River from Diversion Dam to its confluence with the Snake River, and Lake Lowell. Aquifer thicknesses in the Lindgren model were determined from well logs; a 1,000-foot thickness was assumed in areas where no well logs were available.

Aquifer recharge from irrigation was determined on the basis of mapped irrigation areas (Lindgren, 1982). Canal seepage from major irrigation canals was distributed on a reach-by-reach basis. Infiltration from areal precipitation was assumed to be 5% of 12.4 inches (average annual precipitation) in non-irrigated areas and 100% in irrigated areas. Underflow from areas north of the Boise River (Willow Creek, Dry Creek, and Parma Gulch) was simulated based on estimated hydraulic conductivity and hydraulic gradient values.

The Lindgren model was calibrated to 1972 steady-state conditions. A transient calibration was performed for the period of April 1, 1970, to March 31, 1971, using two-week time steps. Calibration difficulty was encountered in the area south of Lake Lowell and in some areas northwest of Lake Lowell, which was attributed to infiltration lags and leakage phenomena.

A second regional model, constructed by the USGS (1991), simulated ground water flow under the 144-mile-long, 50-mile-wide area of the Western Snake River Plain. The model was constructed as part of the USGS's Regional Aquifer System Analysis (RASA) study that began in 1979. The three-layer, finite difference model was constructed using the USGS MODFLOW code (McDonald and Harbaugh, 1984). The model boundary approximated the boundary of the Snake River plain from the junction of Salmon Falls Creek and the Snake River on the east to the confluence of the Payette and Snake Rivers on the west.

The model grid consisted of 25 rows, 72 columns, and 3 layers, with each cell representing an area of 2 miles per side. The model domain was divided into 11 subareas based on geologic and hydrologic characteristics. The uppermost model layer represented an unconfined aquifer in sedimentary (sands and gravels) and volcanic rocks. The top of the upper layer was defined based on 1980 water levels; the bottom of the top layer was assumed to be 500 feet below the 1980 water level contours. The middle layer represented a confined aquifer in about 4,000 feet of mostly fine-grained sedimentary rocks and volcanic rocks. The bottom model layer represented water under high pressure in about 7,000 feet of volcanic rocks.

Model boundaries on the north, south, and west sides of the USGS model were simulated as constant flux boundaries. The flux was derived from water budget estimates because of the lack of actual underflow data. The eastern Snake River boundary was simulated as head dependent in the upper layer and no flow in the middle and bottom layers. The Snake River, Payette River, Salmon Falls Creek, and Lake Lowell were simulated as head dependent cells (i.e., MODFLOW river cells). The average river width was assumed to be 1,300 feet, with an average length per cell of 2 miles. The hydraulic conductivity of river cells was assumed to be 1×10^{-5} ft/s.

Transmissivity values estimated based on specific capacity data were assigned (by model subarea) to the uppermost layer. A uniform transmissivity of 8,600 ft^2/day was assumed for layers 2 and 3. The vertical hydraulic conductivity was assumed to be

9 ft/day between the upper two layers and 22 ft/day between the lower two layers based on published data for similar rock types.

Portions of the Snake, Boise, and Payette River valleys were simulated as drains. The bottom drain elevation was specified as the approximate land surface elevation in the cell. Cells containing both drains and the Boise River were assigned as drain cells. Canals were treated similar to rivers. The average length of major canals in a cell was estimated to be about 9 miles, and the average canal width was assumed to be 20 feet. These dimensions represented about 1.3% of the irrigated area in a cell, or about 33.3 acres per cell. A canal bed thickness of one foot and a vertical hydraulic conductivity of 1×10^{-6} ft/sec (8.6×10^{-2} ft/day) were assumed. Estimated values for effective vertical conductance values between layers were used because of the lack of information describing individual confining zones.

The model was first calibrated under steady-state conditions using 1980 hydrologic data. Calibration parameters included transmissivity, river and drain conductance, and vertical hydraulic conductivity. The model was then calibrated to transient hydraulic conditions based on 1880 (pre-irrigation) through 1980 water level data by adjusting aquifer storage coefficients. Successful calibration was only achieved for the upper layer, where simulated hydraulic heads approximated the measured heads. Insufficient hydrogeologic data for the middle and lower aquifer units prevented an acceptable calibration of the middle and lower model layers. The model was thus deemed useful for understanding the western Snake River aquifer system but not for detailed management analyses. Model calibration indicated that a more refined knowledge of subsurface hydrology was needed, with more data describing the vertical hydraulic head distribution in the upper and middle aquifer units, hydraulic properties of aquifers and confining beds, and underflow.

Brockway et al. (1999) simulated ground water flow in the southeast Boise area as part of an aquifer recharge and recovery evaluation. Built with the USGS MODFLOW code, the model was used for simulations of recharge and recovery scenarios based on injection and withdrawal in a 1,100-foot-deep well at the Micron Technology, Inc., facility. The model area extended from Lucky Peak Reservoir on the east to Cole Road on the west and from the base of the Boise Foothills to Kuna-Mora Road. The model was used to simulate various recharge scenarios (with up to 3,000 gallons per minute of recharge) and recovery scenarios (based on combinations of recovery in 4 wells). The authors concluded that recharge (injection) fully mitigated impacts from increased production.

2. CONCEPTUAL MODEL DESCRIPTION

This section presents a summary of Treasure Valley ground water flow characteristics, water level measurements, and aquifer inflows and outflows (Petrich and Urban, 2004). The summary represents the "conceptual model" of ground water flow that was used as the basis for aquifer simulations.

The Treasure Valley aquifer system is comprised of a complex series of interbedded, tilted, faulted, and eroded sediments extending to depths of over 6,000 feet in the deepest parts of the basin (Wood and Clemens, in press). The valley contains shallow, local flow systems (with ground water residence times ranging from years to hundreds of years) and a deep, regional flow system (with residence times ranging from thousands to tens of thousands of years). Few water wells extend beyond a depth of 1,200 feet.

The Treasure Valley sedimentary section reflects a history of lacustrine, deltaic, fluvial, and alluvial deposition (Wood and Clemens, in press). In general, basin sedimentary deposits grade from coarser, more permeable sediments near the Boise Front[1] to finer, less permeable sediments at the distal end of the basin. At the basin scale, sediments also grade finer with depth. Highly permeable deposits associated with deltaic and/or fluvial deposition are often sandwiched between lacustrine deposits of lower permeability.

Ground water flow in the Treasure Valley is controlled by aquifer characteristics and hydraulic gradient. Aquifer characteristics influencing ground water flow include grain size, sorting, stratigraphic layering, sedimentary layer dip, sediment grain cementation, and the degree of fracturing (e.g., rock aquifers). Additional controls on the movement of ground water are attributed to structural processes, including faulting throughout the basin and along the basin margin.

Ground water chemistry data (Hutchings and Petrich, 2002a) indicate different ground water chemistry north of the fault zone compared to the area south of the fault zone, suggesting restricted flow across the fault zone. Basin downwarping and a downslope trend in sediment deposition contribute to steeply dipping sedimentary deposits that may cause deeper aquifer units to pinch out at depth (Wood, 1997). Based on seismic imaging and outcrop mapping, aquifer sediments of various fault blocks dip at angles ranging from zero to approximately 12 degrees (Wood, 1997).

Fractures within shallow Pleistocene basalts, or along upper and lower surfaces of individual basalt flows, can contribute to ground water movement. For instance, basalt fractures and course-grained sediments underlying the basalt may greatly contribute to

[1] Boise Front describes the portion of the Idaho Batholith that forms the northeastern boundary of the lower Boise River basin.

transmitting leakage from the New York Canal (and other surface water channels) into shallow aquifers.

An erosional unconformity associated with changing lake levels in Pliocene Lake Idaho truncates down-dipping units near the basin margin near Boise (Squires and Wood, 2001; Squires et al., 1992; Wood, 1997). The unconformity separates lacustrine and deltaic sediments (tilted in the Boise area) from overlying lacustrine/deltaic sediments. Coarse-grained sediments associated with the erosional unconformity (Wood, 1997; Squires et al., 1992) appear to serve as a manifold for deeper, regional ground water migrating horizontally into the basin from alluvial fan sediments in the eastern portion of the basin (corroborated by E. Squires, pers. comm., 2002).

Potentiometric surface contours indicate ground water movement in a northwesterly to southwesterly direction, depending on depth and location (Figure 2-1 through Figure 2-4). Potentiometric surface contours in shallow aquifer zones reflect surface hydrologic conditions, such as mounding under the New York and Mora Canals, or discharge to the Boise River. Mounding in the vicinity of the New York Canal represents a local ground water divide, with shallow ground water north of the canal flowing toward the Boise River, and shallow ground water south of the canal flowing toward the Snake River. Potentiometric surface contours from shallow aquifers show ground water flow toward and discharge to the Boise River in mid- to lower reaches. Potentiometric surface contours in deeper zones indicate a more uniform westerly flow direction (e.g., Figure 2-3). Downward hydraulic gradients are indicated along the Boise Foothills, the eastern part of the study area (e.g., TVHP#4, Figure 2-5), and in the vicinity of the New York and Mora Canals. Upward gradients are evident in the central and western portions of the valley (e.g., TVHP#2, Figure 2-5), especially in the vicinity of the lower Boise River.

Individual hydrographs indicate relatively stable water levels in many areas, although water level declines have occurred in a number of wells (Petrich and Urban, 2004). Wells in two areas – southeast Boise and south of Lake Lowell – have experienced declines of approximately 30 feet and 65 feet, respectively. Water levels in these areas appear to have stabilized in recent years. Additional ground water level declines were observed in the areas between northwest Boise and Eagle and southwest Boise, Meridian, and Kuna. Most of the long-term declines in these wells have been less than 10 feet. Reasons for the declines may include increased withdrawals from the measured wells (very few of the monitoring wells are dedicated to monitoring alone), increased nearby withdrawals, and/or changes in local infiltration rates. Further investigation of these apparent declines is warranted to determine if they reflect regional or local conditions. Additional monitoring wells would also be warranted in these areas of apparent declines.

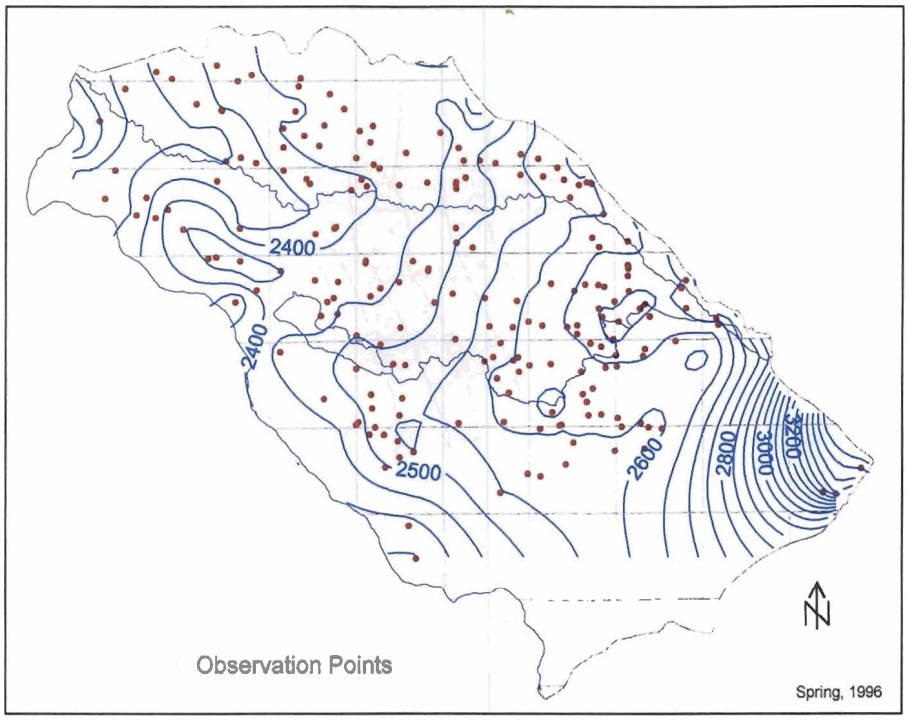

Figure 2-1: Potentiometric surface based on 1996 water level measurements from wells completed in model layer 1.

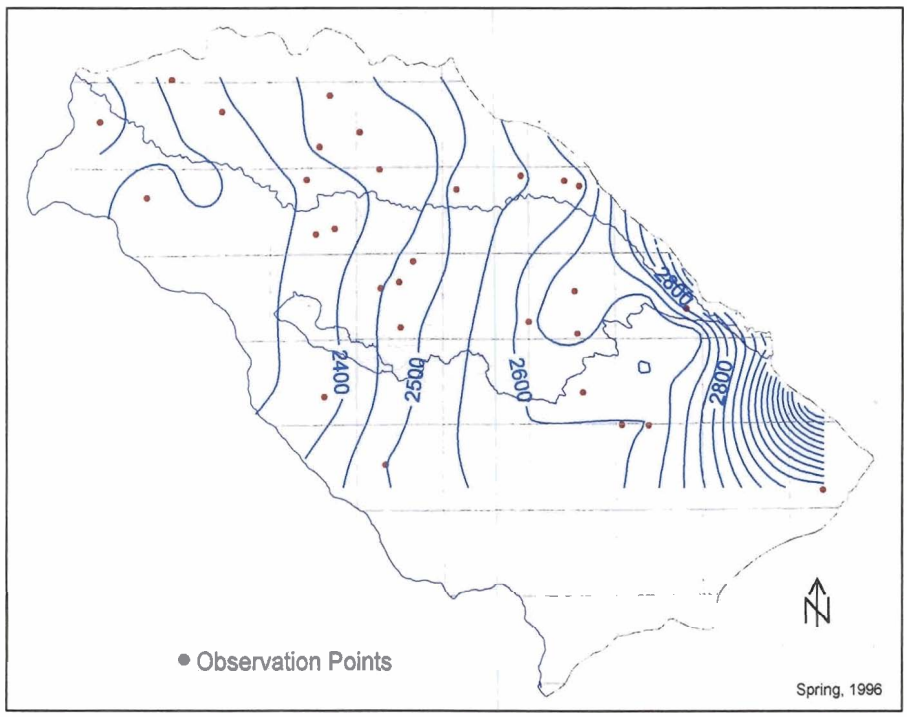

Figure 2-2: Potentiometric surface based on 1996 water level measurements from wells completed in model layer 2.

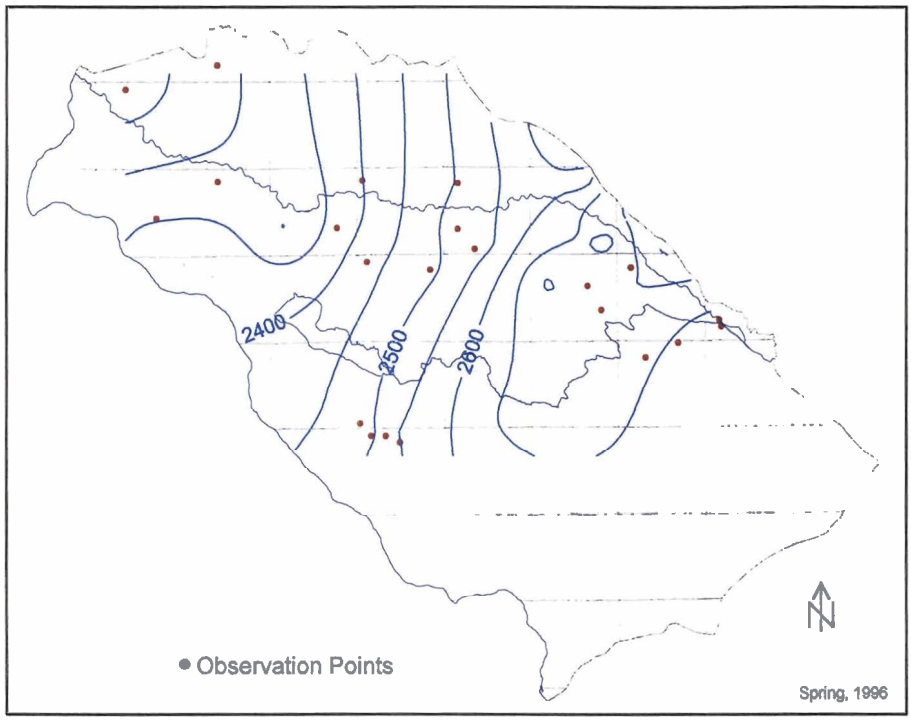

Figure 2-3: Potentiometric surface based on 1996 water level measurements from wells completed in model layer 3.

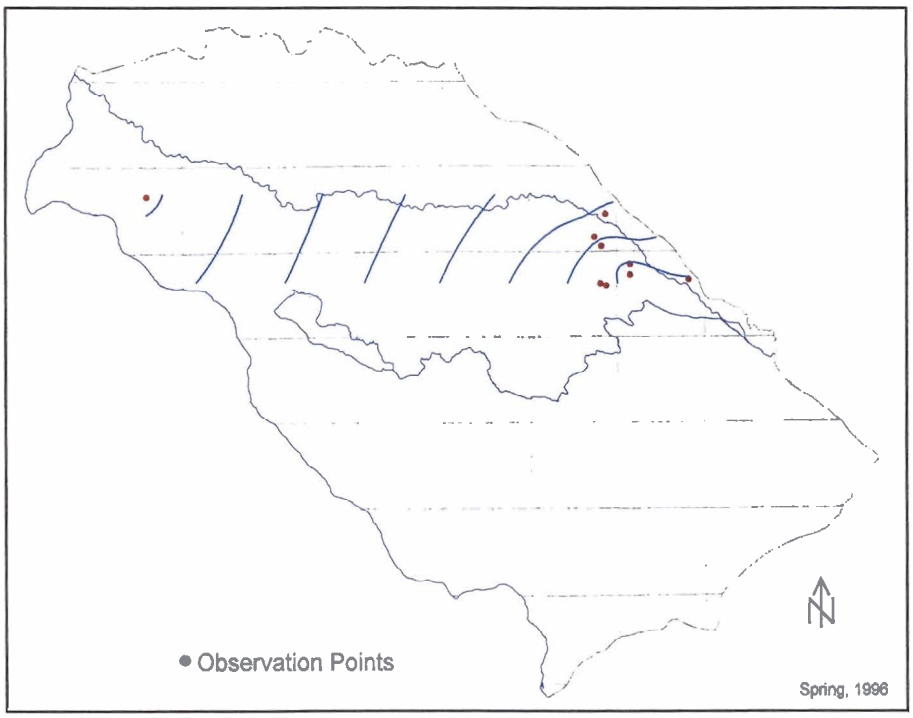

Figure 2-4: Potentiometric surface based on 1996 water level measurements from wells completed in model layer 4.

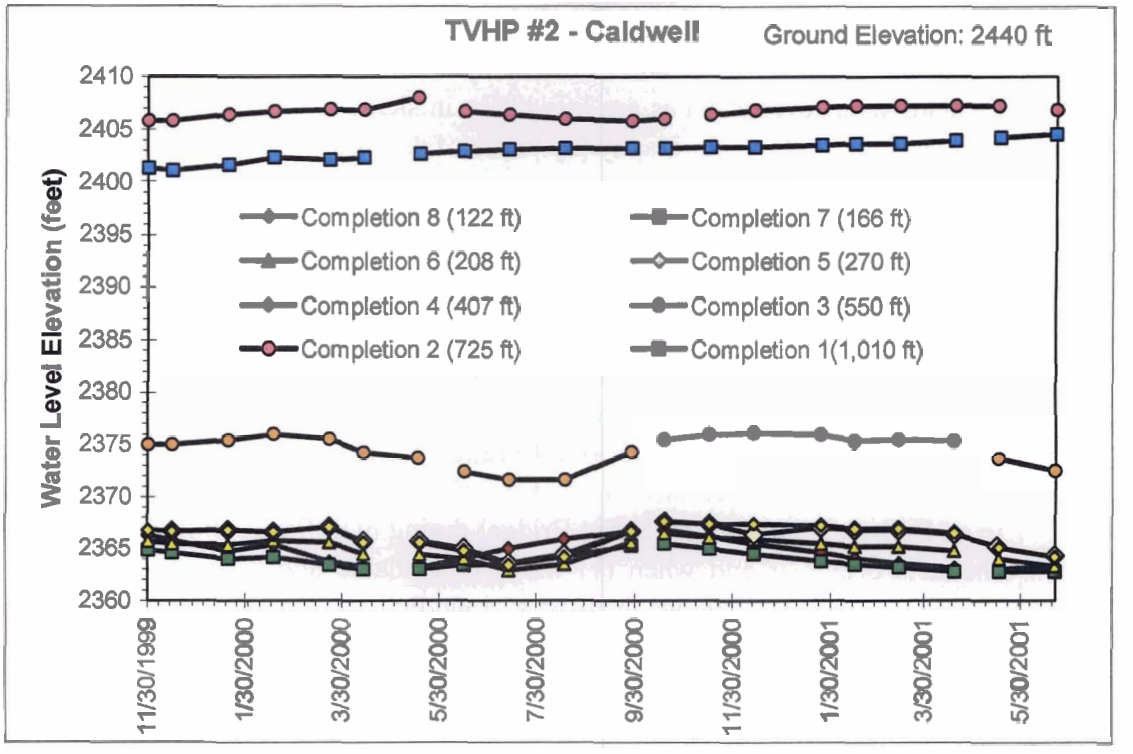

From Petrich and Urban (2004)

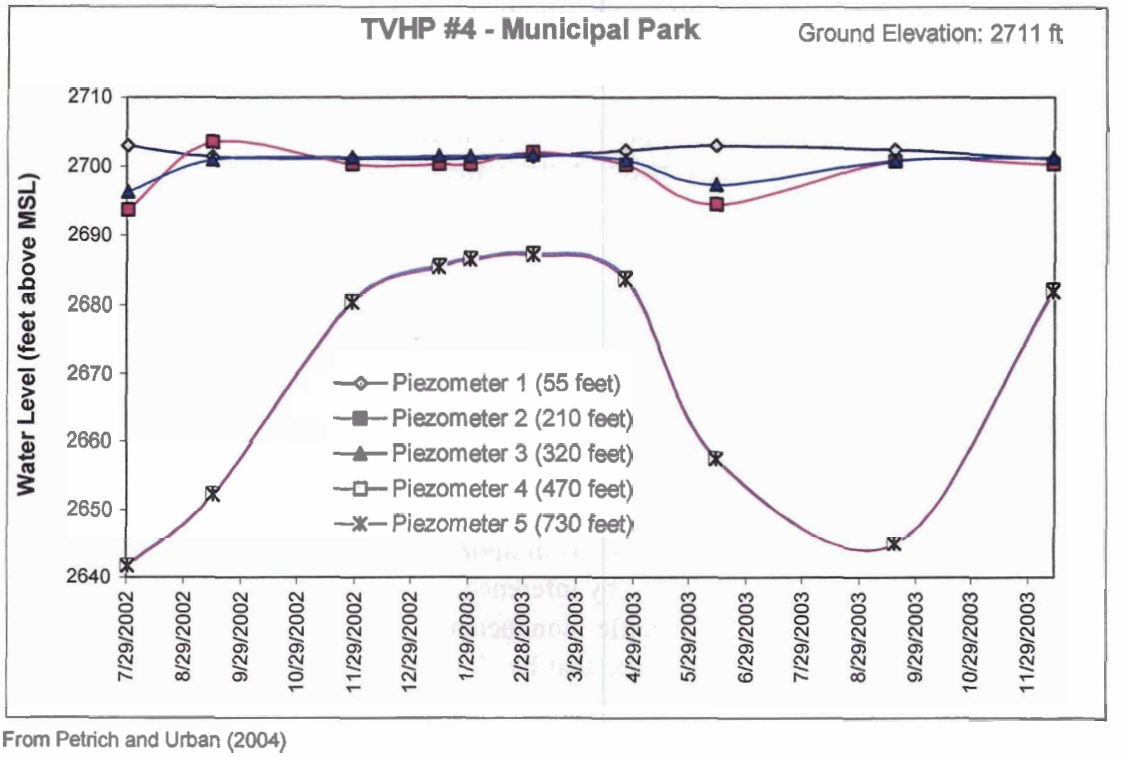

From Petrich and Urban (2004)

Figure 2-5: Water level data from the Caldwell and Boise Municipal Park wells.

A number of shallow monitoring wells indicated water level decreases. Shallow wells may be especially sensitive to changes in local surface water irrigation patterns in areas where the water table is not in direct hydraulic connection with surface channels. Ground water level changes are less likely in shallow wells in areas where the water table is controlled by topography (by virtue of drains and canals).

Seasonal water level fluctuations are evident in many Treasure Valley wells. The fluctuations are generally a response to seasonal increases in withdrawals (e.g., summer irrigation withdrawals) or increases in recharge associated with surface water irrigation.

The largest component of recharge to shallow aquifers is seepage from the canal system and infiltration associated with irrigated agriculture (Urban and Petrich, 1998). Water enters shallow aquifers as infiltration from canals, irrigated areas, and other water bodies (e.g., Lake Lowell), and possibly from upper reaches of the Boise River (e.g., Barber Dm to Capitol Street Bridge) during high flows. Infiltration from surface channels occurs if and when (1) water is available and (2) hydraulic heads in the channel (or lake) are higher than the surrounding aquifer heads. Additional recharge sources include mountain front recharge, underflow from the granitic Idaho Batholith and tributary sedimentary aquifers, and direct precipitation.

Shallow aquifer levels increased by as much as 100 feet in some areas in response to the initiation of large-scale flood irrigation in the late 1800s and early 1900s. Shallow ground water levels rose to and have remained at (or near) ground surface in many areas (at least seasonally), discharging to drains and other surface channels.

Shallow and intermediate aquifers are separated from deeper zones by interbedded silt and clay layers in many parts of the valley. While individual clay layers are not necessarily areally extensive, multiple clay layers in aggregate form effective barriers to vertical ground water movement.

Recharge to the deeper aquifers begins as downward flow through coarse-grained alluvial fan sediments in the eastern portion of the basin and as underflow at basin margins. Ground water is then thought to flow horizontally into the basin via more permeable sediments (e.g., coarse-grained sediments of the geological unconformity overlying Chalk Hills sediments) intersecting the alluvial fan sediments.

This is illustrated in water chemistry data collected from shallow aquifers near the New York Canal. Water in the canal, as in upper portions of the Boise River, has relatively low specific conductance (and by inference, total dissolved solids). In shallow aquifers underlying the canal, specific conductance was found to increase with depth, corresponding with canal water that has infiltrated through soil horizons. In contrast, water in deeper sand units, separated from upper zones by multiple clay layers, has lower specific conductance than water in overlying horizons (Hutchings and Petrich, 2002a; Hutchings and Petrich, 2002b). This finding indicates that water in at least

some deeper aquifers originates at the basin margins and does not enter the ground water regime through the carbon-rich sediments found in Treasure Valley soils.

Residence times of Treasure Valley ground water were generally found to increase with depth and with distance along a regional east-to-west-trending flow path (Hutchings and Petrich, 2002a). Residence time estimates in the regional aquifer system ranged from thousands to tens of thousands of years. The youngest waters entered the subsurface a few thousand years ago and were found along the northeastern boundary of the basin, adjacent to the Boise Foothills. The oldest waters entered the subsurface between 20,000 and 40,000 years ago and were found in the western reaches of the basin near the Snake River. Ground water in the deep deltaic aquifers beneath Boise entered the subsurface between 10,000 and 20,000 years ago.

Comparisons between measured water chemistry constituents and established models of geochemical processes (Hutchings and Petrich, 2002a) show that (1) ground water near the northeastern basin margin has experienced little interaction with aquifer minerals, and (2) ground water beyond the northeastern basin margin has experienced substantial interaction with aquifer minerals. Geochemical evolution of Treasure Valley ground water appears to be influenced by solution of both carbonate and silicate minerals.

Ground water discharge to rivers, drains, and canals represents the dominant form of discharge from the Treasure Valley aquifer system (Urban and Petrich, 1998). The primary form of natural discharge from the deeper aquifers is thought to be regional upwelling in the southern and western portions of the basin, with ultimate discharge to the Boise River and/or Snake River. Rates of discharge from the deeper aquifers in the western portions of the valley are unknown but are probably low because of the thick accumulation of lacustrine clays separating these aquifers from ground surface.

Relatively long residence times in the regional flow system (over 20,000 years) implies that (1) regional aquifers are not very transmissive, (2) recharge rates to the deeper regional aquifers are limited, and/or (3) regional aquifers are discharge-limited. Although there are abundant silt and clay layers with low hydraulic conductivity, productive sand layers are present throughout central portions of the valley; these sand zones are tapped by many irrigation and municipal wells. Recharge to the deeper, regional system is limited but has generally been sufficient for current rates of withdrawal. Thick lacustrine clays at the distal end of the valley likely inhibit upward (discharge) flow, limiting the amount of water that can flow through the system.

In summary, the Treasure Valley aquifer system consists of shallow aquifers containing local ground water flow systems, and a deeper, regional ground water flow system. Recharge to the shallow system consists largely of infiltration from irrigated fields and canals. Primary discharge is to the Boise and Snake Rivers and other streams and to drains discharging into these channels. The deeper, regional flow system consists of (1) recharge in alluvial sediments in southeast Boise and at the base

of the mountain front north of Boise, (2) movement of ground water from the recharge areas into the deeper Boise area fluvio-lacustrine aquifers, and (3) movement of ground water from the Boise area aquifers into regional lacustrine/deltaic aquifers in the central and western portions of the valley.

3. MODEL CONSTRUCTION

This section describes the basic construction of the Treasure Valley ground water flow model. A description of model inputs in provided in Section 4.

3.1. Model Code

The three-dimensional, finite difference MODFLOW code (Harbaugh et al., 2000; McDonald and Harbaugh, 1988; McDonald and Harbaugh, 1996) was selected for this model because it has been thoroughly validated, continues to evolve and is in common use by Idaho agencies and consultants. Several Graphical User Interfaces (GUIs) were used, including the Ground Water Modeling System (GMS - Brigham Young University, 2002) and PMWIN (Chiang and Kinzelbach, 2001).

The parameter estimation code PEST (Doherty, 1998; Doherty, 2000) was used for model calibration. PEST is a model-independent parameter estimator that is used in the calibration of environmental models, particularly ground water flow models. PEST has the ability to analyze the range of model prediction values, under the constraint that model parameters satisfy constraints imposed by the calibration process. Utility software supplied with PEST allows the use of "pilot points" in conjunction with geostatistically-based regularization criteria in characterizing a three-dimensional model domain.

3.2. Model Domain

The model domain includes the area between the Boise Foothills and the Snake River, which includes the lower Boise River sub-basin (Figure 1-1). The lower Boise River sub-basin begins where the Boise River exits the mountains near Lucky Peak Reservoir. From Lucky Peak Dam, the lower Boise River flows about 64 miles northwestward through the Treasure Valley to its confluence with the Snake River.

The northeastern model boundary follows the base of the Boise Foothills (Figure 1-1). Alternative boundaries for this part of the model include (1) the northern topographic divide for the lower Boise River basin (watershed boundary) or (2) a sediment-granite contact in the foothills. The base of the Boise Foothills was selected because of (1) the lack of well data within the foothills for model calibration and (2) the difficulty in simulating steep hydraulic gradients with grid cells sized for a regional-scale model. The eastern boundary of the lower Boise River basin follows a watershed divide. The southern and southwestern boundary was defined as the Snake River.

3.3. Model Scale

The flow model was designed to simulate ground water flow on a regional (Treasure Valley) scale. A model simulating flow on this scale is suitable for evaluating regional changes in water levels resulting from regional changes in land use or increases in withdrawals. The direct use of the model for evaluating small-scale (e.g., individual wells) issues is limited. However, the regional model provides a basis for constructing submodels that focus on smaller-scale ground water flow questions.

3.4. Model Units

MODFLOW allows the use of any consistent units (e.g., SI [metric] or traditional [English] units). Spatial data covering the Treasure Valley are maintained by IDWR in the Universal Transverse Mercator (UTM) Zone 11 and/or the Idaho Transverse Mercator (IDTM) coordinate systems, which are based on metric units. Most ground water data collected in the study area (e.g., water level data, flow rates, recharge rates, stream fluxes, etc.) are recorded in English units. Errors associated with converting spatial data from metric to English are readily apparent when the spatial data are plotted. However, errors associated with conversion of other data from English to metric units may not be readily apparent when the data are used. For this reason, the model was constructed in English units (feet) with spatial data in UTM Zone 11 (feet). Time units are in days.

3.5. Model Discretization

The Treasure Valley flow model domain was discretized into a four-layer, 61× 49 uniform grid (Figure 3-1 and Table 3-1) with each square cell representing an area of one square mile. The model grid contains 11,956 cells, 5,448 of which are active. One-mile cells were deemed adequate for the regional nature of the simulations.

Grid Corner	Easting (ft)	Northing (ft)	Comment
Northwestern corner	1,610,421	15,941,680	MODFLOW grid origin
Southwestern corner	1,610,421	15,682,960	Standard grid origin
Northeastern corner	1,932,501	15,941,680	
Southeastern corner	1,932,501	15,682,960	

Table 3-1: Grid coordinates (UTM Zone 11).

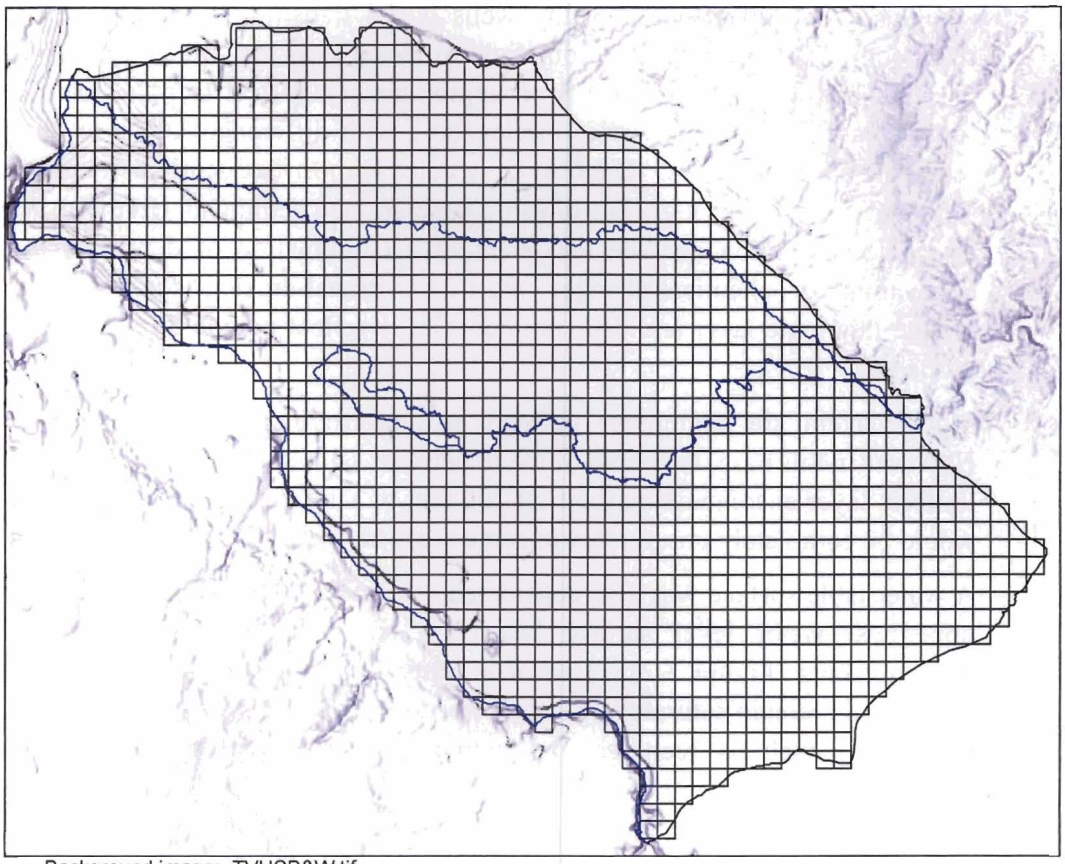

Background image: TVHSB&W.tif

Figure 3-1: Model domain showing uniform, one-mile grid cells.

The model grid was aligned in an east-west direction for two reasons. First, ground water in the deeper, regional flow system in central portions of the Treasure Valley (e.g., the Meridian–Caldwell area) flows in a general westerly direction (Figure 2-2 through Figure 2-4). Second, the east-west orientation simplifies model construction (many data are linked to the east-west land survey system).

Several alternatives for layer definition were considered, including (1) geologic strata, (2) sediment color transitions, (3) ground surface, (4) water table surface, and (5) elevation surface based on Boise and Snake River elevations. Ideally, model layers would be defined based on geological strata or aquifer material characteristics. Several geologic strata were considered for defining layers: (1) the base of the Snake River Formation sediments, (2) the unconformity (where present) separating Chalk Hills sediments from overlying sediments, and (3) the top of the predominantly mudstone section within the Idaho Group sediments. However, the transitions between these strata are neither apparent nor consistent over the entire model domain, or in some cases, even large areas within the domain. When visible (such as the Snake River Formation sediments and basalt), the formation may be above the saturated zone, and the transition may vary substantially in elevation.

Another visible identifier in many wells is the transition from brown to blue-gray sediments. This color change, sometimes referred to as the "blue clay" surface, ranges in depth below ground surface from approximately 30 feet to more than 200 feet in some areas. The surface varies in elevation, with differences of up to 200 feet over relatively short distances. The blue-gray color is most frequently associated with clay sediments in drillers' logs, but bluish coarse-grained sediments have also been noted. The color transition may be the result of a combination of depositional and post-depositional geochemical changes. Post-depositional erosion is not associated with a unique lithologic layer and does not necessarily reflect unique transitions in hydraulic properties.

Model layers are sometimes defined as uniform distances from ground surface. However in this case, the depth of the uppermost saturated zone varies substantially. A uniform layer encompassing the first 200 feet of saturated zone below the Boise River would be completely unsaturated in some areas between the Boise and Snake Rivers.

A water table surface was also considered as a surface for defining layers, such as the uppermost water level surface based on an average of spring and fall 1996 measurements (Figure 3-2). Use of a water level surface would ensure that upper model cells remain saturated, at least prior to an applied stress. However, hydrologic conditions, such as recharge and extraction, influence this surface; it does not necessarily reflect hydrogeologic conditions at depth.

The final alternative for layer definition, an elevation surface based on Boise and Snake River elevations (Figure 3-3), was chosen for the following reasons. First, it represents a relatively uniform surface throughout the model domain. Second, because ground water is in direct hydraulic connection with the Boise and Snake Rivers, a surface connecting these two rivers ensures that the upper model layers remain saturated under initial non-stressed conditions. Third, the surface is dipping basinward, not unlike some of the dipping strata existing in the basin. Finally, this surface offered a basis for defining relatively uniform layer surfaces at depth.

The elevation surface based on the Boise and Snake River elevations was considered to represent a layer "datum" (Figure 3-3 and Figure 3-4). The first model layer was defined as extending 200 feet below the datum (Table 3-2). This zone, at least in the Boise River area, included most of the coarser-grained Snake River sediments. The uppermost model layer is assumed to represent a continuous, unconfined aquifer throughout the model domain. This assumption is valid throughout most of the model area, although some perched aquifers are known to exist. The top of the uppermost model layer is considered to be ground surface. The ground surface in most parts of the model domain is higher than the layer datum (Figure 3-4).

The base of the second layer was defined as extending 200 feet below the base of the first layer (Table 3-2). The bottom of the second layer, 400 feet below the layer datum, roughly corresponds with the geologic unconformity separating Chalk Hills and

overlying sediments (see Section 2). Layers 3 and 4, each extending 400 feet below layer 2, represent the deeper Idaho Group sediments from which the valley's deeper wells draw water. Virtually all water-producing wells in the Treasure Valley are completed at depths above the base of model layer 4.

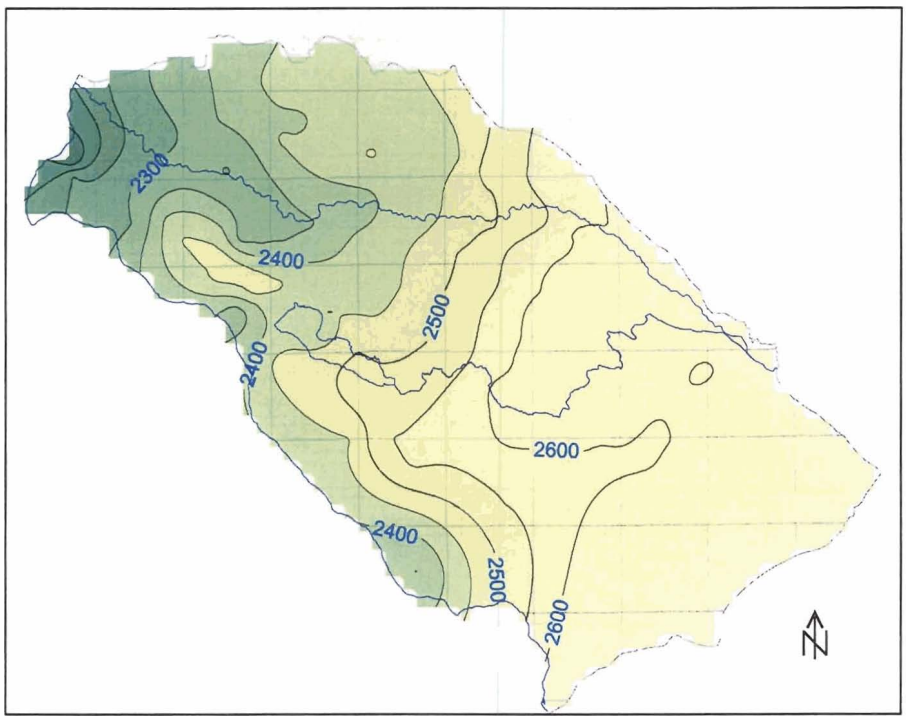

Figure 3-2: Average 1996 potentiometric surface of the uppermost aquifer (ft).

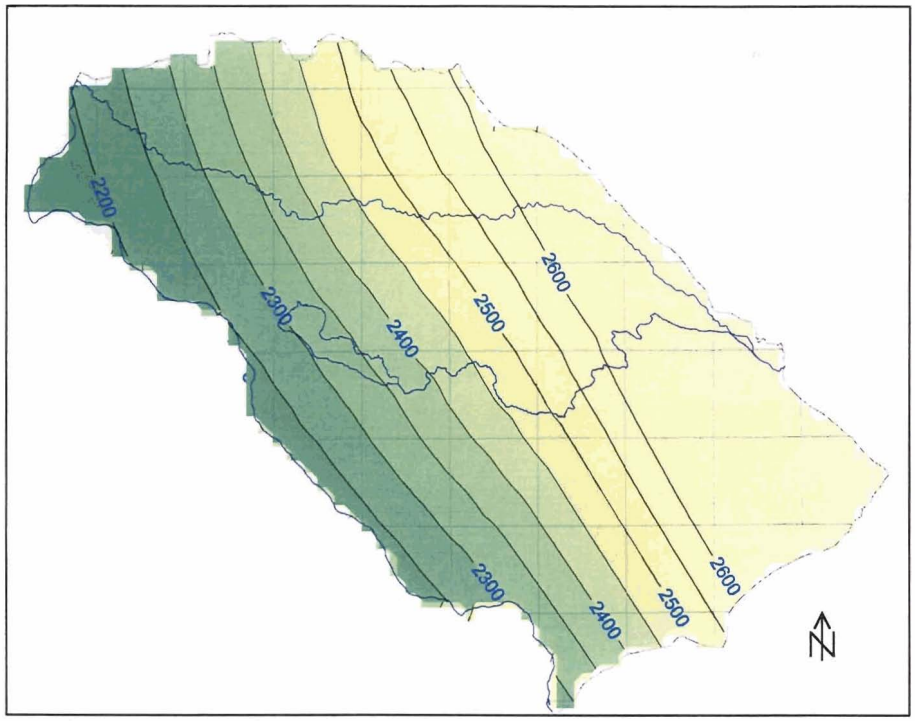

Figure 3-3: Elevation (ft) of uniform layer surface (i.e., layer "datum").

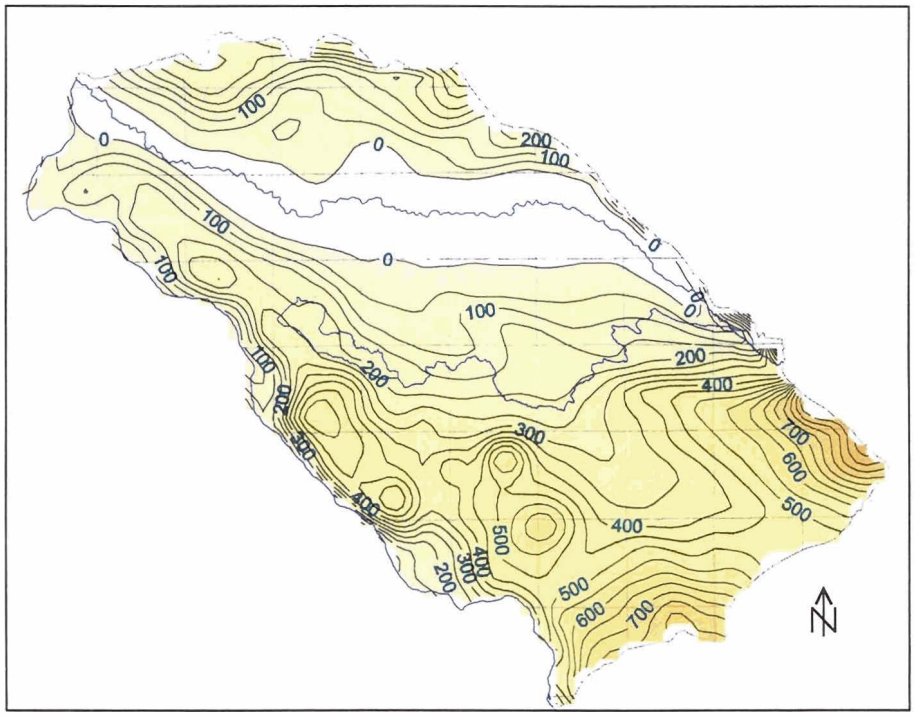

Figure 3-4: Depth from ground surface to layer "datum" (ft).

Layer	Thickness (ft)	Depth from Layer "Datum" to Top of Layer (ft)	Depth from Layer "Datum" to Bottom of Layer (ft)
1	200	0	200
2	200	200	400
3	400	400	800
4	400	800	1,200

Table 3-2: Definition of model layers.

3.6. Boundary Conditions

Boundary conditions were simulated as no-flow, specified flux, head-dependent flux, or free surface (Figure 3-5). No-flow conditions were described for the northern and southeastern sides of the model. The northern edge of the model was assumed to be a ground water flow divide separating the Payette and Boise River drainages. The southeastern boundary (following a hydrologic divide) is relatively parallel to the regional ground water flow lines as presented in Newton (1991) and was therefore assumed to represent a no-flow boundary[2].

No-flow conditions were also defined for the model base. There is evidence that there may be some vertical mixing between geothermal and overlying cold ground water aquifers based on fluoride concentrations, sodium/calcium ratios, and water temperatures (Hutchings and Petrich, 2002a). Nonetheless, it was assumed that on a regional scale, fine-grained sediments at the base of the cold-water system form an effective barrier to substantial upward movement of geothermal ground water into upper cold-water aquifers.

Specified flux boundary conditions were used to simulate recharge (Section 4.6), withdrawals from wells (Section 4.2), and underflow (Section 4.2). Recharge components (Section 4.6) included (1) seepage from canals, (2) seepage from rivers and streams, (3) seepage from Lake Lowell, (4) underflow, (5) infiltration from precipitation and irrigation, and (6) seepage from septic systems.

Ground water withdrawals consist of water that is pumped or flows under artesian pressure from municipal, industrial, agricultural, and rural domestic water supply wells (Urban and Petrich, 1998). This includes water withdrawn from a variety of depths and aquifers. Simulated withdrawal rates are summarized in Section 4.2.

Underflow was assumed along the northeastern edge of the model (simulated a specified flux with injection wells as shown in Figure 3-5). Underflow was included in the model as positive flow to wells (as opposed to negative flow, or withdrawals).

2 There are few wells available along the southeastern model boundary to confirm this assumption.

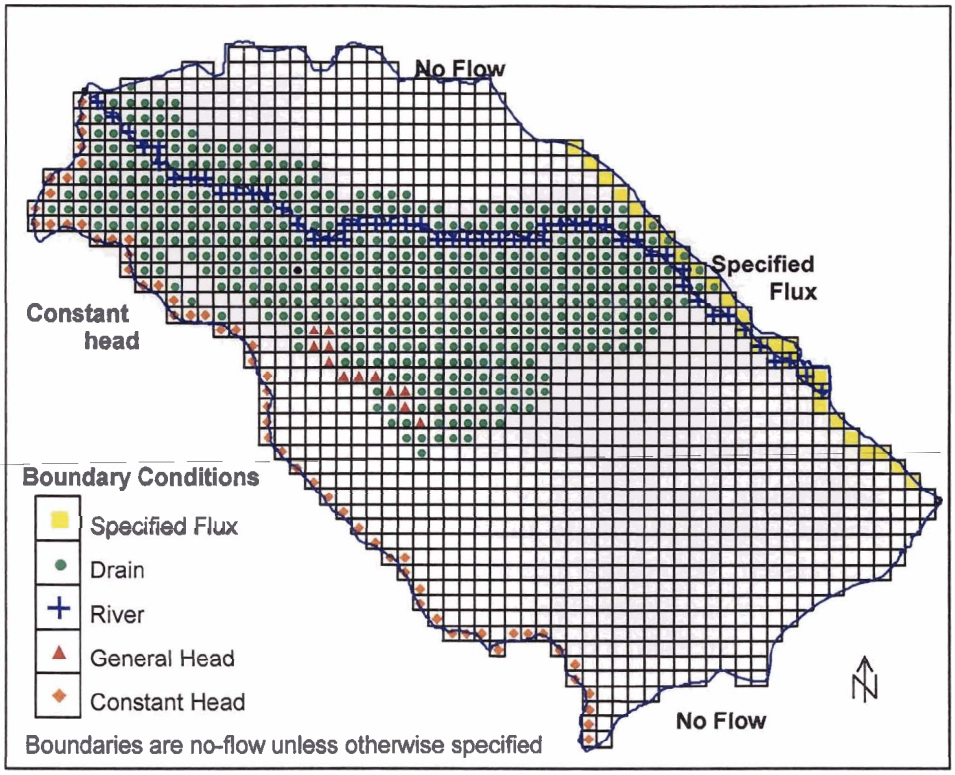

Figure 3-5: Model grid and boundary conditions.

Head-dependent flux boundaries were used to simulate losses to and gains from streams and lakes and flow to drains. Fluxes into and out of the Boise River were simulated using the MODFLOW River Package (Section 4.3). Discharge to drains was simulated using the MODFLOW Drain Package (Section 4.4). Fluxes into and out of Lake Lowell were simulated using the MODFLOW General Boundary package (Section 4.5).

A free-surface boundary represents the water table in model layer 1. The position of the free-surface boundary was calculated by the model in response to surrounding hydraulic heads, other boundary conditions, and aquifer properties.

4. DEVELOPMENT OF MODEL INPUT FILES

4.1. Overview

Multiple files are needed for constructing and calibrating a model. Some of the files are required by the MODFLOW code, some stem from the graphical user interface. This section describes (1) the files that were used for model construction, (2) the data included in the files, and (3) how the files were created. Model files required for the MODFLOW simulations are listed in Appendix B. Files required for model calibration are described in Section 5.10.

Estimated withdrawal, recharge, and underflow rates for 1996 (Urban and Petrich, 1998) were used for model inputs for these simulations. A revised water budget for the year 2000 is being prepared but was not available at the time of model development or calibration.

4.2. Well Package

The MODFLOW well package was used to list (1) ground water withdrawals from cells within the model domain and (2) underflow into the model along model boundaries. Ground water withdrawals consisted of water that was pumped or flowed under artesian pressure from municipal, industrial, agricultural, and rural domestic water supply wells[3].

Withdrawal amounts (Table 4-1) were those estimated in the 1996 water budget (Urban and Petrich, 1998). Withdrawal amounts were estimated[4] on an areal basis (unless withdrawals were associated with known screened intervals in specific wells). The withdrawals were then distributed vertically throughout the model domain based on a distribution of well depths by model layer. The distribution of well depths was drawn from wells listed in IDWR's Well_Log database. The resulting withdrawal distribution by model layer is shown in Figure 4-1. Each cell in the model domain was identified in the well package, although cells without any ground water extraction had values of zero. The spatial distribution of estimated withdrawal rates per model cell is shown in Figure 4-2 through Figure 4-5. In general, ground water withdrawals are greatest in urban areas and in areas of substantial irrigation with ground water.

Estimates of underflow along the northeastern model boundary were made in the Treasure Valley Water Budget (Urban and Petrich, 1998). The magnitude of underflow across the northeast boundary was estimated by assuming all precipitation

[3] The withdrawal estimates for rural domestic wells included all withdrawals. Septic seepage was included in the recharge file (Section 4.6).

[4] The well data were prepared by Scott Urban (IDWR) using the spreadsheet "1996pump-revised-4-21-03.xls".

within the Boise Foothills, less evapotranspiration and stream discharge, enters the model domain as underflow (Urban and Petrich, 1998). This resulted in a total underflow estimate of 8,000 af/yr (8,840 ft^3/day/cell). However, this estimate is uncertain, as is the horizontal and vertical distribution of the underflow along the Boise Foothills. Results from early calibration runs suggested that underflow values might be lower than estimated. Therefore, a lower value of 1,000 ft^3/day/cell was used for the base simulation[5]. Cells in which underflow was specified are indicated (in yellow) in Figure 3-5.

Category	Estimated 1996 Withdrawals		
	Acre-feet (af)	ft^3/day	Percent of total
Domestic and Industrial Withdrawal	66,100	7.89×10^6	34
Municipal Irrigation	9,700	1.16×10^6	5
Self-Supplied Industrial	20,800	2.48×10^6	11
Agricultural Irrigation	71,900	8.58×10^6	37
Rural Domestic Withdrawal	26,600	3.17×10^6	12
Stock Watering	2,600	3.10×10^5	1
TOTAL:	197,700	2.36×10^7	100

(from Urban and Petrich, 1998)

Table 4-1: Estimated ground water withdrawals in 1996.

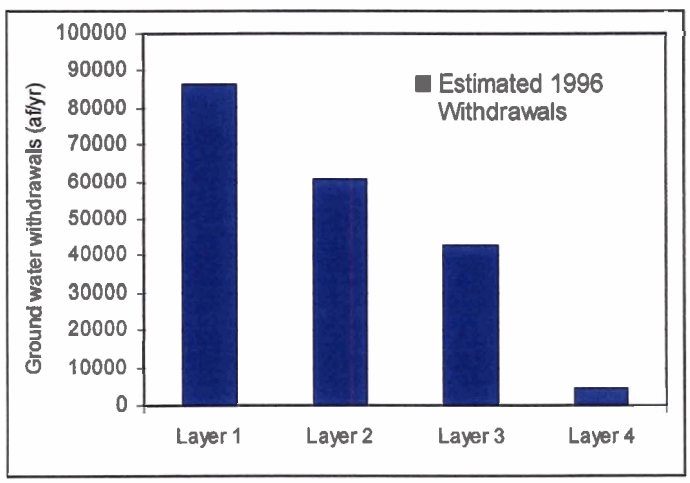

Figure 4-1: Estimated 1996 withdrawals, by model layer.

[5] A higher underflow rate of 8,000 ft^3/day/cell per cell was tested in a sensitivity simulation (see Section 8.3).

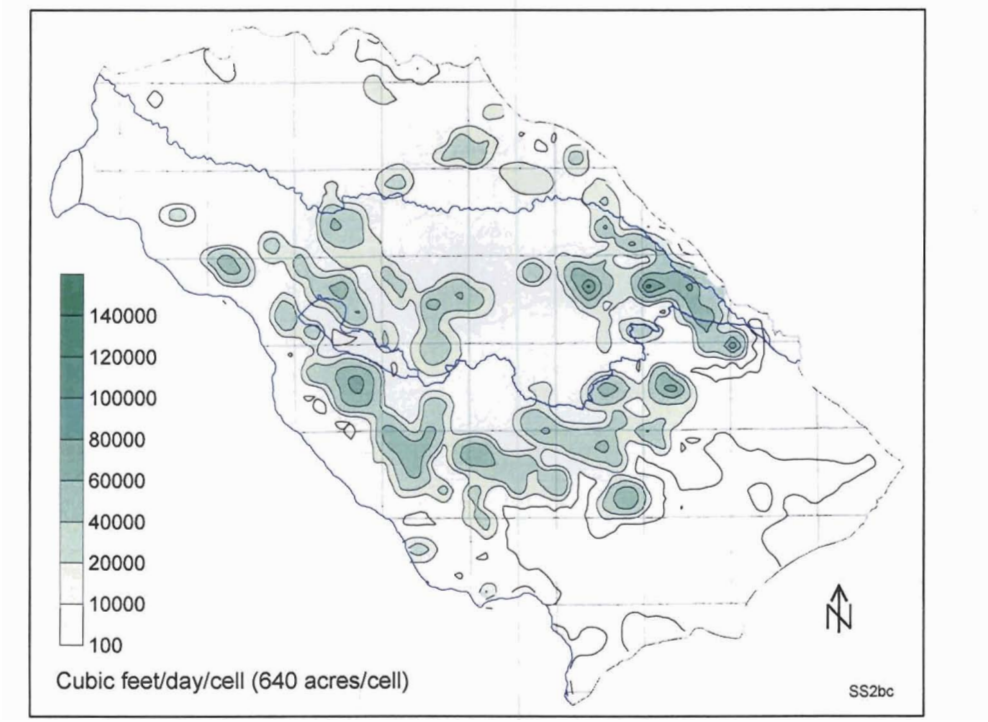

Figure 4-2: Estimated 1996 withdrawals, layer 1.

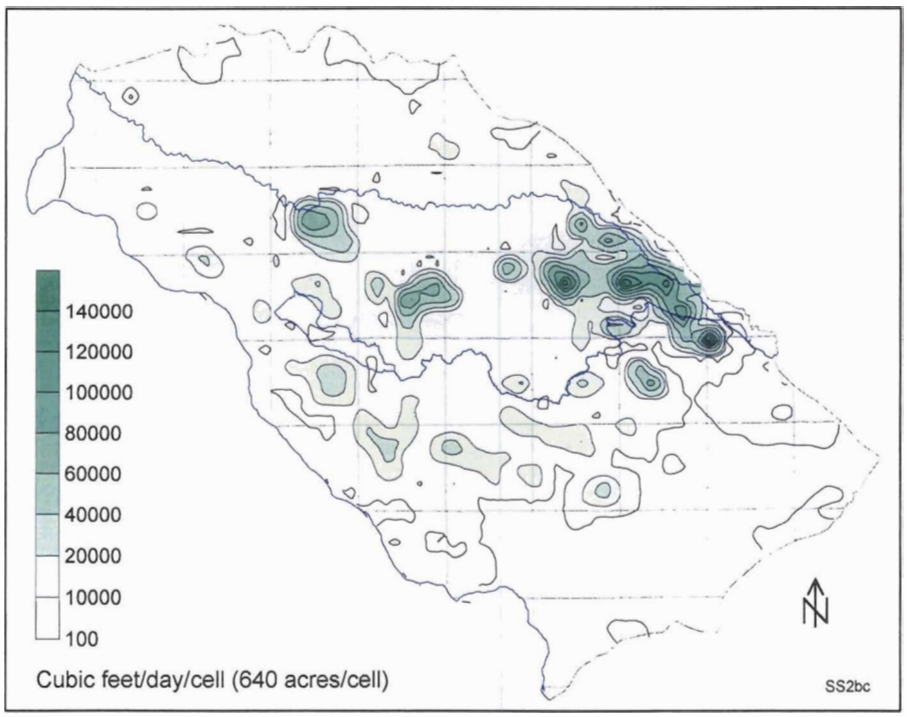

Figure 4-3: Estimated 1996 withdrawals, layer 2.

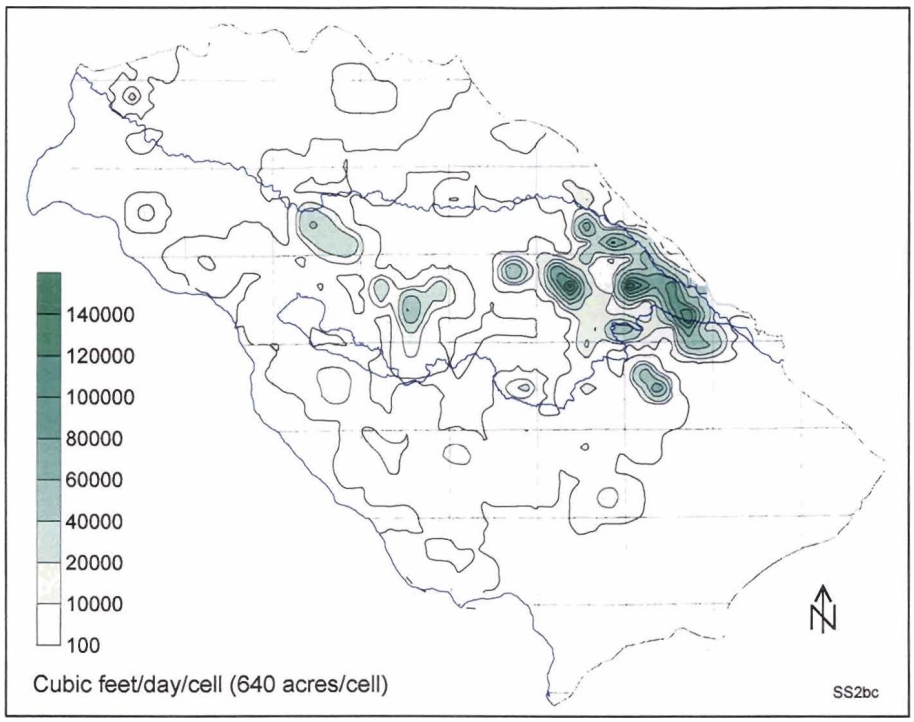

Figure 4-4: Estimated 1996 withdrawals, layer 3.

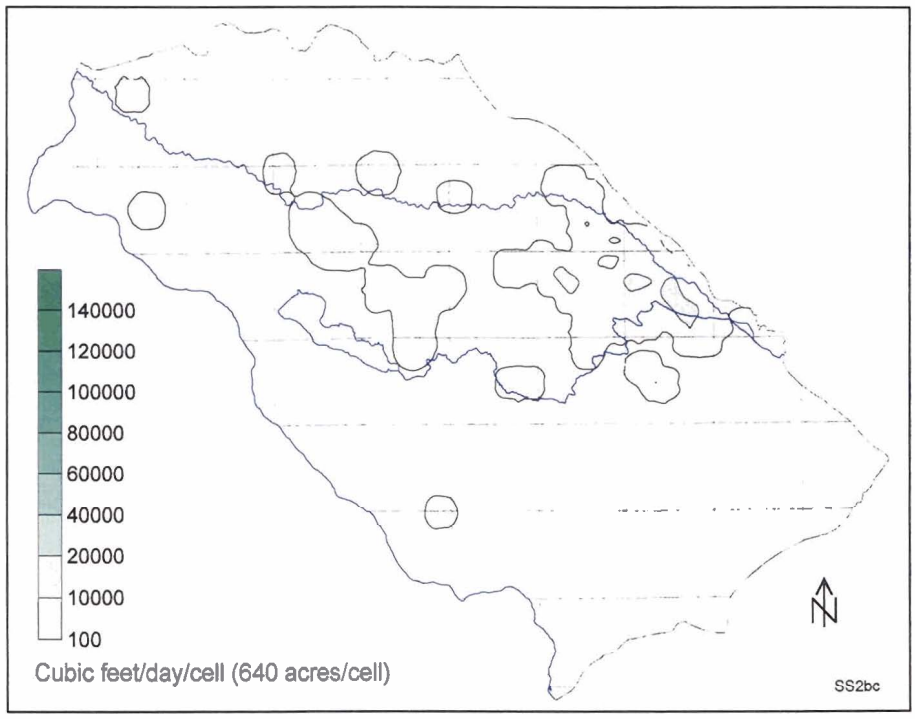

Figure 4-5: Estimated 1996 withdrawals, layer 4.

4.3. River Package

The river package allows simulation of the effects of flow between surface and ground water systems. The rate of flow between a surface channel and an underlying aquifer is calculated in each simulation based on river stage, surrounding ground water levels, channel dimensions, and streambed conductance characteristics. Ground water moves into the surface channel if surrounding ground water levels are higher than the river stage and vice versa if the ground water levels are lower than the river stage.

The river package was used to simulate ground water hydrologic conditions associated with the Boise River to allow for both gaining and losing reaches (the lower Boise River is predominantly a gaining reach). The Snake River was simulated as a constant head boundary because it is predominantly a gaining reach throughout the model domain. Major canals (e.g., New York Canal) were not simulated as river features because seepage from these channels was included in the recharge estimates.

The river stage elevations were based on topographic contour elevations. It was assumed that the river has an average depth of 10 feet. The river bottom elevations were therefore assumed to be 10 feet less than the river stage. River stage varies throughout the year, thus approximate average elevations were assumed. The river stage elevation was assumed to be 2,742 feet[6] where it enters the model domain; the river stage at the confluence with the Snake River was assumed to be 2,170 feet.

The riverbed hydraulic conductance is defined as

$$COND = \frac{K_R L_R W_R}{M}$$

where K_R is the hydraulic conductivity of the riverbed material, L_R is the reach length, W_R is the channel width, and M is the riverbed thickness (McDonald and Harbaugh, 1988). K_R, L_R, W_R, and M vary substantially throughout the model domain, and there is a high degree of uncertainty associated with any estimates of K_R. The riverbed conductance was assumed to be the same for all river cells[7]. The initial conductance value for base calibration simulations was 2.0×10^5 ft^2/day based on the assumptions listed in Table 4-2.

4.4. Drain Package

The drain package is used to simulate the effects of features such as agricultural drains, which enable discharge from an aquifer at a rate proportional to the difference between the aquifer head and the drain elevation (McDonald and Harbaugh, 1988). Simulated

[6] Taken from a USGS 7.5-minute quadrangle map.

[7] A constant river bed conductance (*COND*) was assumed to simplify the model. In actuality, the riverbed conductance would be expected to vary within river cells and among different river cells because of differences in riverbed materials, reach lengths, and river widths.

water enters the drain if the cell head values are greater than the drain elevation; the drains have no effect if the aquifer head levels fall below that of the drains.

Parameter	Value
Aggregate reach length per cell (*L*)	5,280 ft (1 mile)
Aggregate reach width per cell (*W*)	50 ft
Hydraulic conductivity of riverbed material (*K*)	3.8 ft/day
Riverbed thickness (*M*)	5 ft
Streambed conductance (*COND*)	2.0×10^5 ft^2/day

Table 4-2: Streambed conductance values.

Surface topography limits the upper range of shallow ground water levels in the central portion of the basin (i.e., aquifer discharge occurs if ground water levels rise to near ground surface elevations). Drain cells were used to simulate this process – to help the model "remove" this aquifer discharge. Model cells were identified as drain cells if typical shallow aquifer head values, based on fall 1996 water levels, fell within approximately 10 feet of the ground surface elevation. Some additional drain cells were identified if known drains were present in the cells. Factors influencing discharge to a drain include the difference between local aquifer heads and drain heads, drain dimensions, and drain-bottom sediment characteristics.

The drain conductance is a lumped parameter that describes head loss between a drain and underlying aquifer. The conductance was defined similar to river conductance (see Section 4.3). Drain conductances were kept has high as possible (to drain as much water as necessary) without creating model instability. Assumed parameter value assumptions for drain cells are given in Table 4-3.

Parameter	Value
Aggregate reach length per cell (*L*)	26,400ft (5 miles)
Aggregate reach width per cell (*W*)	5 ft
Hydraulic conductivity of lake sediment material (*K*)	3.79×10^{-1} ft/day
Lakebed thickness (*M*)	1 ft
Drain cell conductance (*COND*)	5.0×10^4 ft^2/day

Table 4-3: Initial drain conductance values.

4.5. General Head Boundary

The general head boundary package was used to simulate the effects of flow between Lake Lowell and underlying shallow aquifers (Figure 3-5). The mathematical basis for this package is similar to that of the river (Section 4.3) and drain (Section 4.4) packages, in that flow from an external source (in this case, Lake Lowell) is proportional to the difference in head between the external source and the aquifer. The

conductance of the external source (Lake Lowell bottom sediments) was assumed to be 4,000 ft^2/day/cell (Table 4-4).

Parameter	Value
Aggregate reach length per cell (*L*)	5,280 ft
Aggregate reach width per cell (*W*)	5,280 ft
Hydraulic conductivity of lake sediment material (*K*)	1.15×10^{-3} ft/day
Lakebed thickness (*M*)	8 ft
General head boundary conductance (*COND*)	4.0×10^{3} ft^2/day

Table 4-4: Initial general head boundary conductance values.

4.6. Recharge Package

The recharge package was used to simulate areally distributed recharge over the uppermost Treasure Valley aquifers. The primary sources of recharge consisted of (1) seepage from canals, (2) seepage from rivers and streams, (3) seepage from Lake Lowell, (4) infiltration from precipitation and irrigation, and (5) seepage from septic systems (Urban and Petrich, 1998). A summary of estimated annual recharge rates is shown in Table 4-5.

The MODFLOW recharge file[8] was created based on estimated Treasure Valley ground water recharge rates (Urban and Petrich, 1998) for the 1996 calendar year. Average daily recharge rates in the MODFLOW recharge file were calculated based on annual recharge estimates. The recharge file does not include seepage from the Boise River (which is simulated as a head-dependent boundary based on river package parameters, see Section 4.3). It also does not include seepage from Lake Lowell, (which is simulated as a head-dependent boundary based on general head boundary package parameters, see Section 4.5).

The MODFLOW recharge file represents a smaller recharge volume (973,711 af/yr) than that listed in Urban and Petrich (1998), for two reasons. First, the model domain represents a slightly smaller area than that used to estimate total recharge for the Treasure Valley. Second, the model also simulates recharge via river, underflow, and head-dependent boundary cells. Total simulated recharge is reconciled with estimated water budget inflows in Table 7-2.

The areal distribution of recharge (as applied on a cell-by-cell basis in the model) is shown in Figure 4-6. The greatest simulated recharge rates were along the New York Canal and areas of flood irrigation in central portions of the valley. Losses from (or gains to) the Boise River are not specified in the recharge package but were simulated as a head-dependent boundary in the MODFLOW river package (Section 4.3).

[8] MODFLOW recharge files were created by Scott Urban, IDWR (*1996rechnew.xls*).

Sources of Recharge	Estimated Recharge for 1996		
	Acre-feet (af)	ft^3/day	Percent of Total
Canal Seepage	637,000	7.60×10^7	61
Seepage from Rivers and Streams	16,000	1.91×10^6	1
Seepage from Lake Lowell	19,000	2.27×10^6	2
Underflow	8,000	9.55×10^5	1
Flood Irrigation and Precipitation	302,000	3.60×10^7	30
Recharge by Other Land Uses	48,000	5.73×10^6	4
Rural Domestic Septic Systems	5,000	5.97×10^5	<1
Total	1,035,000	1.24×10^8	99

(from Urban and Petrich, 1998)

Table 4-5: Estimated recharge to shallow Treasure Valley aquifers in 1996.

4.7. Solver Package

MODFLOW comes with several solver options: Slice-Successive Over-Relaxation (SSOR), Strongly Implicit Procedure (SIP), and the Preconditioned Conjugate-Gradient Method (PCG2). Different solvers may work better for different problems. The PCG2 solver was successful in solving the Treasure Valley model simulations; other solvers were not required.

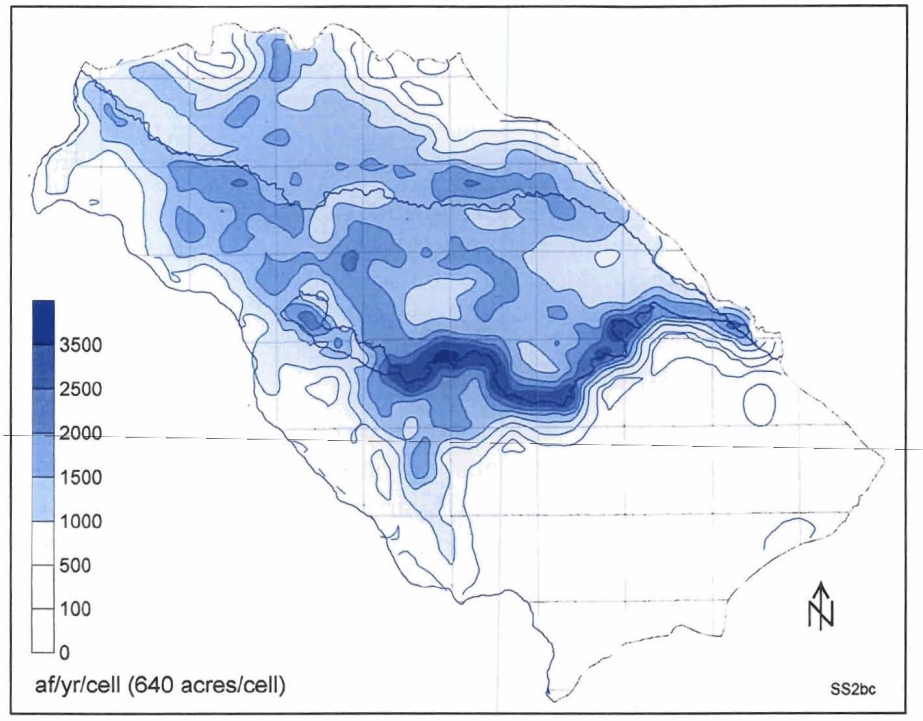

Figure 4-6: Areal distribution of estimated recharge.

5. MODEL CALIBRATION

5.1. Introduction

Model calibration is the process of adjusting model parameters so simulated observations match measured or estimated observations as closely as possible. This chapter describes the calibration of the Treasure Valley ground water flow model under steady-state hydraulic conditions.

5.2. Automated Parameter Estimation

Initial model calibration was conducted using "trial-and-error" manipulation of individual cells or zones of cells. Trial-and-error calibration involves manually manipulating parameter values (e.g., hydraulic conductivity, vertical conductance, etc.) such that simulated head values are as close as possible to observed head values.

Automated parameter estimation involves the use of codes that automatically manipulate parameter values to minimize an objective function (e.g., sum of squares of the residuals between simulated and observed heads). Automated calibration methods generally yield descriptive statistics[9] that quantify the uncertainty of the calibration.

Several parameter estimation codes existed at the time of calibration (Doherty, 1998; Doherty, 2000; Harbaugh, 2000; Hill, 1992; Hill et al., 2000; Poeter and Hill, 1998). PEST (Doherty, 2000) was initially selected because of it's ability to limit parameter value ranges, availability of utilities designed to ease the use of MODFLOW input of files created in GMS[10] (a graphical user interface), and parallel processing utilities. Subsequent improvements in PEST that were used in this model calibration included regularization with pilot points and predictive analysis tools (Doherty, 2000).

PEST's regularization scheme allows estimation of a larger number of parameters than would otherwise be possible without incurring parameter instability and non-uniqueness. Preferred values for parameters, or relationships between parameters, were used as supplementary information to help constrain model calibration. Regularization and pilot points (see Section 5.6) allowed an increased number of calibration parameters.

PEST operates independently of the MODFLOW code or the graphical user interface. Using the Gauss-Marquardt-Levenberg method, PEST adjusts specified model parameters and/or stresses (excitation) values on an iterative basis until an objective function is minimized.

---

[9] Some of PEST's descriptive statistics may not apply with the use of regularization (see Section 5.6).

[10] http://www.ems-i.com

The parameter estimates from any model calibration may have a degree of non-uniqueness, whereby additional adjustments of any given parameter have no material impact on the overall calibration (i.e., the objective function will not be lowered further with additional parameter adjustments). The degree of non-uniqueness depends on the general strength of the calibration, the nature of the individual parameters, and the number and quality of observation data. PEST's predictive analysis tools help estimate maximum and minimum outcomes within the context of a set of "calibrated" parameters.

5.3. Steady-State versus Transient Calibration

Model calibration can be performed under steady-state and/or transient hydraulic conditions. Steady-state conditions require the assumption that hydraulic conditions, fluxes and water levels, are at equilibrium. Fluxes and water levels change over time under transient conditions. Steady-state calibration parameters generally include hydraulic conductivity; transient calibrations require the calibration of aquifer storativity as well. Ground water flow models generally are calibrated to steady-state conditions first and to transient conditions[11] if data allow.

A steady-state calibration is appropriate if the model questions focus on equilibrium aquifer conditions, or long-term aquifer sustainability. Similarly, model predictions under steady-state simulations are appropriate to evaluate questions of long-term (i.e., equilibrium) water levels, or aquifer sustainability. Simulated equilibrium water levels are determined by hydraulic conductivity values, which are estimated in a steady-state calibration. Transient flux and water level data will not help estimate hydraulic conductivity parameters; they would only help in estimating the time required to reach equilibrium.

Basing a steady-state calibration on water levels that are experiencing long-term rises or declines may yield inaccurate results. In general, water levels in the Treasure Valley have been relatively constant over time (years). However, two areas have experienced substantial declines, an area south of Lake Lowell and the southeast Boise area, although water levels in these areas appear to have stabilized in recent years.

Many areas experience seasonal variations in ground water levels. To reduce errors introduced into the steady-state simulations from seasonal variations, the flux rate inputs (underflow, recharge, extraction rates, etc.) were converted to daily average rates based on 1996 totals. For example, daily rates for summer irrigation-dominated recharge were divided into uniform daily rates based on total recharge for the 1996 calendar year (see Section 4.6). Similarly, water level observations used for model

11 Hydraulic conductivity and/or transmissivity values often are correlated with storativity values, and thus, a transient calibration might focus first on adjusting storativities while using hydraulic conductivity and/or transmissivity values from a steady-state calibration.

calibration represent an average between spring and fall 1996 observations. Thus, simulated recharge and withdrawal rates, and river, general head, constant head, and drain flux rates, represent daily rates averaged over an entire year.

A transient model was not constructed, for two reasons. First, detailed temporal flux data are required to help calibrate aquifer storativity in a transient simulation[12]. Detailed flux data were not yet available during model construction and simulation. The USBR and IDWR are currently compiling more detailed irrigation diversion and return data for the valley, which would be essential for transient simulations (especially those focusing on shallow aquifer conditions). Second, successful transient simulations depend on well-defined temporal water level changes. Temporal water level change information enables calibration of aquifer storativity. Without these data, simulated storativity parameters may be excessively correlated with hydraulic conductivity[13] parameters.

Transient simulations with temporal water level change data can be conducted over short or long time periods, depending on data availability. With some exceptions, long-term Treasure Valley water levels have remained relatively steady over the last several decades, and therefore, may not provide adequate long-term changes that could be used to calibrate a transient model. Exceptions include the areas south of Lake Lowell and southeast Boise, but these two areas are probably not extensive enough to provide a sufficient basis for a regional transient model calibration.

The Treasure Valley also experiences seasonal water level changes (see hydrographs in Petrich and Urban, 2004). Seasonal fluctuations are dominated with two general patterns. Water levels in wells are influenced either by water level rises corresponding with irrigation applications or by summer irrigation withdrawals, or both. Variations in local withdrawals and/or shallow recharge, even if well defined, may reduce the reliability of simulated regional storativity estimates. Thus, these seasonal water level fluctuations may be insufficient for a solid seasonal transient calibration for a model covering the entire Treasure Valley area.

However, transient calibrations are probably feasible for local ground water flow models within the Treasure Valley or submodels of the regional model. These calibrations would be possible (depending on the specific type of question to be answered by the model) if detailed local water level and surface recharge/discharge data were available.

[12] Aquifer storativity was assumed to be zero during a steady-state simulation because the steady-state simulation does not account for water level changes over time.

[13] Aquifer hydraulic conductivity and storativity represent independent physical characteristics of an aquifer. However, the effect of these parameters in a model calibration may, if not adequately constrained, appear correlated.

5.4. Calibration Parameters

Primary calibration parameters for the steady-state calibration were horizontal hydraulic conductivity (K_h) and vertical hydraulic conductivity (K_v). Underflow was also varied between several runs, but generally held constant within runs because of correlation with hydraulic conductivity parameters.

Areal recharge was also a potential calibration parameter. However, recharge is often correlated with K_h and K_v (a change in recharge values and a corresponding change in K_h or K_v may lead to the same calibration result). The range of recharge values might be constrained if detailed system discharge data (e.g., ground water discharge to discrete reaches of the Snake and Boise Rivers) were available at the time of calibration.

Layers 3 and 4 were considered to be one layer for model calibration for two reasons[14]. First, there were relatively few observation wells in these layers (Section 5.5), many of which are concentrated in the Boise area. Some of the wells that extend to depths encompassed by these layers were completed in multiple model layers, excluding their use as layer-specific observation wells. Second, the nature of aquifer materials represented in these layers probably is more consistent (interbedded sand, silt, and clay, with increasing finer-grained sediments with depth) than overlying layers. Thus, K_h and K_v parameters for model layers 3 and 4 were tied together because of the relatively small number of water level data points in these lower model layers.

5.5. Calibration Observations

Calibration observations included (1) ground water levels based on mass ground water level measurements (Petrich and Urban, 2004) and (2) estimated or observed vertical differences in potentiometric surface. The steady-state calibration was conducted based on 1996 water levels, which coincides with water budget estimates for this same year.

5.5.1. Ground Water Levels

The 1996 spring and fall mass measurements (Petrich and Urban, 2004) included 339 and 331 wells, respectively. Candidate wells for the mass measurement were selected by the USGS from the USGS Ground Water Site Inventory (GWSI) database. Criteria for observation well selection included (1) available drillers' reports, (2) completion depths falling within the layer intervals, and (3) horizontal and vertical distribution (where possible) throughout the model domain. Several wells with screen openings spanning both layers 3 and 4 were used as observation wells because they were located in areas with few observation alternatives.

[14] Two layers were used in the lower portion of the model to allow future parameter and/or flux variations.

Not all observations taken during the mass measurement were used for calibration for several reasons. First, several of the measurements were made in areas that were later removed from the model domain (e.g., Boise Foothills). Second, wells that were located in the half of a cell adjacent to an exterior boundary were excluded (or moved to the interior half of a cell) because of errors incurred by GMS's spatial interpolation function by which cell heads were calculated based on surrounding grid nodes. Third, a number of observations appeared to represent suspect data caused by active pumping or other reasons.

Finally, a number of shallow wells were located in areas where drains are present (see Section 4.4). Measurements from these wells were given a calibration weight of zero because the water levels in these wells were at or above drain elevations. Water level data in areas where topography was actively controlling the water table are not appropriate for estimating hydraulic conductivity because the water level (i.e. hydraulic gradient) reflects the topography (or drain elevations), not aquifer characteristics[15]. Furthermore, water levels from shallow wells near drains can confound model calibration because PEST attempts to force the model to match these water level elevations but cannot match them because the simulated drains siphon away water that is above the drain elevations. Non-zero calibration weights for these wells would have caused a contribution to the objective function that would have been impossible for PEST to reduce. In the end, 200 observations with weights greater than zero were used for model calibration (Figure 5-1 through Figure 5-3, and Appendix C). These are shown in Figure 5-1 through Figure 5-4.

Water levels vary throughout the year in response to well withdrawals, nearby pumping, and/or seepage from surface water and irrigation. Of 284 project observations (not all of which were used for calibration), 154 wells experienced a water level rise between the spring and fall mass measurement, 106 wells experienced a water level decline, and the remaining wells experienced no change (Table 5-1). With five exceptions, average water levels between spring and fall measurements were taken for each well for the simulation under steady-state hydraulic conditions. The spring measurements for 5 wells in layer 4 were used instead of an average because (1) these wells were not measured in the fall, and (2) elimination of these wells would have meant a substantial reduction in observations in layer 4.

[15] Darcy's law implies describes the relationship between flow, hydraulic conductivity, and hydraulic gradient: $q = K\frac{\partial h}{\partial L}$, where q is unit flow, K is hydraulic conductivity, and $\frac{\partial h}{\partial L}$ is the hydraulic gradient. The purpose of the calibration is to estimate K on the basis of the hydraulic gradient. If the hydraulic gradient is controlled by ground surface (i.e., drain elevation), then the observation is not necessarily appropriate for use in model calibration.

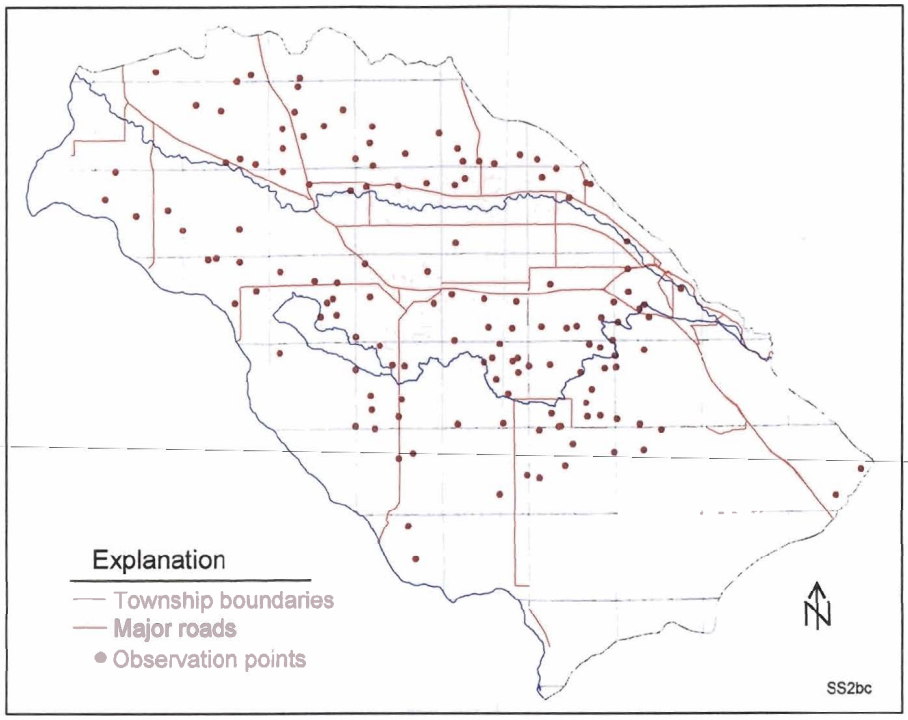

Figure 5-1: Locations of water level observations, layer 1.

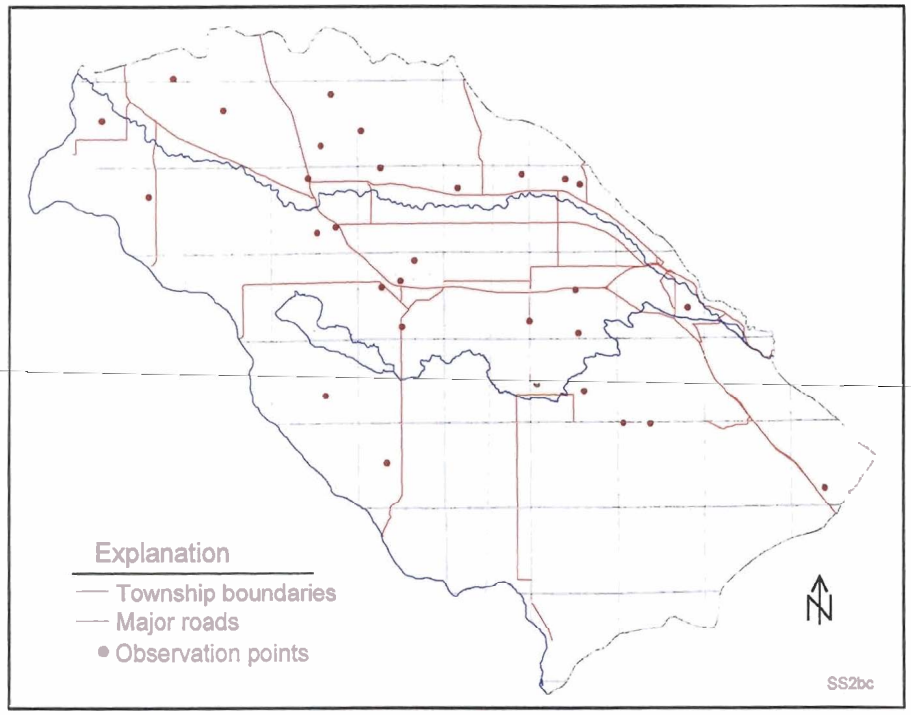

Figure 5-2: Locations of water level observations, layer 2.

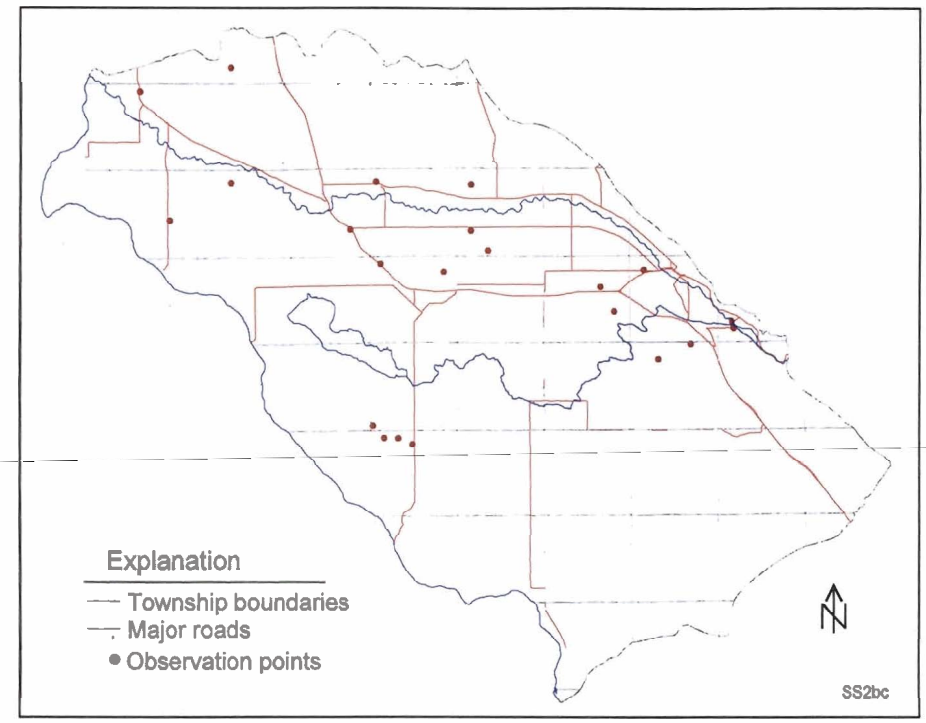

Figure 5-3: Locations of water level observations, layer 3.

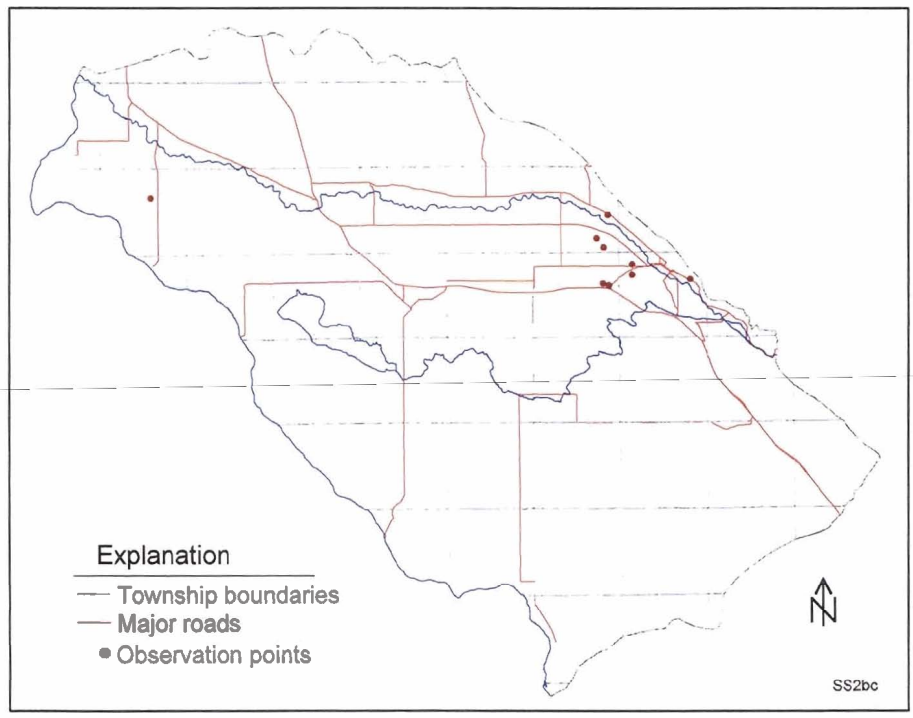

Figure 5-4: Locations of water level observations, layer 4.

Parameter	Value
Total number of wells	284
Observations with weight > 0	200
Number of wells increasing in water level (weight > 0)	93
Maximum water level increase from spring to fall	48 ft
Median water level increase	3 ft
Percentage of wells with less than 10 ft increase	82.8 %
Number of wells decreasing in water level	91
Maximum water level decrease from spring to fall	-45 ft
Median water level decrease	-3 ft
Percentage of wells with less than 10 ft decrease	81.3 %

From "Final 1996 obs Data.xls"

Table 5-1: Statistics for water level changes in observation wells between the spring and fall mass measurements, 1996.

The quality of model calibration depends, in part, on potential errors associated with the calibration data. Water level measurements taken by the USGS generally have an accuracy of ±0.01 foot. However, other potential errors may influence model calibration. Potential sources of error associated with the water level observations include the following:

1. Ground surface elevations used for calculating water level elevations were taken either from 7.5-minute topographic maps or resource-grade global positioning system (GPS) device. This may have contributed to elevation errors at least as great as 10 feet.
2. Errors may have occurred during water level measurement, although USGS protocols are intended to minimize measurement error.
3. Errors may have occurred in identifying the spatial location of a well.
4. Recent pumping may have influenced water levels in some wells. The USGS reduces the risk of inadvertently measuring water levels immediately after a pump shuts off by taking two measurements in succession. The measurement is recorded if the measurements are within 0.01 foot of one another. Despite precautionary measures, water levels may reflect long-term drawdown or influence from nearby wells.
5. An inaccurate water level reading may result in artesian wells if the measured well is currently flowing or has recently flowed or if a nearby well is flowing or has recently flowed.
6. An inaccurate drillers' report may result in water level measurements from a well being attributed to an incorrect model layer.
7. Interpolating observation point measurements to node locations (locations at which heads are simulated) may introduce some interpolation error, particularly near the model boundary where head gradients are high, and near sources of significant recharge/discharge (e.g., near pumped wells and leaking channels) where there may be curvature of the potentiometric surface.

8. Error may be introduced because water levels in some wells represent a composite value of hydraulic head over a vertical distance (depending on the screened interval of the well), while the model simulates a single head value that represents an average over the thickness of a model cell.
9. Finally, calibration data quality is influenced by grid design. Water level measurements represent hydraulic head at a point – the well – and simulated heads represent an interpolated average over an entire grid cell. The larger a cell, the greater the potential for differences between a measured water level and the simulated head for the same location. Again, the potential error is greatest for areas in which the water levels vary spatially (i.e., steeper horizontal hydraulic gradients), such as along the Snake River.

Flux data, such as aquifer discharge measurements, may be useful for model calibration. Some reach-gain estimates are available for the Boise and Snake Rivers (Table 5-2). However, the individual contributions from ground water discharge to river and streams, irrigation returns, or the contributions of ground water discharge to drains have not yet been determined (the USBR is compiling these data as part of the TVHP, but the data were not available at the time of model calibration).

Component	Estimated flux (af/yr, 1996)
Discharge to Boise River *Includes direct ground water discharge to the Boise River and flows from drains. The flows from drains includes both irrigation return flows and ground water discharge to drains.*	523,200
Discharge to Snake River *Includes direct ground water discharge to the Snake River and flows from drains. The flows from drains includes both irrigation return flows and ground water discharge to drains. Estimated discharges entering the south side of the Snake River have been excluded.*	290,800
Total discharge to rivers and drains	814,000

From Urban and Petrich (1998)

Table 5-2: Summary of discharge to the Boise and Snake Rivers.

5.5.2. Vertical Gradient Measurements and Observations

Vertical differences in water levels can be used in a model to help calibrate vertical hydraulic conductivity estimates. There is abundant anecdotal information regarding vertical head differences in the Treasure Valley based on observations while drilling wells. Substantial, areally-extensive, subsurface, fine-grained sediments associated with lacustrine depositional environments contribute to confined-aquifer conditions.

However, relatively few reliable vertical gradient data are available. Exceptions include the multiple-completion monitoring wells installed as part of the TVHP. The

two deepest project wells with multiple vertical gradient data (Petrich and Urban, 2004) are in Caldwell and Boise's Municipal Park (Figure 2-5). The vertical head difference in the Caldwell well ranged from 35 to 41 feet (upward gradient) with an average of 37 feet between November 30, 1999, and June 20, 2001. Water levels in the Boise Municipal Park monitoring well ranged from 15 to 61 feet (downward gradient) with an average of 28 feet between July 29, 2002, and April 24, 2003. The lower summer water levels in the deeper Boise Municipal Park well piezometers probably reflect impacts from summer irrigation withdrawals in nearby wells.

Six vertical gradient "observations" were established to help calibrate vertical hydraulic conductivity. These "observations" (Figure 5-5) included (1) real data collected in the Caldwell monitoring well and (2) synthetic values based on anecdotal water level information. Downward water level differences of 35 feet are not uncommon in the eastern portion of the valley; 40-foot upward differences are not uncommon in the central and western portions of the valley (E. Squires, pers. comm., 2000). **Thus, six vertical gradient observation points were specified:** (1) three observations with a difference in 40 feet (upward gradient) between model layers 1 and 4; (2) two observations with 30 feet (upward gradient); and (3) one observation with a downward gradient of 30 feet. All but those shown at location "Grad 6" represented synthetic points[16].

[16] These "observation" estimates were made prior to the construction of the Boise Municipal Park monitoring well. The Municipal Park well indicated vertical water level differences consistent with the assumed 30-foot downward gradient represented by "Grad 6" (Figure 5-5).

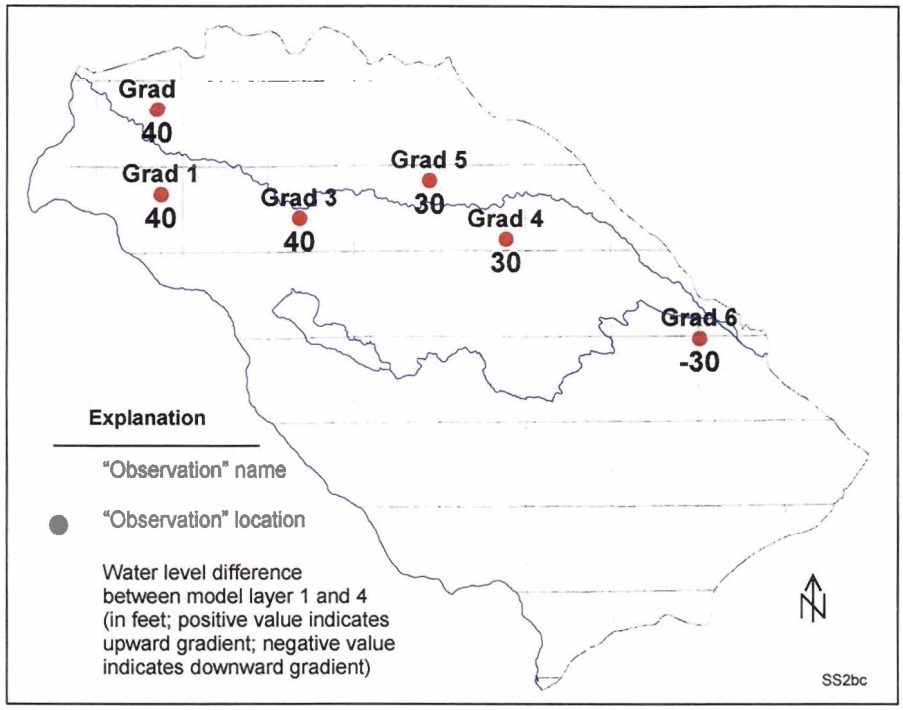

Figure 5-5: Vertical gradient "observation" locations.

5.5.3. Observation Weights

Calibration data were assigned weights in the PEST control file. Theoretically, the weights are inversely proportional to the standard deviations of the field measurements to which they pertain (Doherty, 2000). In this case, all weights for head observations were made equal (with a value of 0.196). All hydraulic head differences were given a weight of 25.0.

The weights for the vertical head differences were a somewhat subjective choice. The vertical head differences were given a substantially greater weight than water levels for the following reasons (Doherty, 2003):

1. There were fewer head differences used in the observation dataset than direct head measurements. A weight of 25.0 allowed the total contribution of vertical head differences to roughly equal the total measurement head differences in the objective function. This allowed better estimation of parameters to which these head differences are most sensitive (e.g., vertical conductivities), as the objective function was not "dominated" by general water level residuals to which these parameters were very insensitive.
2. It is likely that the errors associated with head measurements in different layers are correlated. This is an outcome of both the measurement procedure (including the fact that well reference elevation errors affect both of these heads equally when heads are measured for different layers in the same well)

and "model structural error" (i.e., the inability of the model to represent every detail of system behavior), which tends to affect model-generated heads in overlying layers in the same way. This results in correlation between measured heads in neighboring layers. The variance of a head difference is thus represented by the formula:

$$\sigma^2_{h1\text{-}h2} = \sigma^2_{h1} + \sigma^2_{h2} - 2\sigma_{h1,h2}$$

where the last term is the correlation between the two individual measurements. This can be as large as the variance of the measurements themselves, resulting in a relatively small value for $\sigma^2_{h1\text{-}h2}$, hence requiring that it be assigned a higher weight in the inversion process.

3. The head differences assigned to a particular location within the model domain were intended to represent average head differences over broader area, and thus, can accommodate the use of a higher weight.

5.6. Parameterization using a Pilot Points Regularization Scheme

The use of too many model parameters may lead to numerical instability or non-uniqueness of parameter estimates. To reduce the number of parameters, a model is sometimes divided into a number of zones with assumed parameter homogeneity in each zone. Individual zones might be designated based on common geological or hydrological characteristics. This was attempted in early simulations with the Treasure Valley model. However, there is little basis for areal zone boundaries in the Treasure Valley because of the nature of lacustrine deposition over much of the area. Faulting might represent a basis of zonation, but many fault locations have not yet been identified, and many of the known or suspected faults may not extend throughout the entire stratigraphic sequence. Furthermore, use of zones may result in abrupt parameter transitions for which there is no physical justification.

A related problem with highly parameterized systems (i.e., a large number of parameters) is that individual parameter estimates may show a large degree of spatial variability. Calibration by trial-and-error or with a parameter estimation code may result in individual simulated parameter value variations to accommodate nuances in an observation data set, even though the nuances may merely represent "observation noise."

PEST includes an option for regularization that imposes a smoothing constraint on parameter values (Doherty, 2000). The regularization consists of defining preferred relationships ("prior information") between pairs of parameter values and then attempting to minimize variations from these preferred relationships. In particular, PEST seeks to minimize the (1) measurement component of the objective function (e.g., sum of the squared differences between simulated and observed values) and (2) variation between the preferred relationships necessary to minimize the measurement component of the objective function.

The extent to which parameter smoothing is enforced at the cost of reducing the amount of model-to-measurement misfit is dictated by a "regularization weight factor". The regularization weight factor is calculated by PEST as part of the regularized inversion process. This weight factor can be considered as the Lagrange multiplier in a constrained optimization problem (Doherty, 2003). In this problem, PEST was asked to minimize the "regularization objective function" (i.e., maximize the extent of parameter smoothing) subject to the constraint that the measurement objective function (which is inversely proportional to the degree of model-to-measurement misfit) falls no lower than a certain user-specified value. This value was set high enough to prevent PEST from estimating parameters that reflect observation noise rather than data. Thus, when used in "regularization mode," PEST gave priority in choosing parameter values to those which maximized model-to-measurement fit but did not obtain a better fit than was deemed appropriate.

In general, if a preferred level of fit cannot be obtained because the level of observation noise (or model structural error) is greater than anticipated, PEST will still allow estimation of many parameters. It does so by using the regularization process to obtain the best fit achievable, with as smooth a parameter set as can be calculated to achieve it under numerically stable conditions.

The prior information used in the regularization process has a role in the model calibration similar to that of measured observations, and consequently increases the number of parameters that might otherwise be calibrated because of the higher information content available for use by the calibration process. Regularization can make insensitive parameters (e.g., parameters distant from field measurements) more sensitive because of relationships between parameters that are enforced as part of the calibration process.

Regularization should include a substantial number of relationships between most or all of the parameters involved in the parameterization process and should encapsulate some "preferred state" of the system. Deviations from this preferred state, (e.g., non-zero differences between parameter pairs) are tolerated only to the extent that they allow the model to provide an acceptable fit to field measurements (Doherty, 2000). Homogeneity conditions were the most common preferred state for Treasure Valley model parameters. Prior information was used to keep values for similar parameters (e.g., K_h) within a layer the same unless individual parameter variation was necessary to reduce local measurement residuals.

Regularization can be applied to individual parameters, parameter zones, or pilot points. Calibration using individual parameters, especially if based on individual MODFLOW cells, would generally exceed even the most robust data sets available for most ground water simulations. Calibration using parameter zones, if not based on specific geologic or hydrogeologic characteristics, may result in abrupt parameter value transitions at zone boundaries. Also, the use of a limited number of parameters prevents the parameter estimation process from extracting maximum information from

the dataset used in the calibration process. Calibration with pilot points is a parameterization scheme in which parameter values are estimated for a series of points within the model domain. Values from these points are then spatially interpolated before each model run to individual model cells using kriging or some other spatial interpolation method (Doherty, 2000). Regularization using prior information can then be used to limit the degree of spatial parameter variation between pilot points; this was the approach taken in the Treasure Valley model.

Locations for pilot points used in the calibration of the Treasure Valley model (Figure 5-6) were established using three general criteria. First, pilot points were placed throughout the areas of greatest interest. Second, pilot points were placed in the vicinity of observation points so observation information could guide parameter estimation.

Finally, a number of pilot points were placed near model boundaries to help estimate parameter values near the boundaries. Although lack of observation data in these areas prevented robust estimation of these parameters, values were estimated through the regularized inversion process undertaken by PEST. Parameters represented by these pilot points were estimated on the basis of smoothing relationships between them and parameters closer to the center of the model domain, where more data were available for estimation of parameters.

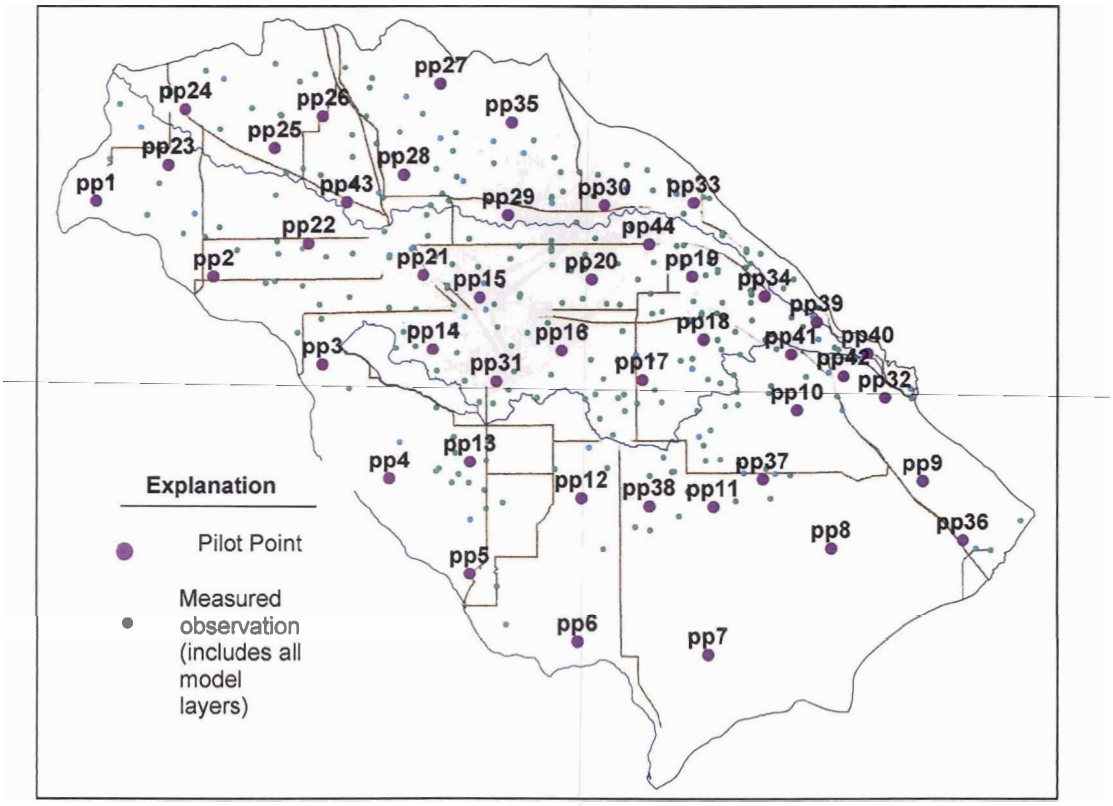

Figure 5-6: Distribution of pilot points.

The use of pilot points and regularization led to the estimation of 270 model parameters (Table 5-3), consisting of K_h and K_v, at each pilot point for model layers 1 through 4. Of these, some parameters were tied together and were calibrated in groups to further reduce the number of parameters requiring estimation. Tied parameters, if all in one area, form *de facto* parameter zones. However, the boundaries are not as discrete as those of the parameter zones normally employed in the calibration process because of the pilot point spatial interpolation. Areas with tied K_v values are shown in Figure 5-7and Figure 5-8. Data describing spatial variations in K_v, especially in deep layers, were unavailable. Geologically, it seemed reasonable to assume that K_v values of fine-grained materials associated with large-scale lacustrine deposition would not vary greatly over some subareas. This reduced the number of parameters requiring estimation to 149 (Table 5-3). This number of parameters is insufficient to define all heterogeneities within the flow system (such as heterogeneities caused by faulting, basalt intrusions, and basalt flows). However, the number of parameters was thought reasonable given the amount and resolution of subsurface data describing large-scale aquifer heterogeneities and the amount of observations available for model calibration.

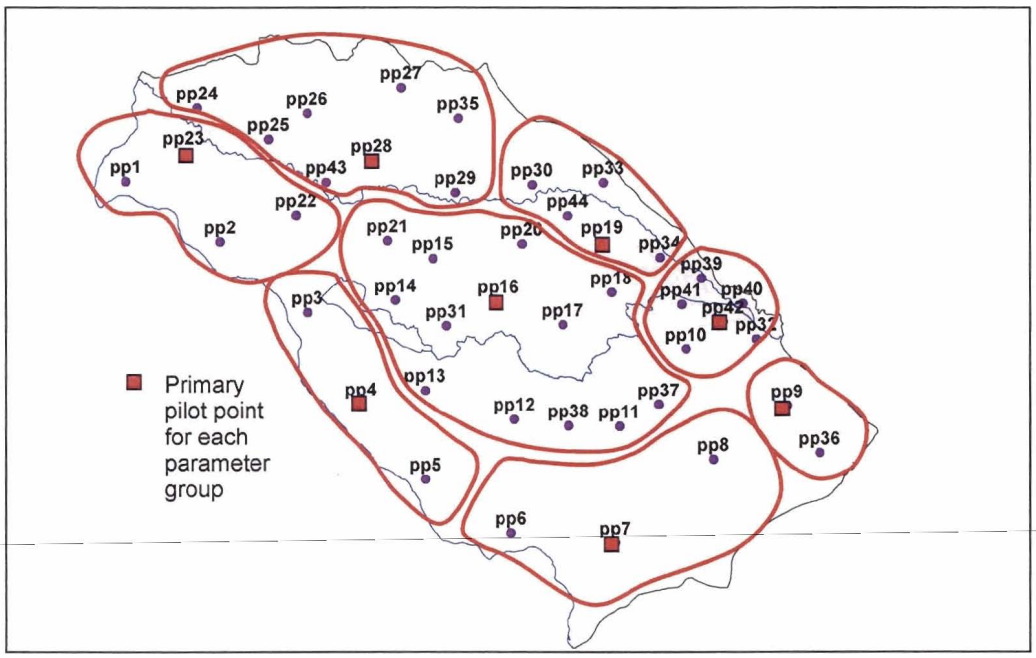

Figure 5-7: Tied K_v parameters in layer 1.

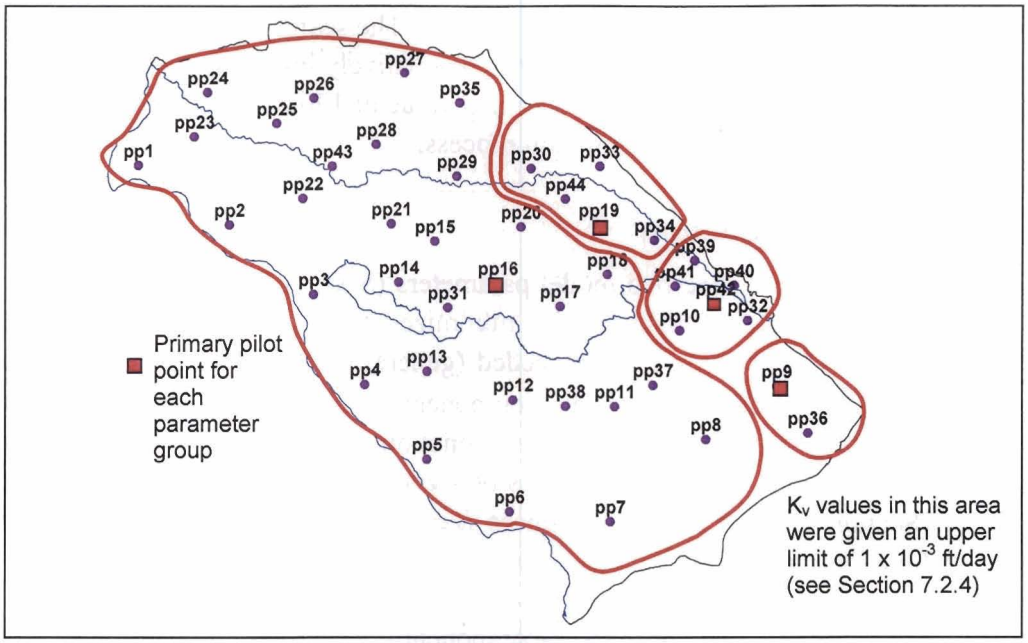

Figure 5-8: Tied K_v parameters in layers 2 and 3.

Parameter	Total Number of Parameters	Number of Tied Parameters	Comments
Layer 1 K_h	44	1	
Layer 2 K_h	44	2	
Layer 3 K_h	44	2	
Layer 1 K_v	44	36	Individual pilot point parameters tied to one of the following: PP4, PP7, PP9, PP16, PP19, PP23, PP28, and PP42
Layer 2 K_v	44	40	Individual pilot point parameters tied to one of the following: PP9, PP16, PP19, and PP42
Layer 3 K_v	44	40	Individual pilot point parameters tied to one of the following: PP9, PP16, PP19, and PP42
Underflow	6		Fixed values
Total Parameters	270	121	

See Sections 4.2 and 8.3.

Table 5-3: Parameter distribution (Simulation *SS2bc*).

There are several spatial interpolation options available with PEST (as separate utilities) for interpolating pilot point parameter values to model cells. Kriging was used for the Treasure Valley model calibration. The kriging parameters (variogram model, range, sill, search radius, transform, etc.) are specified in a control file. Some of these parameters can be estimated through the calibration process if desired, or they can be specified in the calibration. In this case, the variogram was fit using an

exponential model with a nugget of zero. The search radius was estimated through the calibration process but was found to be relatively insensitive. Thus, in most PEST runs the search radius was assigned a fixed value of 150,000 feet. The variogram sill has no effect on the spatial interpolation process.

5.7. Objective Function

PEST adjusted specified model parameters (Section 5.4) on an iterative basis until the primary objective function was minimized to a specified value or until a specified number of iterations were exceeded (generally 50 iterations). The primary objective function (Φ) consisted of two components: (1) the regularization objective function and (2) the measurement objective function. The regularization component consisted of the sum of squared differences between parameter differences and preferred values (Section 5.9) for these differences (zero in all cases). The measurement objective function consisted of two sub-components. The first sub-component consisted of the sum of the squared differences between measured and simulated water level observations. The second sub-component (the vertical gradient component) consisted of the sum of the squared differences between measured and simulated vertical head differences.

Targets set for the objective function in regularization mode (variable *PHIMLIM*) influenced the base calibration. Setting the target too low forced PEST to manipulate parameter values at pilot points by creating heterogeneities into the model domain that may or may not exist. This would be done at the expense of reducing the regularization constraints (increasing the regularization component of the objective function). There are two ways to limit the amount of unrealistic parameter distortion required to calibrate the model. The first is to set an objective function target that is not too low (a judgment call based on initial simulations). The second is to limit the number of iterations that PEST can use to meet the objective function target.

5.8. Initial Values

Initial parameter values are shown in Table 5-4. The initial values for K_v and K_h are not particularly relevant because the simulations are conducted under steady-state hydraulic conditions. The upper and lower parameter value limits were used to constrain the calibrated parameter values to "reasonable" values based on an anticipated mix of aquifer sediments within a given layer thickness. The upper limits on parameter values are consistent with gravel sediments (Freeze and Cherry, 1979). The lower limits are consistent with silt sediments; the lower limit value for K_v is consistent with marine clay.

5.9. Prior Information

Prior information consists of preferred relationships between pairs of parameter values (Section 5.6). The basis for these relationships is information that is not necessarily represented in other calibration observations. For instance, differences between individual K_v values may be minimal over large areas of lacustrine sediments. Prior information indicating that K_v values may be the same throughout a given area adds information to the model calibration that is not added in other ways. PEST (Doherty, 2000) attempts to minimize the deviation from the preferred relationships, deviating only if necessary to reduce the primary measurement component of the objective function.

Parameter	Units	Initial Value	Lower Limit	Upper Limit	Comment
Horizontal hydraulic conductivity (K_h)	ft/day	10	0.001	1,000	Fixed, tied, or log value[(a)]
Vertical hydraulic conductivity (K_v)	ft/day	0.1	1×10^{-8}	1,000	Fixed, tied, or log value[(a)]
Range[(b)]	ft	150,000	50,000	2×10^6	Fixed
Underflow[(c)]	ft^3/day	5,000	100	50,000	Fixed
Notes:					
(a) See Table 5-3.					
(b) Refers to the search radius used in calculating variograms for spatial interpolation of pilot point parameter values (Doherty, 2000).					
(c) See Figure 3-5 for locations of underflow cells.					

Table 5-4: Initial parameter values.

The primary objective function contains measurement and regularization components (Section 5.7). At the beginning of a calibration, the regularization objective function began with a value of zero and increased as prior information relationships were altered to reduce the measurement objective function. Prior information components (Table 5-5) are listed in the PEST control file (**.pst,* Section 5.10). The objective function values were printed for each PEST iteration in its run record file (**.rec*).

Prior Information (preferred-state homogeneity relationships)	Prior Information Variable Names	Number of Prior Information Relationships
Attempt to keep K_h values in layer 1 the same	ppreg1 – ppreg946	903
Attempt to keep K_h values in layer 2 the same	ppreg947 – ppreg1892	861
Attempt to keep K_h values in layer 3 the same	ppreg1893 – ppreg2838	861
Attempt to keep K_h values in layer 1 the same as those in layer 2	pvh1 – pvh44	42
Attempt to keep K_h values in layer 2 the same as those in layer 3	pvhb1 – pvhb44	42
Attempt to keep keep K_v values in layer 2 the same as those in layer 3	pvvb16, pvvb42 – pvvb44	5
Attempt to keep K_v values in layer 1 the same	Pvlat13 – pvlat39	27
Attempt to keep K_v values in layer 2 the same	Pvlat4 – pvlat6	3
Attempt to keep K_v values in layer 3 the same	Pvlat10 – pvlat12	3
	Total	2,747

Table 5-5: Prior information in steady-state simulations.

5.10. Calibration Input Files

PEST requires three types of input files: template files, instruction files, and the PEST control file. PEST uses one template file (**.tpl*) for every model input file that contains parameter values to be adjusted through the parameter estimation process. Instruction files (**.ins*) guide PEST to locations in model output files for reading specific output data. The PEST control file (**.pst*) supplies the names of all template and instruction files and corresponding model input/output files. The control file also gives PEST the model name (or a batch file that runs one or more models or utilities), initial parameter estimates, observations, prior parameter information, and PEST variables that control the calibration.

PEST can be used to calibrate any model using ASCII input and output data. Consequently, files used by the calibration process include those that are specific to the model and specific to the particular calibration exercises that are being undertaken. A calibration includes files that are unique to the particular simulation being calibrated. Files used for this Treasure Valley steady-state model calibration are listed in Appendix D. Some of the files are required by the PEST code, some are MODFLOW or GMS files, and some are utility files. More detailed file descriptions of the PEST files are available in the PEST manual (Doherty, 2000). Files produced in a Treasure Valley model calibration are listed in Appendix E.

5.11. Processing Calibration Results

The calibration process results in a number of PEST and model files (Appendix E). The steps taken in processing a typical calibration run are outlined in Table 5-6.

	Process	File
1.	Check for "dry" model cells.	MODFLOW output file (**.out*)
2.	Check percentage discrepancy in the volumetric budget .	
3.	Load head values into GMS, view in map and cross-section views.	MODFLOW head file (**.hed*)
4.	Review optimization record; check objective function ($\phi_{measurement}$ and ϕ_{regul}) values, check "optimization results".	PEST run record (**.rec*)
5.	Review highest and lowest eigenvalues *As a rule of thumb, the highest and lowest values should be within 7 orders of magnitude (Doherty, pers. comm., 2001).*	
6.	Review high eigenvalues and identify correlated parameters. *Eigproc.exe is a utility that provides eigenvector values for high eigenvalues.*	PEST run record (**.rec*); eigproc.exe
7.	Review parameter sensitivity values. *The larger the sensitivity value, the more sensitive the calibration is to the parameter, and hence, the better the estimate of that parameter is likely to be. Conversely, the smaller the number, the less sensitive the calibration is to this parameter, and hence, more uncertainty will normally be associated with estimates of that parameter.*	PEST parameter sensitivity file (**.sen*)
8.	Plot head values. *This can be done in a variety of ways. The head values illustrated in this report were loaded into GMS, exported as ASCII data files, loaded into "HeadProcessor.xls" in which values are distributed to separate worksheets by layer, and then graphed in Surfer™ (eliminating all values of z = -999).*	**.hed* HeadProcessor.xls Runname Heads.xls Sim Head.lvl
9.	Plot residual values. *1. Copy the residual data from run record file into SS residuals.xls, process the residual data, and create Surfer™ grid files. Review "print page" data.* *2. In Surfer™, open Grid, Data, select file, set columns, open Grid Blanking, select Active.bln, save as grid file (e.g., run_name L# res.grd).* *3. Map contours in Map menu; use "ResCont.lvl" for contour fills.*	PEST run record (**.rec*) SS Residuals.xls
10.	Plot K_h and K_v distributions. *The batch file "real2surf.bat" runs "real2srf.exe, which uses the *.ref files created during a MODFLOW run to create .grd files for Surfer™. Contour maps can then be created with Surfer™ using the "K Distribution.lvl" file to color-fill the contours.*	real2surf.bat runs real2srf.exe, requiring the following files: kh1.in; kv1.in; kh2.in; kv2.in; kh3.in; kv3.in tvm.spc kh1.ref; kv1.ref; kh2.ref; kv2.ref; kh3.ref; kv3.ref

Table 5-6: Simplified outline for simulation/calibration review.

6. MODEL ASSUMPTIONS AND LIMITATIONS

There are many assumptions, limitations, and potential errors associated with the numerical simulation of ground water flow (Table 6-1). These assumptions and limitations should be kept in mind when reviewing model results.

There are several specific potential sources of error in this Treasure Valley model. First, there is a high degree of geologic uncertainty throughout the system. Many strata, although substantial, are not spatially continuous over the model domain. While it is clear that there are shallow and deep aquifers, with markedly different flow characteristics, residence times, and recharge rates, there are not clearly identifiable strata that separate these aquifers over the entire model domain. There are some areas within the model domain with little or no hydrogeologic data (e.g., southern Ada County) because few or no wells have been drilled in these areas. Horizontal and vertical aquifer heterogeneity is seen in lithologic, chemical, and aquifer test data. In addition, faulting can and does influence ground water flow. The locations of some faults are known or have been inferred. Offsets of some of the faults appear to be greater than 800 feet, but the hydraulic influences of most faults are unknown.

Second, flux rates at boundaries are unknown. There is substantial uncertainty in the estimates of underflow into the model domain. Streambed and drain conductances are unknown, as are lakebed conductance values.

Third, parameter uncertainty is high in some portions of the model domain because of the lack of observation data (again, because there are few wells in some portions of the model domain). In general, there are fewer deep wells than shallow wells, and the distribution of deep wells is limited primarily to more highly populated areas. This limits the number of observation points for deeper aquifers in some portions of the model domain.

Observation data were collected from a variety of wells. Some are clearly influenced by ground water pumping, either from within the observation well or from nearby wells. The elevations of some of the wells are known only within general limits (e.g., ±10 feet). Spatial discretization of areas with substantial variations in potentiometric surfaces (e.g., drawdown) can lead to model errors. Some water level measurements from shallow wells, if influenced by surface drainage, may lead to model calibration errors (these were removed where surface influences were recognized).

The water table elevation in some parts of the model domain is controlled by the elevation of land surface. The water table elevations in these areas do not contain information for estimating hydraulic conductivities in these areas, leading to high uncertainty in local K_h estimates.

Category	Potential Limitations, Assumptions, and Errors
Potential conceptualization errors	Incorrect flow system conceptualization
	Incorrect application of numerical approach
	Incorrect layer and/or grid definitions
	Errors in assumed boundary conditions
	Errors in parameter regularization assumptions
Basic ground water flow assumptions required for using MODFLOW	Ground water flow does not meet Darcian flow assumptions, which include the following: flow is laminar, fluid is incompressible, fluid density is constant, gravitational acceleration is constant, and water movement is caused mechanical (e.g., hydraulic) gradients.
	Borehole storage is negligible.
	There is no change in hydraulic characteristics with respect to degree of saturation.
Limitations and assumptions associated with the discretization of space and time	Grid resolution is inappropriate for model objectives.
	Simulated head values are based on heads in surrounding nodes; steeply sloping and/or non-linear heads (or other dependent variable) and may not be accurately represented by finite difference grid.
	Aquifer characteristics, inflows and outlows, and other properties are assumed to be constant within a grid cell.
	Flux characteristics are assumed to be constant within time steps.
	Hydraulic properties are assumed to be constant in time.
	Wells are assumed to be fully penetrating in assigned layers.
	Simulated observations are averaged over too large an area (this may be a concern if water level observations are based on wells experiencing substantial drawdown). Model grid is not fine enough to reproduce head curvature in the vicinity of lines and points of groundwater extraction and inflow.
Potential causes for numerical errors	Model cells go dry
	Incorrect solution closure criteria
	Truncation error, roundoff error
Potential model input errors	Errors in recharge package inputs (e.g., data errors, interpolation errors, etc.)
	Errors in well package inputs (e.g., data errors, interpolation errors, etc.)
	Errors in drain package inputs (e.g., data errors, interpolation errors, etc.)
	Errors in river package inputs (e.g., data errors, interpolation errors, etc.)
	Errors in general head boundary package inputs (e.g., data errors, interpolation errors, etc.)
Potential observation measurement errors	Physical measurement errors
	Water levels influenced by pumping in observation well
	Water levels influenced by nearby pumping
	Water levels observation based on approximated or incorrect well elevation

Table 6-1: Sources of possible error leading to parameter uncertainty.

The nature of the steady-state simulations also contributes to parameter uncertainty. Flux data (e.g., recharge, withdrawals, etc.) are averaged over an entire year, even though the stress may occur only during one season (e.g., irrigation season). Observation data for the steady-state simulations also consisted of averaged water levels based on 1996 spring and fall measurements.

Calibration errors can result from incorrect parameterization, assignments of pilot point locations, and parameter regularization relationships. Parameter non-uniqueness and/or correlation can also lead to calibration errors. Some indication of parameter uncertainty is given during the calibration process. PEST output includes parameter sensitivity values, which are strongly influenced by parameter correlation. However, it is important to remember that some parameter values may be highly uncertain but not relevant to a particular model prediction. Predictive analysis (Doherty, 2000) is probably a more useful approach (Section 9) for evaluating a scenario in the context of various parameter uncertainties.

It is also important to note that no ground water model can be calibrated without some form of implicit or explicit regularization. Regularization is the process by which model parameterization is simplified to the extent that parameter estimation can take place. Where zones are used, regularization is implicit. Where PEST's regularization functionality is used, regularization is explicit, with regularization constraints enforced to the extent necessary (through calculation of an appropriate regularization weight factor). In either case, the complexity of the parameter estimation problem is reduced to a level that is compatible with the information content of the data used for calibration. The less observation data, the greater the role of regularization in the calibration process.

The parameter field that results from the calibration process cannot be considered the "true" hydraulic property field prevailing within the model domain – even if the fit between model outputs and field data is perfect. It is one of many possible parameter fields that could fit the data. Where PEST's regularization functionality is used, it is the smoothest of all these fields; where zones are used, it is the "blockiest" field. In either case, the calibrated field cannot reflect small- or even medium-scale heterogeneity of true aquifer hydraulic properties; these are simply beyond the ability of the calibration process to capture.

In general, where model predictions depend on regional or averaged hydraulic properties, this model's performance should be relatively good. Where model predictions depend on local detail, use of this model may result in error or a higher degree of uncertainty.

7. CALIBRATION RESULTS

7.1. Introduction

This section presents a set of model calibration results for steady-state hydraulic conditions. Calibration results are presented in the form of (1) objective function values and other PEST output, (2) mass balance results, (3) comparisons between simulated and observed water levels, (4) comparisons of simulated and observed potentiometric surfaces for each model layer, (5) spatial distribution of K_h and K_v values, (6) distribution of residuals (difference between measured and simulated observations) values, and (7) simulated vertical ground water flow rates.

7.2. Steady-State Calibration Results

Model construction, testing, and calibration invariably result in a large number of simulations. The simulation[17] described in this section was the product of many model development runs and was considered a "base run" for comparison with subsequent predictive analysis simulations.

The base run calibration consisted of 50 PEST iterations and approximately 14,300 individual model runs. Values for objective function (Φ) components are listed in Table 7-1. The largest residuals occurred in the lowest layers. The highest and lowest eigenvalues are within 6 to 7 orders of magnitude, as they should be (Doherty, pers. comm., 2002). A comparison between simulated and observed hydraulic heads is shown in Figure 7-1. The PEST calibration could have been allowed to continue beyond 50 iterations, although attempts to match observation data more closely would have begun to result in simulated heterogeneities that may or may not have corresponded with actual aquifer properties.

7.2.1. Mass Balance

The mass balance for the calibration is shown in Table 7-2[18]; 1996 water budget (Urban and Petrich, 1998) values are listed for comparison in Table 7-3. The well and recharge components in the model are specified values; constant head, river leakage, and Lake Lowell seepage are head-dependent values. The total simulated inflows (1,036,212 af/yr) are similar to the total estimated 1996 inflows (1,035,000 af/yr) (Urban and Petrich, 1998). The total simulated outflows are virtually the same as the simulated inflows (as would be expected with conservation of mass in the steady-state

[17] Simulation *SS2bc*.

[18] In this and similar tables, the difference between inflows and outflows provides an indication of numerical error. Under steady-state hydraulic conditions, the difference between inflows and outflows should be zero. Any deviation from zero indicates some numerical error within the simulations.

model simulations), while the estimated 1996 outflows are approximately 36,000 af/yr less. The 36,000-af/yr difference is within the estimated error of water budget components, and therefore probably not meaningful.

Base Run Results (based on observations with PEST weights greater than zero)				
Contribution to Φ from heads	3,220			
Contribution to Φ from regularization	3,150			
Contribution to Φ from gradients	56.46			
Highest eigenvalue	1.176			
Lowest eigenvalue	1.89×10^{-7}			
Number of PEST iterations	50			
Number of MODFLOW runs	~14,300			
Run Statistics				
	Total	**Layer 1**	**Layer 2**	**Layers 3 and 4**
Maximum positive residual	73.59	62.86	57.05	73.59
Minimum negative residual	-67.08	-67.08	-52.48	-44.14
Average absolute residual	14.62	12.42	16.01	23.29
Median absolute residual	9.49	8.74	9.714	19.03
Number of values	200	140	29	31

Table 7-1: Run information for steady-state simulation (base simulation).

7.2.2. Potentiometric Surfaces

Comparisons between potentiometric surface contours based on simulated and observed water level measurements are shown in Figure 7-2 through Figure 7-5. Potentiometric surface contours based on observed data are limited to those areas within the model domain containing actual data. The simulated potentiometric surface contours extend throughout the model domain because they are based on simulated head values in each active model cell.

The potentiometric surface contours based on simulated and observed data are in closer agreement in areas where there are abundant data than in areas of less data. For instance, potentiometric surface contours are closer in the central portion of the valley than in the southeastern portion of the model domain. The general agreement between simulated and observed head values are shown in Figure 7-1.

It is important to note that the contours drawn in Figure 7-2 through Figure 7-5 are drawn from different data. The observation heads were drawn from observation data (the locations of these data are shown in each plot). Contours drawn a long distance from an observation point (e.g., near model boundaries) are likely in error. The model-generated heads are calculated at every cell, although the uncertainty of hydraulic parameters in areas void of observation points also may be high. These contours should be compared with caution, especially in areas void of observation points.

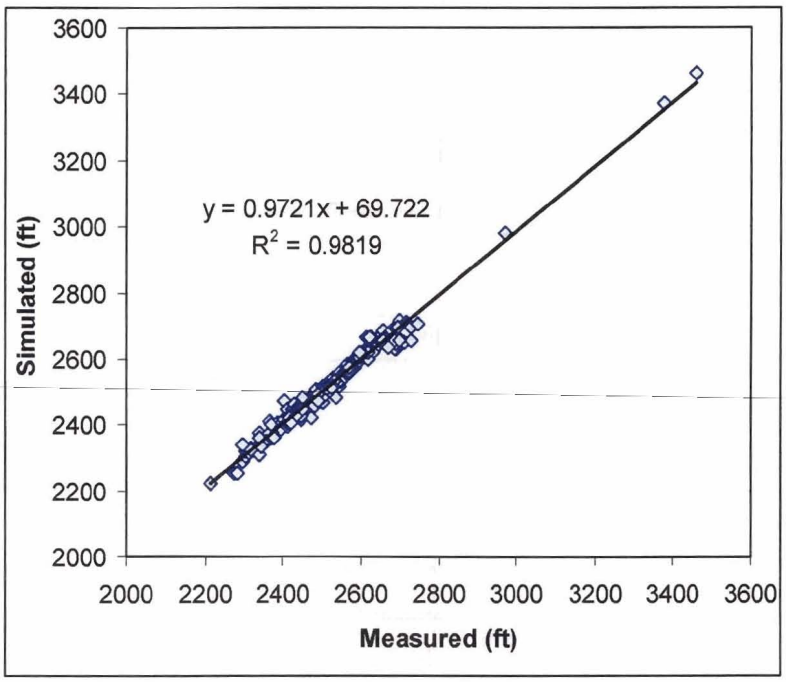

Figure 7-1: Simulated versus measured hydraulic head observations, steady-state hydraulic conditions (base simulation).

Base Simulation Inflows	Flux (ft3/day)	Flux (af-yr)
Constant head (Snake River)	28,891	242
Wells (underflow)	108,000	905
Drains	-	-
River leakage (Boise River)	5,784,138	48,467
Head-dependent boundaries (Lake Lowell)	1,537,895	12,886
Recharge (excluding recharge from underflow, wells, drains, river leakage, and head-dependent boundaries)	116,205,088	973,711
Total Inflows	123,664,008	1,036,211
Base Simulation Outflows		
Constant head (Snake River)	17,350,556	145,385
Wells	23,076,956	193,368
Drains	36,667,716	307,248
River leakage (Boise River)	46,486,872	389,525
Head-dependent boundaries (Lake Lowell)	81,962	687
Recharge	-	-
Total Outflows	123,664,064	1,036,212
Summary		
Inflows–Outflows	(56)	(0)
Percent discrepancy	0.00	0.00

Table 7-2: Base simulation mass balance.

1996 Water Budget – Inflows	Annual flux (af-yr)
Canal seepage, seepage from rivers and streams, flood irrigation and precipitation, recharge by other uses, and recharge from rural domestic septic systems	1,008,000
Seepage from Lake Lowell	19,000
Underflow	8,000
Total Inflows	1,035,000
1996 Water Budget – Outflows	**af-yr**
Domestic and industrial withdrawals, municipal irrigation, self-supplied industrial, agricultural irrigation, rural domestic withdrawals, and stock watering	199,000
Discharge to rivers and streams	800,000
Total Outflows	999,000
Difference	+36,000

Table 7-3: 1996 Water budget components (Urban and Petrich, 1998).

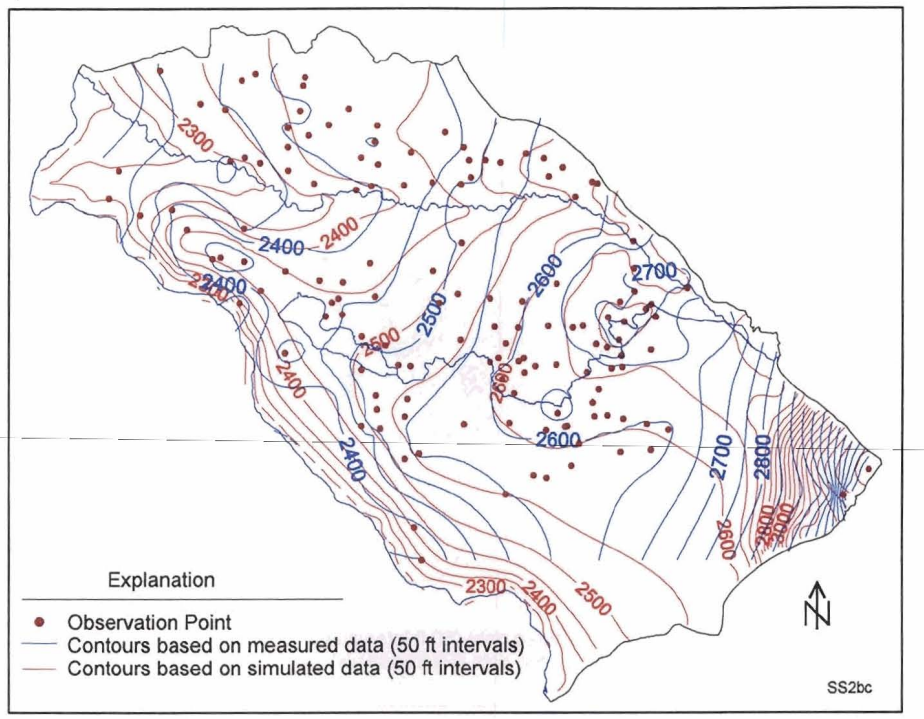

Figure 7-2: Simulated and observed potentiometric contours, layer 1.

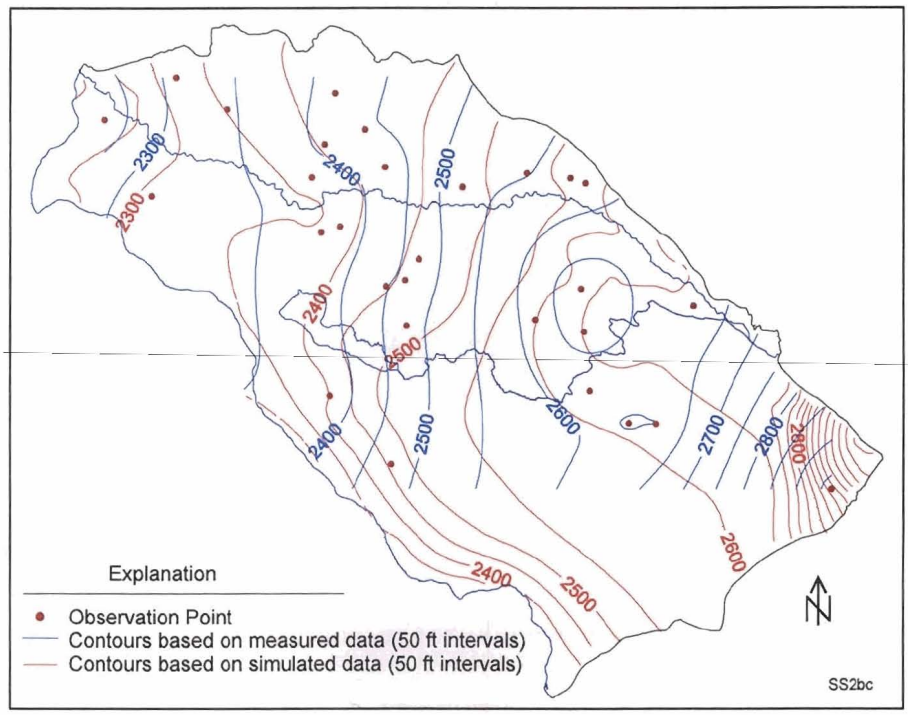

Figure 7-3: Simulated and observed potentiometric contours, layer 2.

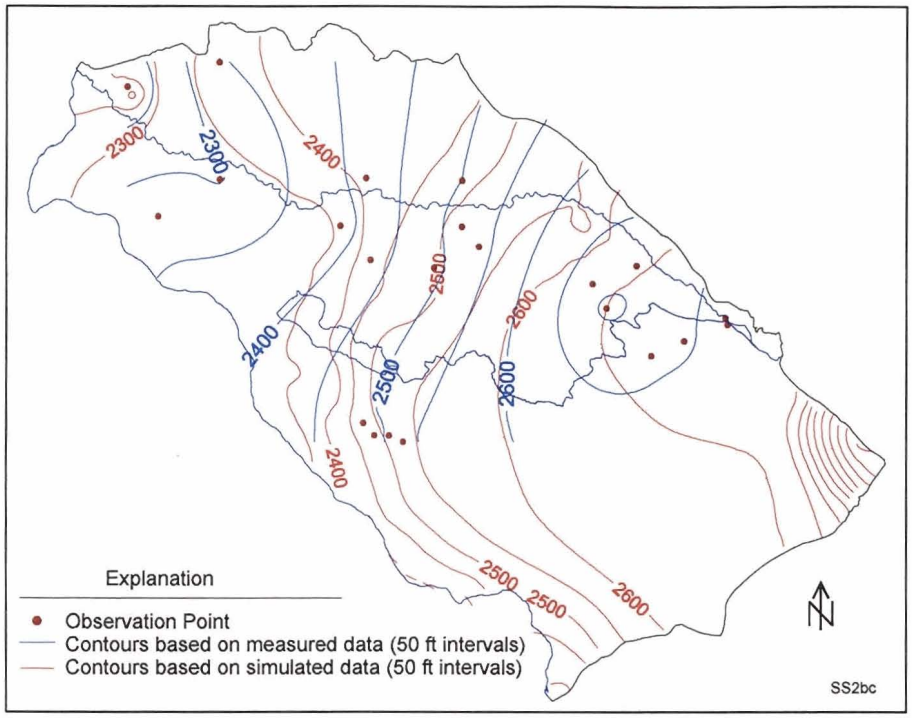

Figure 7-4: Simulated and observed potentiometric contours, layer 3.

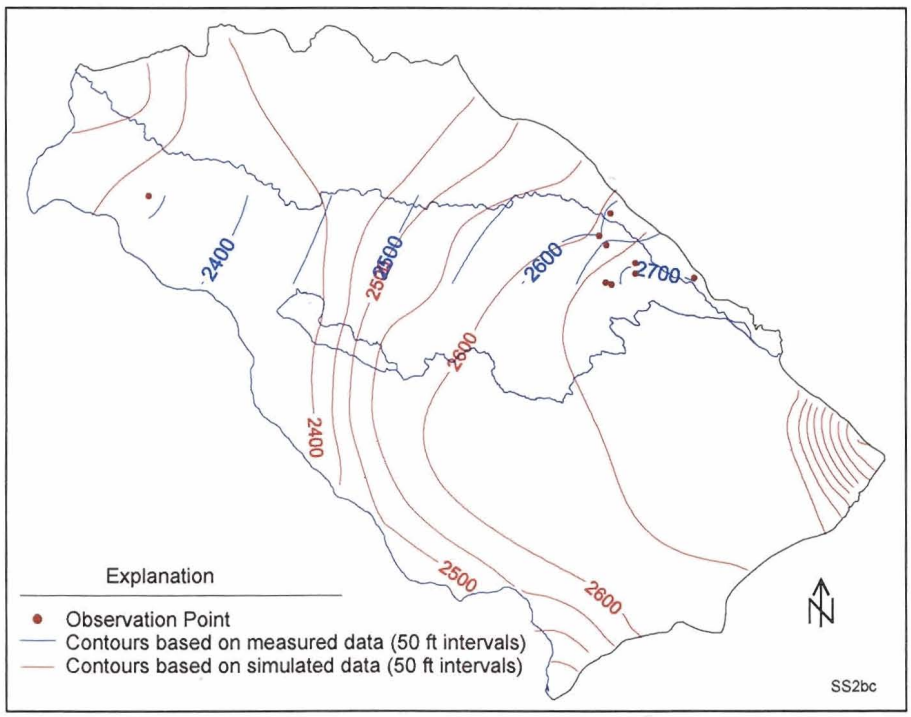

Figure 7-5: Simulated and observed potentiometric contours, layer 4.

7.2.3. Spatial Distribution of Residuals

The distribution of residuals between simulated and observed head values is another measure of calibration results. Two areas of positive residuals occurred along the northeastern and southwestern boundaries (Figure 7-6). Negative residuals occurred in one area in the northern portion of the model (based mostly on 2 to 3 observations) near the New York Canal and west of Lake Lowell. Residual values in layers 2, 3, and 4 show more spatial bias; there are larger areas of positive or negative residuals. In addition, there are several areas (e.g., the north central portion of the model domain) where observations with positive and negative residuals are located in close proximity. The residuals may reflect differences in observed water levels, errors in estimated well elevations, local heterogeneities (e.g., faults) not expressly incorporated into the model, or differences in local drawdown conditions. The residuals in these areas may also reflect averaged-cell characteristics. PEST attempts to reconcile the differences during the model calibration but ends up estimating hydraulic parameter values that lead to minimized residuals.

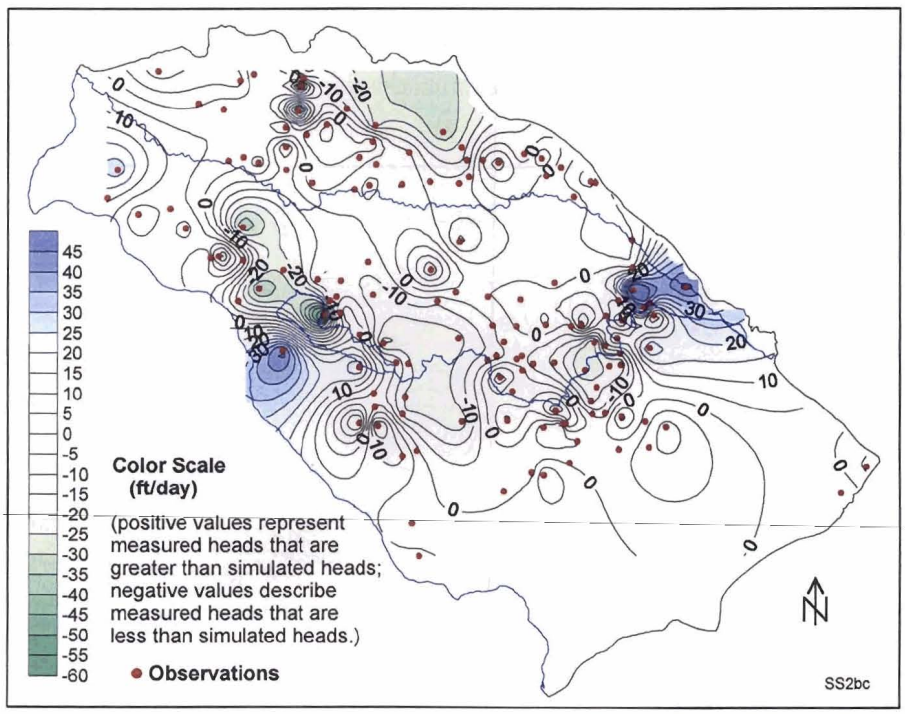

Figure 7-6: Base simulation residuals, layer 1.

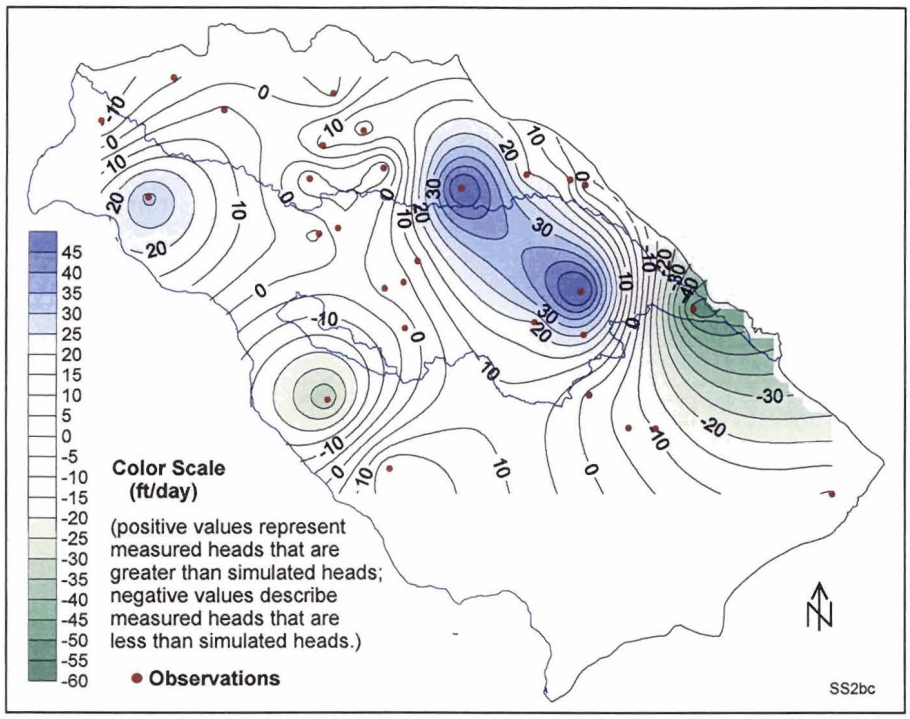

Figure 7-7: Base simulation residuals, layer 2.

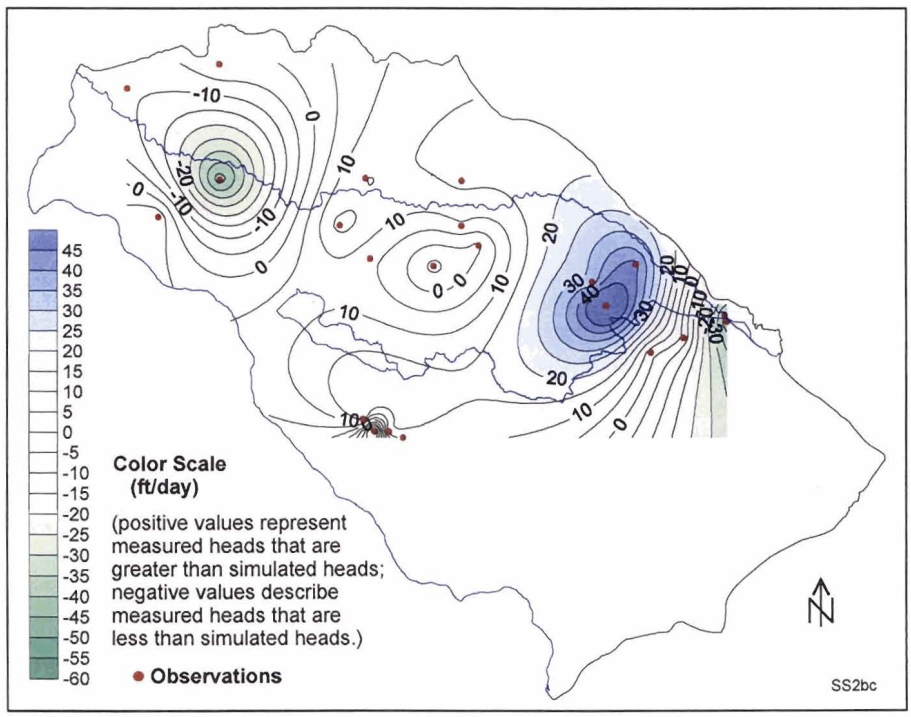

Figure 7-8: Base simulation residuals, layer 3.

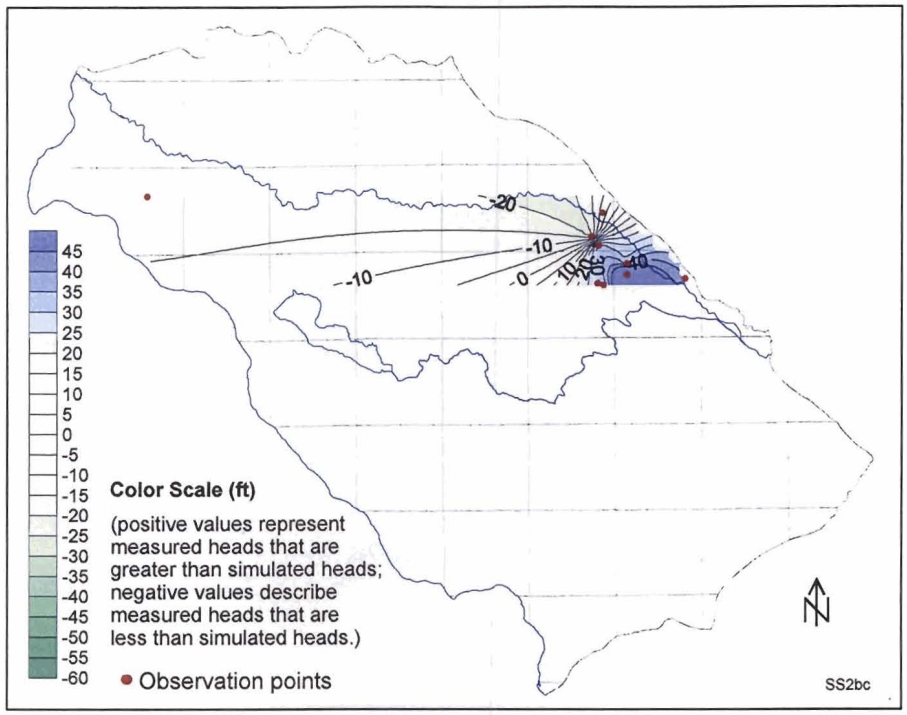

Figure 7-9: Base simulation residuals, layer 4.

It should be noted that the degree of spatial correlation exhibited by the residuals is not cause for concern (Doherty, 2003), in spite of the commonly-held belief that residuals should be uncorrelated at the completion of the model calibration process (see, for example, Anderson and Woessner, 1992). In fact, wherever regularization is used in the solution of the inversion problem (whether this be explicitly through PEST's regularization functionality or implicitly through the use of zones), model-to-measurement residuals will show spatial correlation (Christensen and Cooley, 2002; Nolet et al., 1999).

7.2.4. Estimated Parameter Value Distributions

The distribution of K_h and K_v values within the model domain are shown in Figure 7-10 through Figure 7-15. The K_h and K_v values for layers 3 and 4 are the same because the parameters are tied together (Section 5.6).

Several patterns emerge from the PEST-calibrated K_h and K_v values. First, the calibration suggested a higher K_h zone in the Boise vicinity, especially in layers 3 and 4. This corresponds with coarse-grained alluvial and fluvial sediments present in this area. The higher K_v values extend toward the central portions of the basin in layers 3 and 4, which appear to correspond with the occurrence of fluvial deltaic sediments. The higher K_h values also extend south and southeast of the Boise area, which may be unsupported because of the lack of observation points in this portion of the model domain.

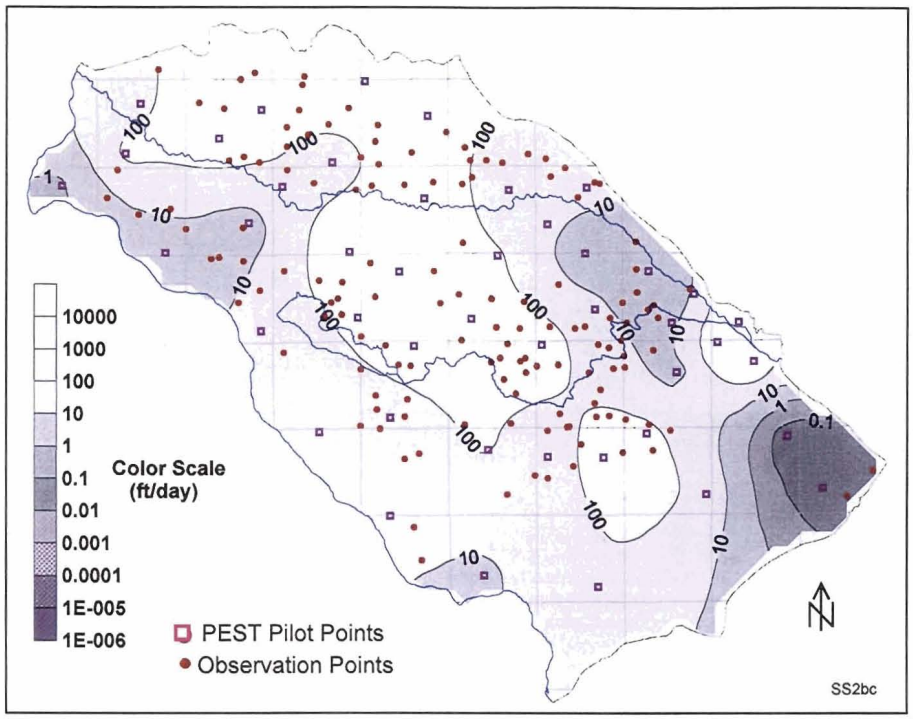

Figure 7-10: Estimated horizontal hydraulic conductivity distribution, layer 1.

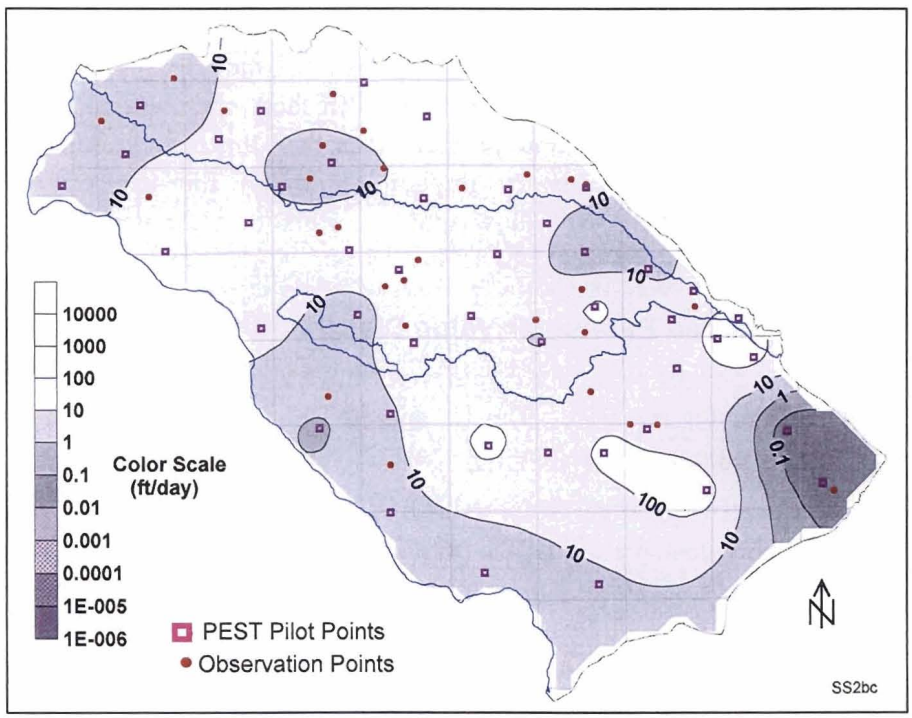

Figure 7-11: Estimated horizontal hydraulic conductivity distribution, layer 2.

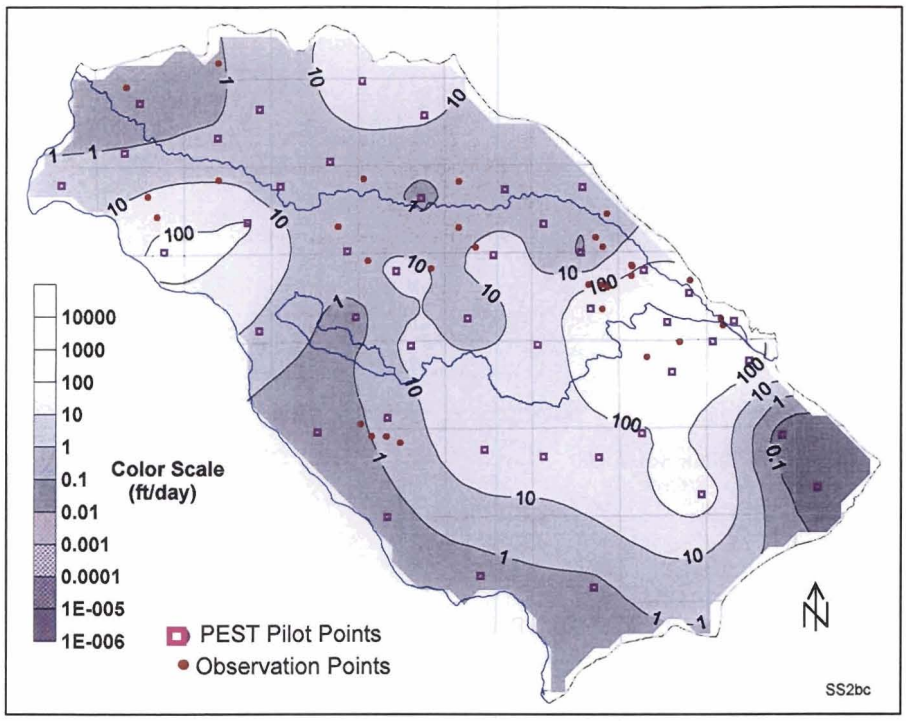

Figure 7-12: Estimated horizontal hydraulic conductivity distribution, layers 3 and 4.

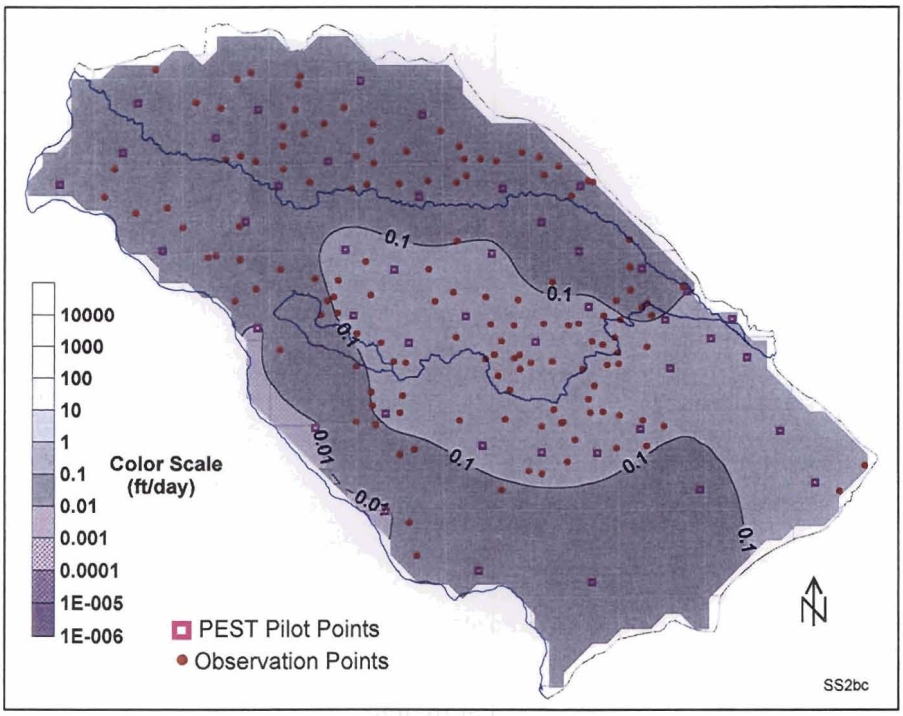

Figure 7-13: Estimated vertical hydraulic conductivity distribution, layer 1.

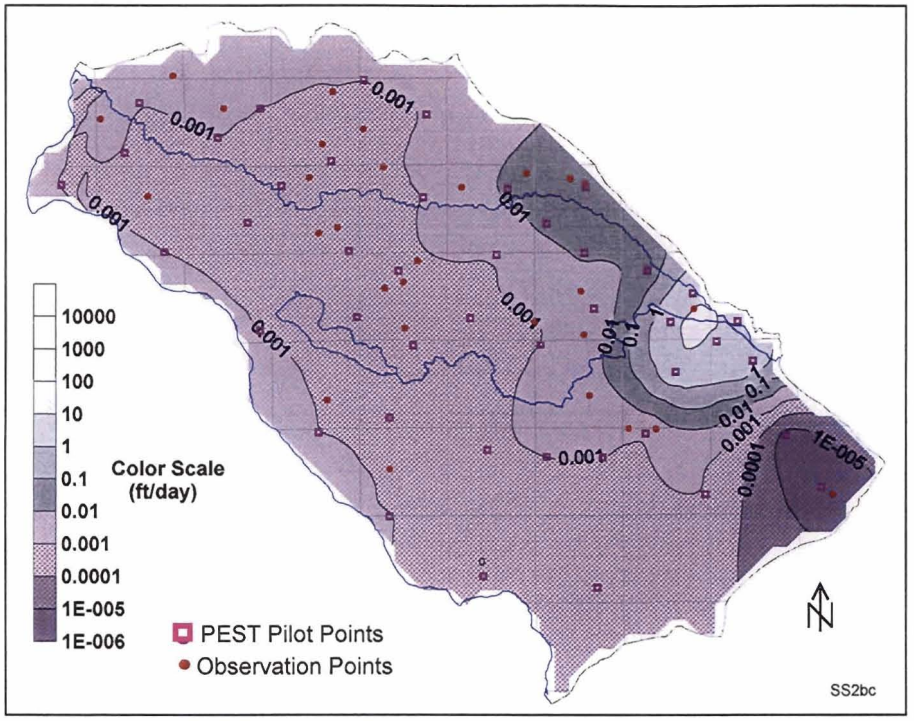

Figure 7-14: Estimated vertical hydraulic conductivity distribution, layer 2.

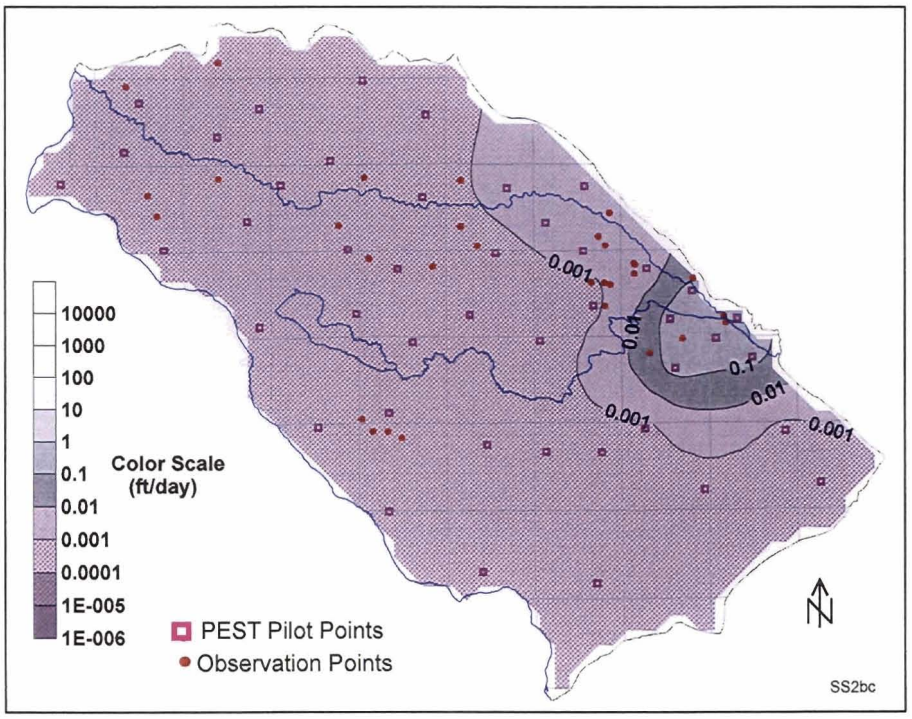

Figure 7-15: Estimated vertical hydraulic conductivity distribution, layers 3 and 4.

Second, low K_h values are seen in the far eastern portion of the model domain. This represents the model's attempt to maintain ground water levels that are substantially higher in this area than other parts of the model domain.

Third, a low K_h zone appears in the northwest Boise–Eagle area. This appears to correspond with fine-grained sediments (clay and silt) that are present in this area (such as those profiled in the TVHP#1 monitoring well).

Next, calibrated K_v values are lower in the central and western portions of the model domain than in the Boise area. The maximum K_v values were limited to an upper value of 1×10^{-3} ft/day in layers 2 through 4 in a large portion of this area (Section 5.4 and Figure 5-8), which is consistent with the extensive layers of lacustrine clays in this area. Upper limits for simulated K_v values in the eastern portion of the model domain (e.g., Boise area) were much higher (e.g., 1×10^{3} ft/day), allowing the model to simulate greater downward movement of water to deeper zones (although PEST-estimated K_v values remained below 10 ft/day). The higher K_v values are consistent with coarser-grained silts and sands in this area.

Finally, it is important to recognize that simulated parameter values are much less certain at the model boundaries, especially in areas of few data. Parameters in these areas were generally less sensitive than in areas with more data and may be highly correlated with one another. In fact, estimation of parameters in this area is only possible through deployment of PEST's regularization functionality.

7.2.5. Potentiometric Cross-Sections

Cross-sections of potentiometric contours in model row 18 and column 36 (Figure 7-16) provide an indication of hydraulic gradients at depth. These potentiometric contours should, however, be read with caution because the ground water flow directions (based on observed gradients) may not be along the x-y axes shown in the cross-sections.

Several general flow characteristics are evident in the cross-sections. First, there is a general upward gradient over much of the central portion of the basin. A ground water flow divide is evident in the north-south cross-section in the vicinity of the New York Canal. Simulated ground water flow (in the north-south cross-section) moves from the New York Canal area toward the Boise River, but deeper (simulated) ground water flow has a more southerly component toward the Snake River.

7.2.6. Flooded Cells

The water table is very close to ground surface in some parts of the basin, such as the central portion in which substantial flood irrigation occurs. Irrigation system drains were installed to collect and remove shallow ground water from these areas. Simulating ground water flow in these areas resulted in a number of "flooded" cells, as indicated in Figure 7-17. However, the median residuals in this calibration run, at 9.5 feet, is very close to the difference in drain elevation and ground surface (10 feet,

Section 4.4). Therefore, it is not surprising that some cells appear to be flooded. This simulated flooding represents a natural process (drainage) and is not cause for concern. Theoretically, increasing drain conductances should reduce cell flooding (if simulated ground water levels are below those of the drains), but excessively high drain conductances can lead to numerical instability.

7.2.7. Vertical Ground Water Flow Rates

The vertical flow rates into and out of each model layer were estimated from the steady-state simulations (Table 7-4). The total amount of vertical downward flow through the aquifer system is a small portion of the total amount of recharge from ground surface to the uppermost aquifer (Table 7-3). Most of the difference between downward and upward flux between the lower model layers was attributed to extraction by wells.

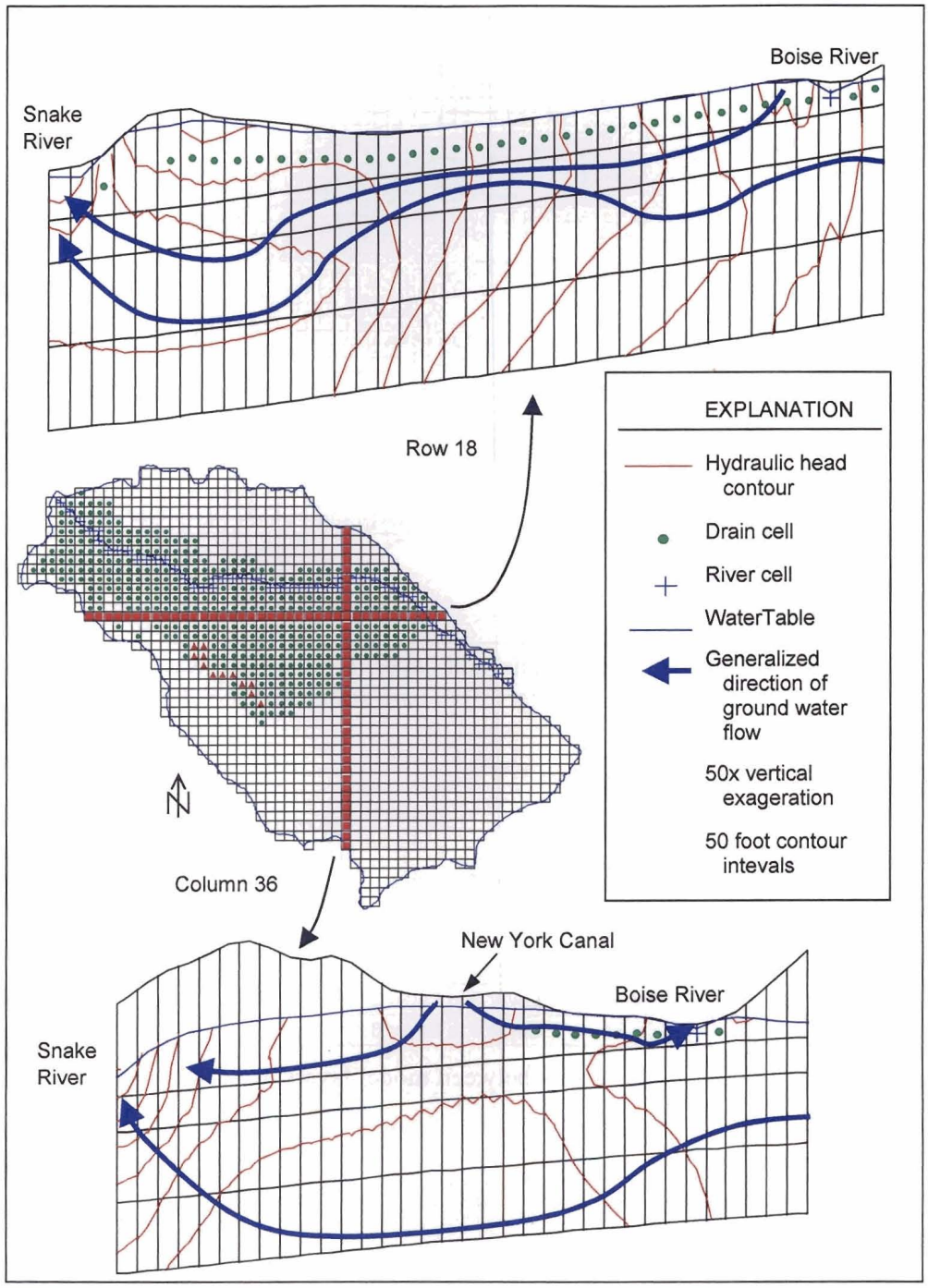

Figure 7-16: Potentiometric contours, base simulation, row 18 and column 36.

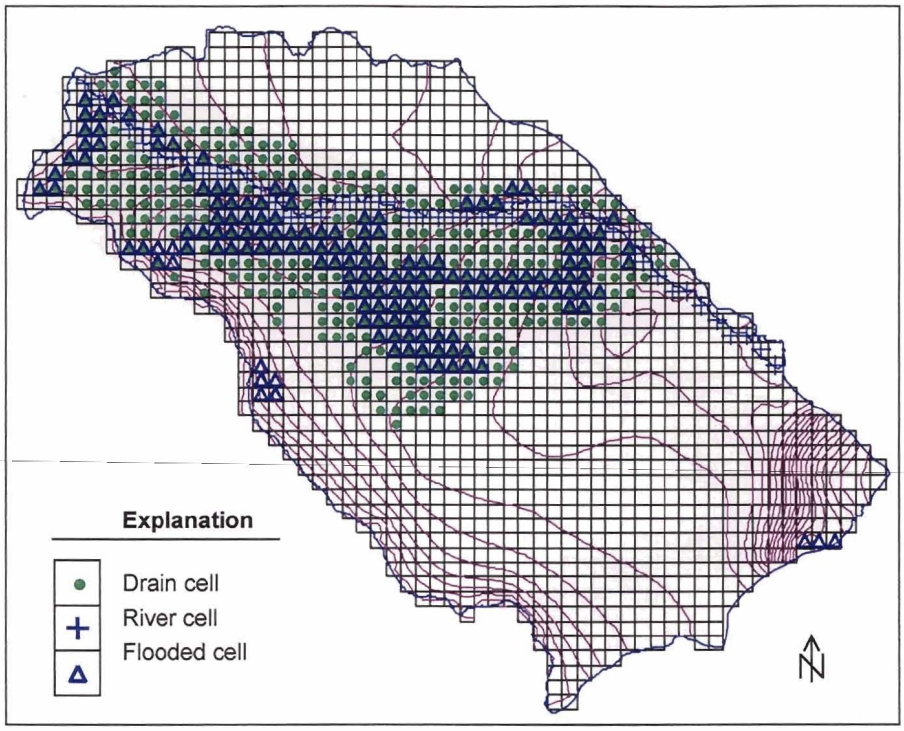

Figure 7-17: Flooded cells and layer 1 simulated water level contours (50-foot contour interval) in base simulation (*SS2bc*).

Flux Direction	Simulated Downward Flux Between Model Layers (af/yr)	Flux Direction	Simulated Upward Flux Between Model Layers (af/yr)	Difference (af/yr)	Estimated Withdrawals by Wells (af/yr)
Layer 1 to Layer 2	146,257	Layer 2 to Layer 1	38,976	107,282	(60,538)
Layer 2 to Layer 3	68,406	Layer 3 to Layer 2	21,436	46,970	(42,934)
Layer 3 to Layer 4	15,633	Layer 4 to Layer 3	11,371	4,263	(4,489)

Table 7-4: Simulated flux between model layers, base simulation.

8. SENSITIVITY ANALYSES

Two general types of parameter sensitivity influence model results and predictions. First, individual parameters have different degrees of influence in any given simulation. Some individual parameters may have substantial influence on model results; others may have very little influence. Some individual correlated parameters may be highly sensitive. However, there is a certain linear combination of these parameters that is relatively insensitive. PEST calculates these parameter sensitivity values during a calibration.

Second, there is parameter sensitivity to various model input variables, such as recharge or underflow. The model sensitivity to these inputs is often evaluated by varying the parameter by a certain amount (e.g., 10%), running the calibrated model and evaluating the effect on model output (e.g., water levels or observation residuals). However, change in an input stress, such as recharge, alters the hydrologic conditions under which the model was originally calibrated. A more thorough evaluation of sensitivity to different inflow rates is to recalibrate the model using the altered sensitivity stress.

Three sensitivity calibrations were conducted to evaluate the effect of increases and/or decreases in selected inflow rates. These additional calibrations were based on the following conditions:

1. 10% increase in recharge over estimated 1996 levels
2. 10% decrease in recharge over estimated 1996 levels
3. Increase in underflow along the northeastern model boundary

8.1. Increased Recharge

8.1.1. Description

The first sensitivity simulation consisted of a 10% across-the-board increase in recharge to the model. The 10% increase could represent error in the 1996 recharge estimates or an increase in recharge over 1996 levels.

8.1.2. Results

Results from a calibration with increased recharge are summarized in Table 8-1. The contribution to the objective function from observations (heads) was higher (see Table 7-1) than in the base simulation. The maximum and the average and median absolute residuals were the same as or higher in each layer compared to the base simulation. A water budget comparison (Table 8-2) between this calibration and the base simulation shows that most of the recharge increase ends up as discharge to the Boise River ("river leakage"), Snake River ("constant head"), and drains.

Increased Recharge Simulation Results (SS7a) (based on observations with PEST weights greater than zero)				
Contribution to Φ from heads	3,646			
Contribution to Φ from regularization	2,271			
Contribution to Φ from gradients	0.909			
Highest eigenvalue	2.1			
Lowest eigenvalue	2.24×10^{-7}			
Number of PEST iterations	50			
Number of MODFLOW runs	~14,300			
Run Statistics				
	Total	**Layer 1**	**Layer 2**	**Layers 3 and 4**
Maximum positive residual	78.21	67.08	66.15	78.21
Minimum negative residual	-65.18	-65.18	-51.52	-53.95
Average absolute residual	15.64	13.01	17.88	25.39
Median absolute residual	10.75	9.40	10.70	19.75
Number of values	200	140	29	31

Table 8-1: Run information for simulation with 10% increase in recharge.

Volumetric Budget Comparison					
		Base Simulation (*SS2bc*)	**10% Increase in Recharge (*SS7a*)**	**Difference from Base Simulation**	**Change as a Percentage of Increased Recharge**
Inflows	Constant head	28,891	32,646	3,755	3%
	Wells	108,000	108,000	0	0%
	Drains	0	0	0	0%
	River leakage	5,784,137	6,576,735	792,598	7%
	Head-dependent boundaries	1,537,895	1,615,971	78,076	1%
	Recharge	116,205,088	127,825,584	11,620,496	100%
	Total In	123,664,008	136,158,944	12,494,936	
Outflows	Constant head	17,350,556	21,689,984	4,339,428	37%
	Wells	23,076,956	23,076,956	0	0%
	Drains	36,667,716	39,523,332	2,855,616	25%
	River leakage	46,486,872	51,759,356	5,272,484	45%
	Head-dependent boundaries	81,961	109,265	27,304	0%
	Recharge	0	0	0	0%
	Total Out	123,664,064	136,158,896	12,494,832	

Table 8-2: Volumetric water budget, 10% increase in recharge.

The simulation resulted in a very slight increase in the number of flooded cells (Figure 8-1). The layer 1 water level contours (Figure 8-1) were almost identical to those for the base simulation (Figure 7-17), so additional contour plots are not provided for the increased recharge simulation.

Residuals for this run (Figure 8-2) were similar to those in the base calibration (Figure 7-1). The residual patterns from the increased recharge simulation run (Figure 8-3 through Figure 8-6) were very similar to those in the base simulation (Figure 7-6 through Figure 7-9). This suggests that the aquifer system is able to accommodate the additional water, especially in the uppermost layer, with the current distribution of hydraulic conductivity. Additional recharge (proportional to current recharge amounts) enters the shallow flow system and discharges in surface channels (e.g., canals and drains) without substantially influencing water levels. Relatively high hydraulic conductivity values estimated for both the increased recharge simulation (Figure 8-7) and the base simulation (Figure 7-10) make this possible. These relatively high K_h values are consistent with the general coarse-grained nature of the Snake River Group sediments.

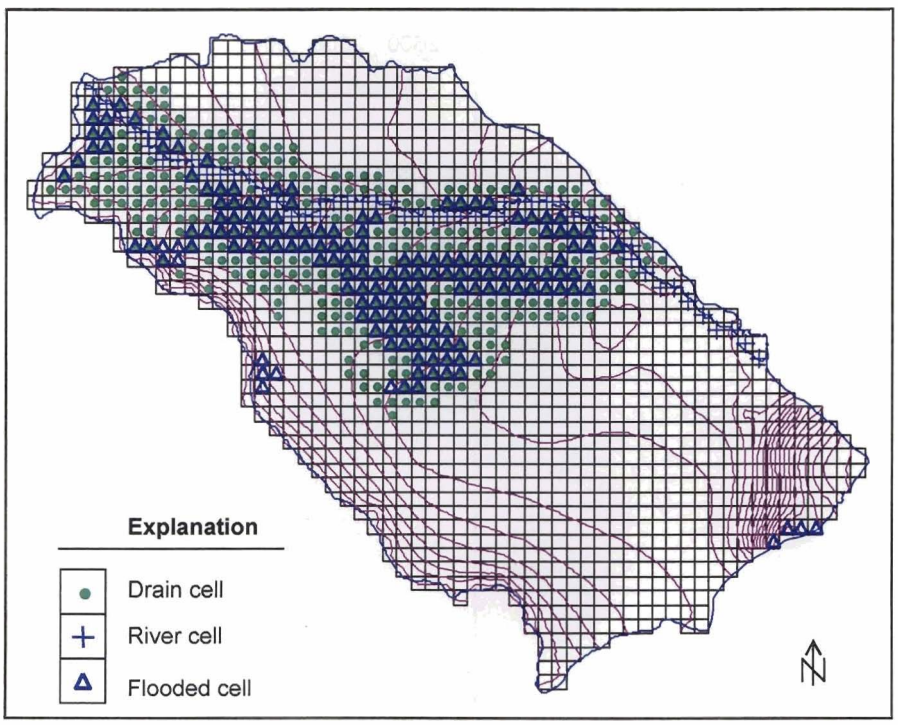

Figure 8-1: Flooded cells and layer 1 simulated water level contours (50-foot contour interval) in increased recharge simulation (*SS7a*).

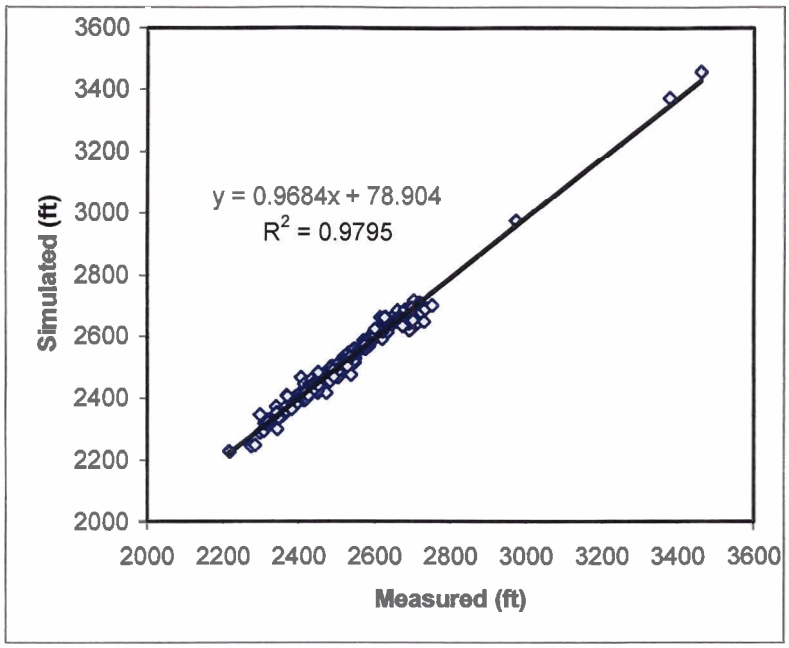

Figure 8-2: Simulated versus measured hydraulic head observations, increased recharge (simulation *SS7a*).

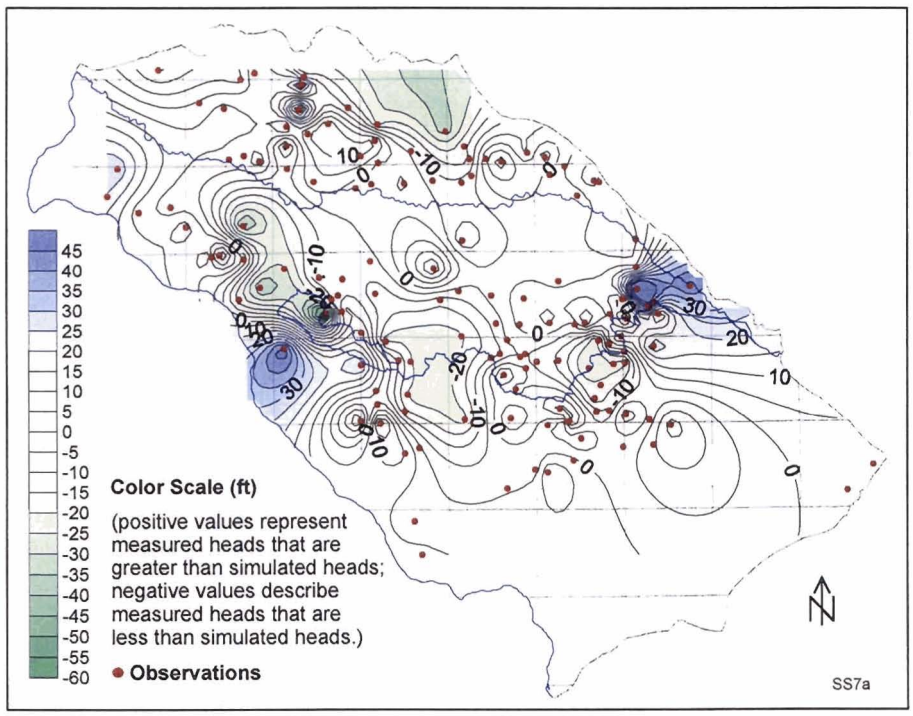

Figure 8-3: Increased recharge simulation residuals, layer 1.

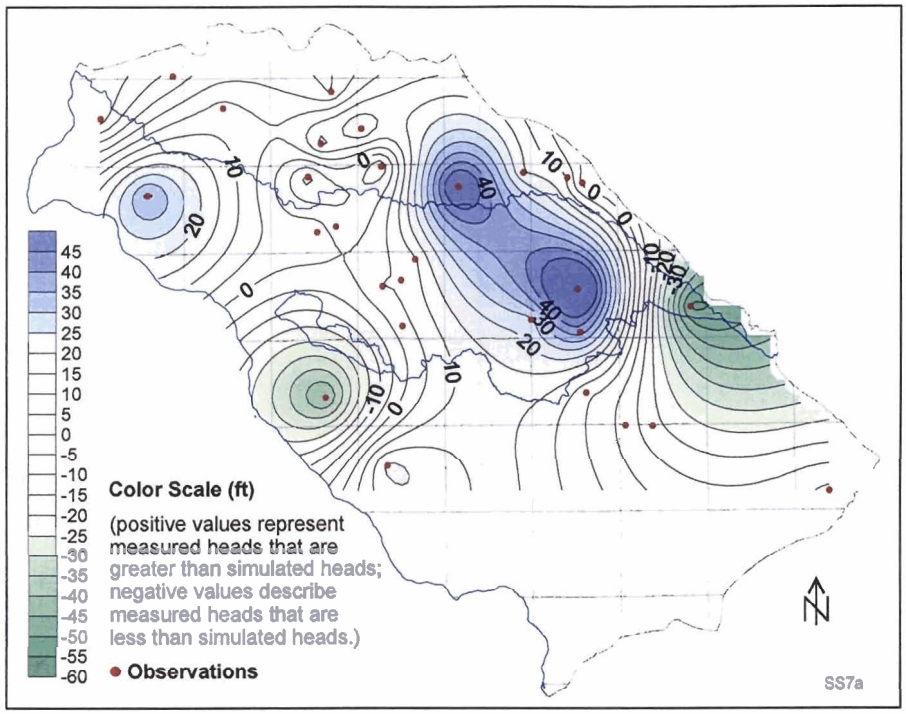

Figure 8-4: Increased recharge simulation residuals, layer 2.

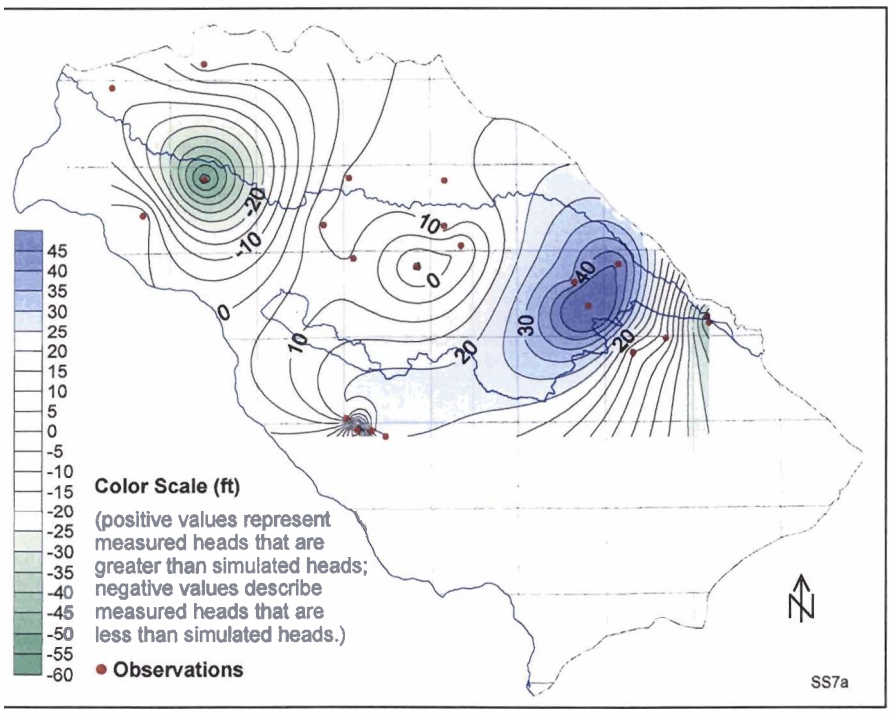

Figure 8-5: Increased recharge simulation residuals, layer 3.

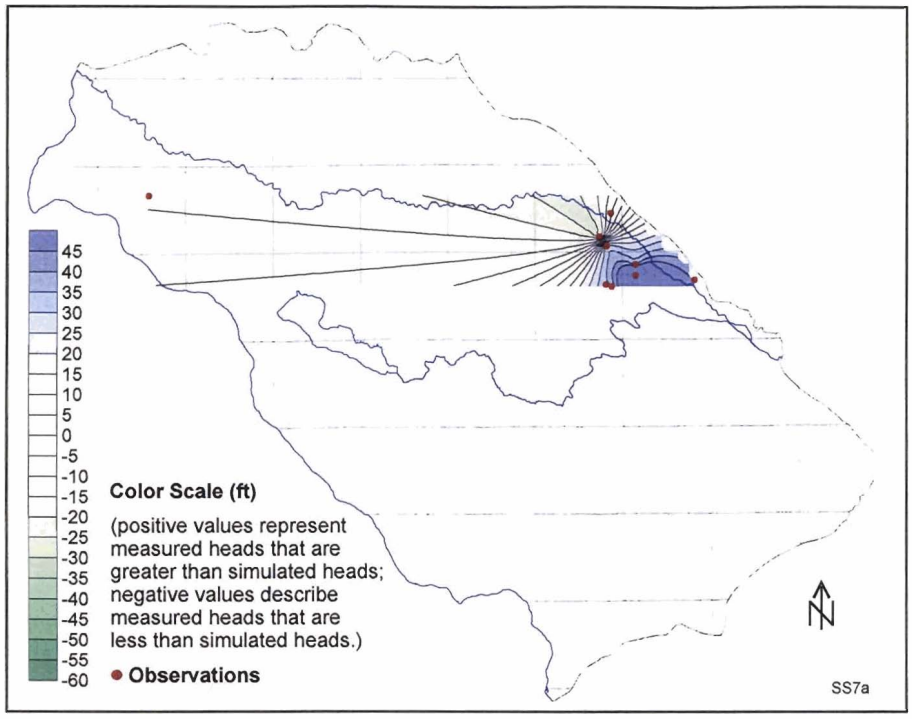

Figure 8-6: Increased recharge simulation residuals, layer 4.

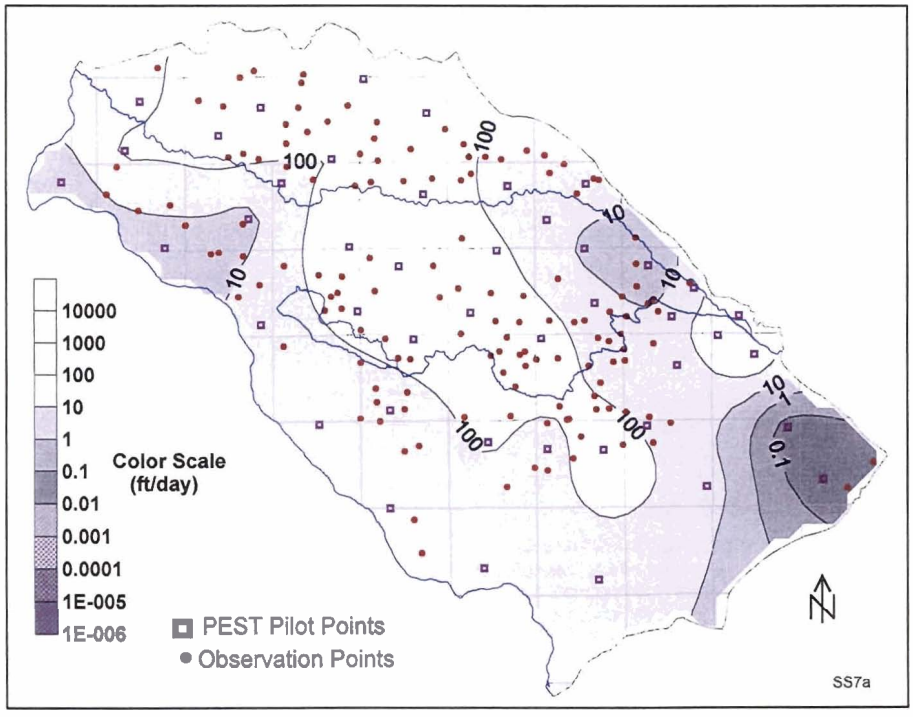

Figure 8-7: Horizontal hydraulic conductivity distribution for increased recharge simulation, layer 1.

8.2. Decreased Recharge

8.2.1. Description

This sensitivity simulation consisted of a 10% across-the-board decrease in recharge to the model. The 10% decrease could represent error in the 1996 recharge estimates or a decrease in recharge over 1996 levels.

8.2.2. Results

Results from a calibration with decreased recharge are summarized in Table 8-3 and Figure 8-8. The contribution to the objective function (ϕ) from head observations was greater than in the base simulation. The sum of the squared residuals from head values was greater than in the base simulation (see Table 7-1). The average and median absolute residuals were similar to those in the base simulation. The maximum absolute residuals (located primarily in the eastern, higher elevation portion of the aquifer – Figure 8-8) were much greater in this simulation. The distribution of residuals in the uppermost layer (Figure 8-9) was similar to that in the base simulation (Figure 7-6), except that the decreased recharge led to much lower simulated water levels in the eastern portion of the basin. The residuals in the second layer (Figure 8-10) were similar to those in the base simulation (Figure 7-7), except in the eastern portion of the basin, in which one well had a simulated water level much less than the observed one. Residuals in layers 3 and 4 (Figure 8-11 and Figure 8-12) were very similar to those of the base simulation (Figure 7-8 and Figure 7-9).

The K_h distribution (Figure 8-13) derived in the decreased recharge simulation for the uppermost model layer was very similar to both that of the base simulation (Figure 7-10) and the increased recharge simulation (Figure 8-7). The parameter estimation suggests that the layer 1 sediments are relatively conductive and increasing or decreasing recharge by 10% does not materially change the conductivity of these sediments. The one exception is in the far eastern portion of the model domain, where PEST indicates very low conductivity sediments in an effort to maintain the relatively steep apparent hydraulic gradient in this area. A water budget comparison (Table 8-4) between this calibration and the base simulation shows that the decrease in recharge results in decreased discharge to the Boise River ("river leakage"), Snake River ("constant head"), and drains.

Decreased Recharge Simulation Results (*SS7b*) (based on observations with PEST weights greater than zero)				
Contribution to Φ from heads	4,767			
Contribution to Φ from regularization	256			
Contribution to Φ from gradients	5.6			
Highest eigenvalue	8.64			
Lowest eigenvalue	1.21×10^{-7}			
Number of PEST iterations	50			
Number of MODFLOW runs	~14,300			
Run Statistics (based on observations with weights > 0)				
	Total	**Layer 1**	**Layer 2**	**Layers and 4**
Maximum positive residual	168.86	168.86	40.57	69.26
Minimum negative residual	-166.23	-60.94	-166.23	-43.41
Average absolute residual	14.48	12.65	16.669	20.69
Median absolute residual	8.64	8.17	4.24	18.97
Number of values	200	140	29	31

Table 8-3: Run information for simulation with 10% decrease in recharge.

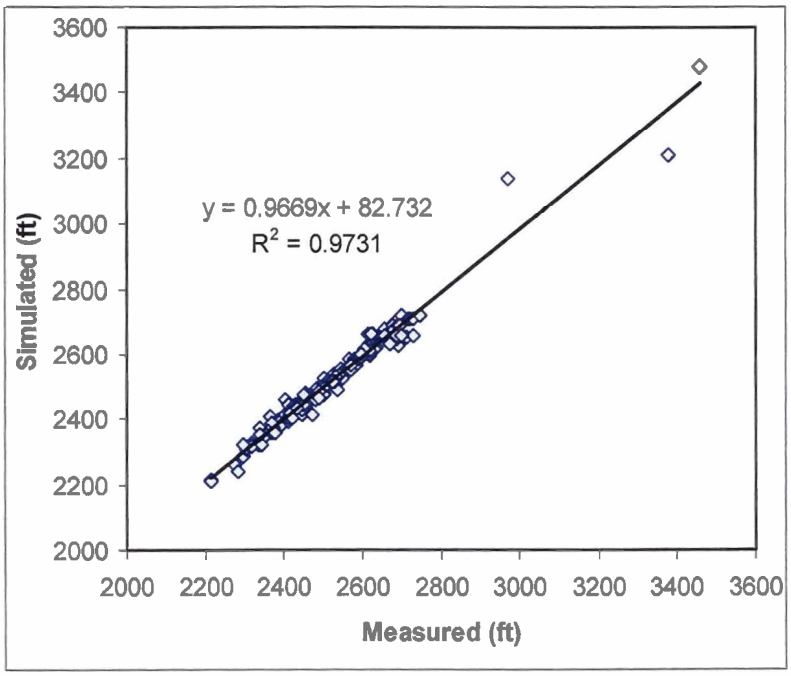

Figure 8-8: Simulated versus measured hydraulic head observations, steady-state hydraulic conditions (decreased recharge simulation).

Volumetric Budget Comparison					
		Base Simulation (*SS2bc*)	10% Decrease in Recharge (*SS7b*)	Difference from Base Simulation	Change as a Percentage of Decreased Recharge
Inflo	Constant head	28,891	24,386	-4,505	0%
	Wells	108,000	108,000	0	0%
	Drains	0	0	0	0%
	River leakage	5,784,137	5,904,424	120,287	1%
	Head-dependent boundaries	1,537,895	1,927,328	389,433	3%
	Recharge	116,205,088	104,584,592	11,620,496	-100%
	Total In	123,664,008	112,548,728	-11,115,280	
Outflo	Constant head	17,350,556	14,411,841	-2,938,715	-25%
	Wells	23,076,956	23,076,956	0	0%
	Drains	36,667,716	34,972,756	-1,694,960	-15%
	River leakage	46,486,872	40,042,612	-6,444,260	-55%
	Head-dependent boundaries	81,961	44,520	-37,441	0%
	Recharge	0	0	0	0%
	Total Out	123,664,064	112,548,680	-11,115,384	

Table 8-4: Volumetric water budget comparison, 10% decrease in recharge.

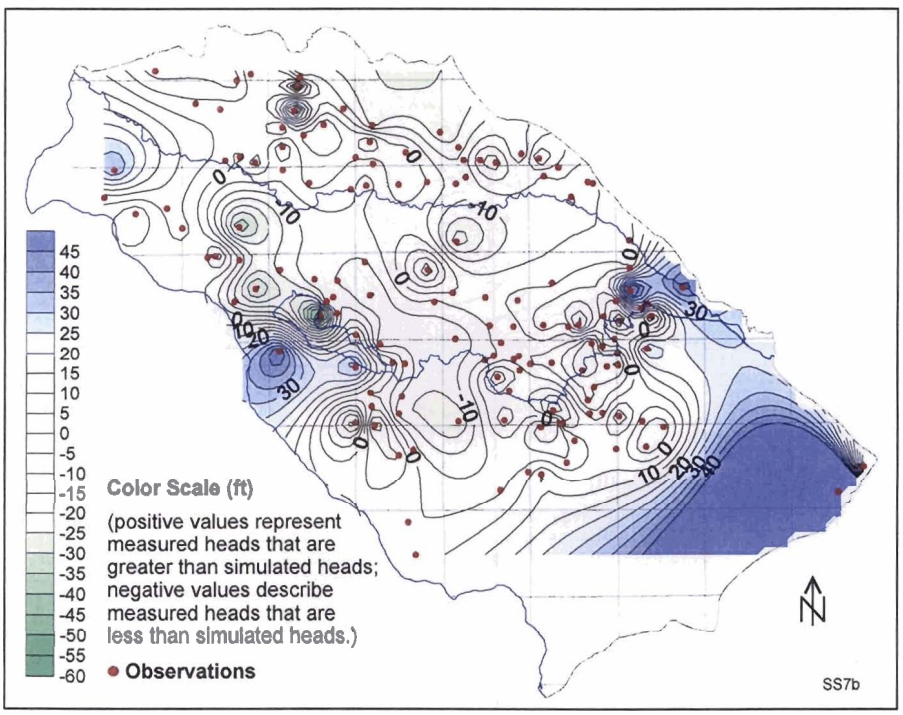

Figure 8-9: Decreased recharge simulation residuals, layer 1.

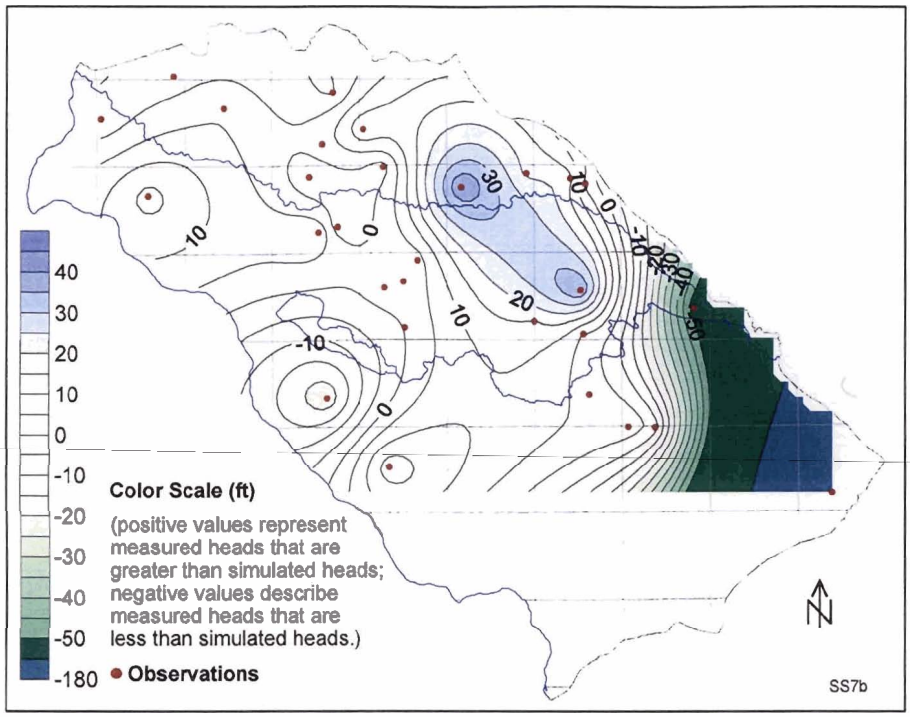

Figure 8-10: Decreased recharge simulation residuals, layer 2.

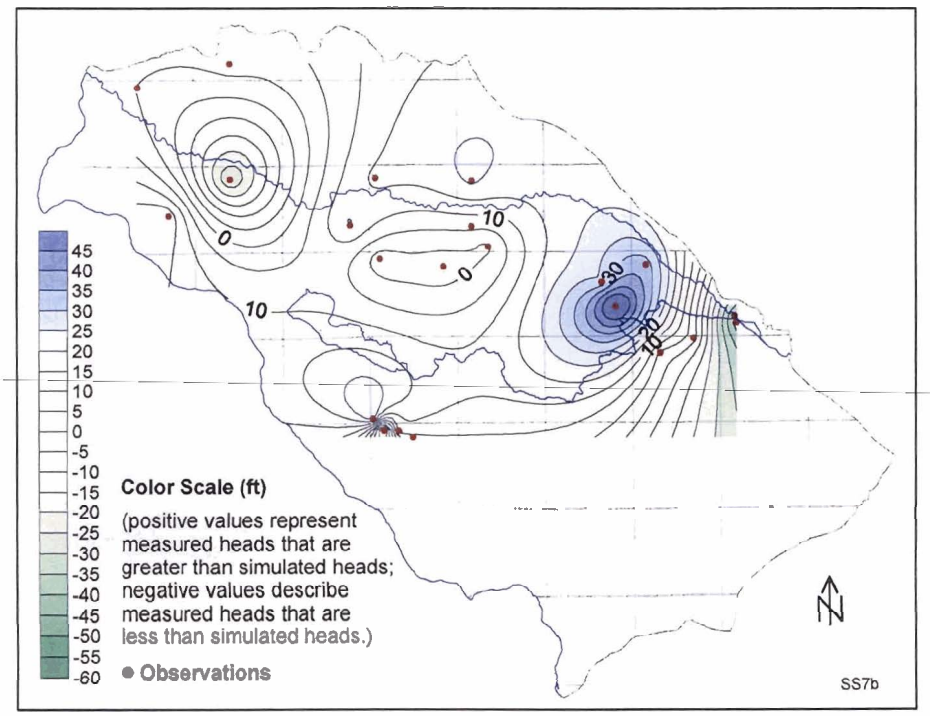

Figure 8-11: Decreased recharge simulation residuals, layer 3.

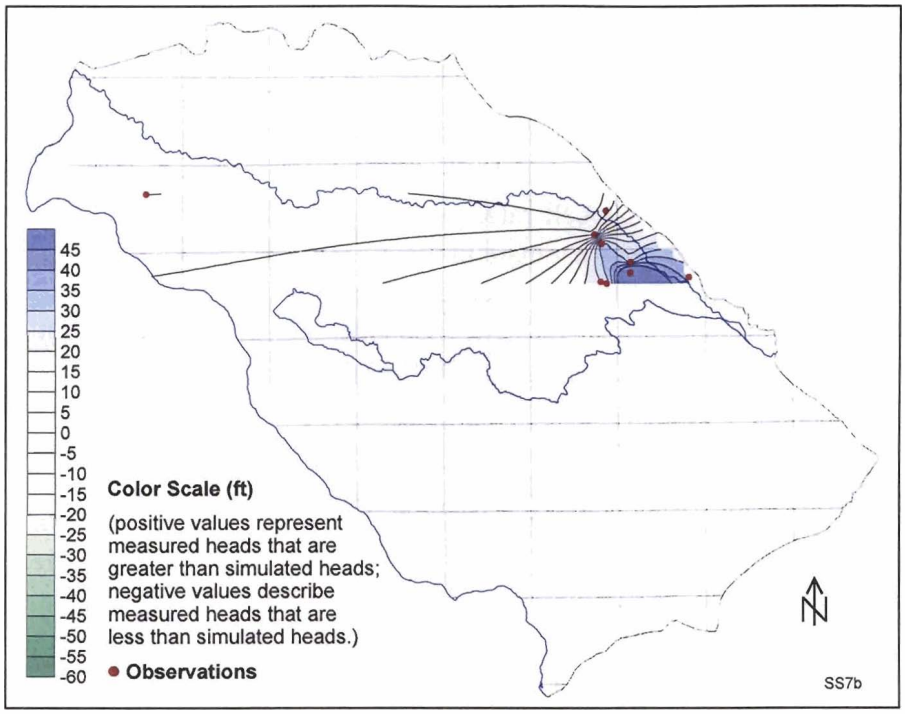

Figure 8-12: Decreased recharge simulation residuals, layer 4.

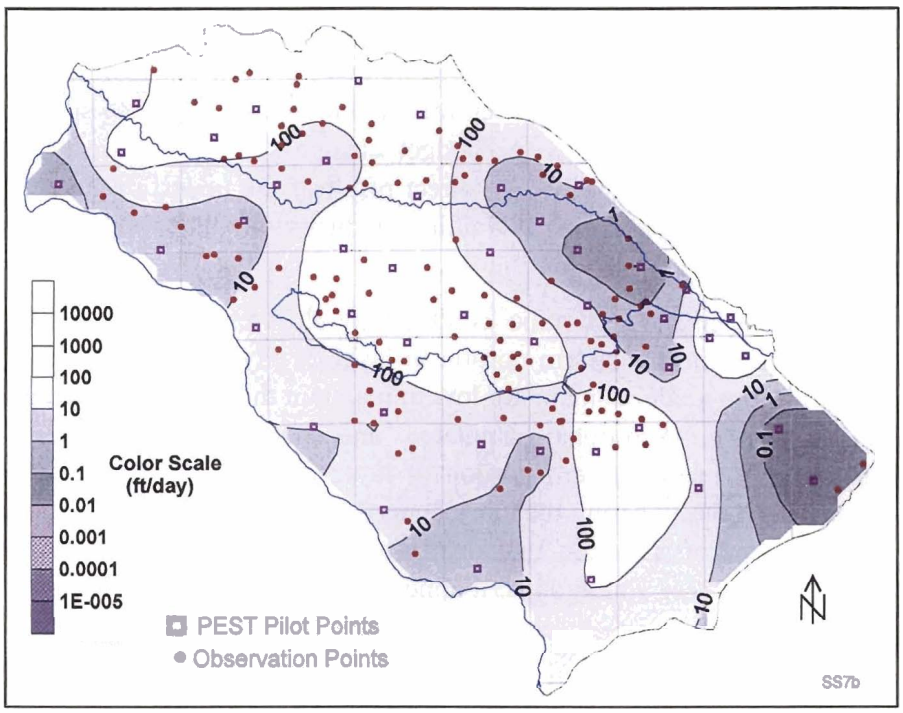

Figure 8-13: Horizontal hydraulic conductivity distribution for decreased recharge simulation, layer 1.

8.3. Increased Underflow

8.3.1. Description

This simulation consisted of increasing underflow (simulated as a specified flux) from 1,000 to 8,000 ft^3/day/cell. Cells in which underflow is specified are shown in Figure 3-5. The 8,000 ft^3/day/cell rate, yielding a total underflow of 7,239 af/yr, is much closer to the 8,000 af/yr estimate in the 1996 water budget (Urban and Petrich, 1998). However, there is substantial uncertainty about the amount and horizontal and vertical distribution of underflow rates into the model domain. Early simulations during initial model construction used lower underflow rates that led to higher objective function (sum of squared residuals) values, suggesting that the model had a difficult time accommodating the higher flux rate. Underflow rates in the base simulation therefore were decreased for the base simulation. The purpose of this model run was to show the effects of the increased underflow rate.

8.3.2. Results

Results from the calibration with increased underflow rates are summarized in Table 8-5. The contribution from head and gradients to the objective function were higher than in the base simulation (Table 7-1). The maximum and minimum residual values were higher and lower, respectively, than the base simulations, although the total average and median residual values were similar. A plot of the measured versus observed water levels (Figure 8-14) shows a slightly poorer fit than the base simulation (Figure 7-1). Residuals are portrayed by layer in Figure 8-15 through Figure 8-18. A water budget comparison between this calibration and the base simulation (Table 8-6) indicates that numerous water budget changes occur as a result of the increased underflow. Some of these are a direct result of the underflow increase, but some are the result of changes in hydraulic conductivity values forced by the increased underflow.

One of the largest hydraulic conductivity differences between this and the base simulations is in the eastern portion of layer 2. Hydraulic conductivity values in this portion of the model domain are low to maintain the steep hydraulic gradient observed in this area. Additional simulated underflow causes simulated heads to rise substantially in the eastern portion of layer 2, suggesting that the model had some difficulty accommodating the extra underflow in this area. This reflects a weakness in the underflow assumption that underflow is probably not uniform along the Boise Front. From these simulations, it appears that the underflow along the eastern portion of the model domain (e.g., east of the Boise River) is probably much less than that west of the Boise River.

Increased Recharge Simulation Results (*SS7c*) (based on observations with PEST weights greater than zero)				
Contribution to Φ from heads	4,183			
Contribution to Φ from regularization	2,797			
Contribution to Φ from gradients	134			
Highest eigenvalue	1.261			
Lowest eigenvalue	1.71×10^{-7}			
Number of PEST iterations	50			
Number of MODFLOW runs	~14,300			
Run Statistics (based on observations with weights > 0)				
	Total	**Layer 1**	**Layer 2**	**Layers 3 and 4**
Maximum positive residual	86.0	86.0	43.2	68.5
Minimum negative residual	-172.5	-64.6	-172.5	-45.1
Average absolute residual	14.8	12.6	18.7	21.2
Median absolute residual	9.7	8.9	8.6	18.3
Number of values	200	140	29	31

Table 8-5: Run information for simulation with increase in underflow.

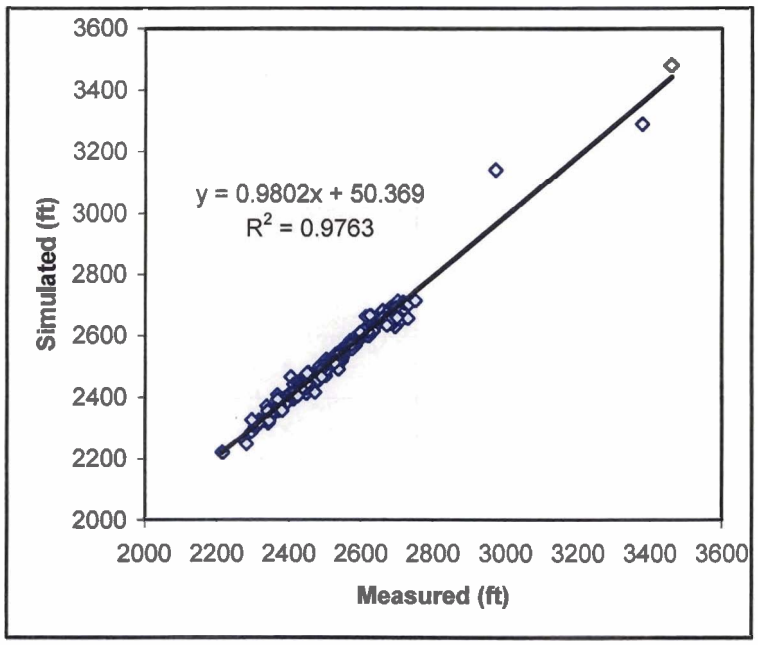

Figure 8-14: Simulated versus measured hydraulic head observations, steady-state hydraulic conditions (increased underflow simulation).

Volumetric Budget Comparison					
		Base Simulation (*SS2bc*)	Increase in Underflow (*SS7c*)	Difference from Base Simulation	Change as a Percentage of Increased Underflow
Inflows	Constant head	28,891	26,620	-2,271	0%
	Wells	108,000	864,000	756,000	100%
	Drains	0	0	0	0%
	River leakage	5,784,137	5,010,208	-773,929	-102%
	Head-dependent boundaries	1,537,895	1,697,406	159,511	21%
	Recharge	116,205,088	116,205,088	0	0%
	Total In	123,664,008	123,803,320	139,312	
Outflows	Constant head	17,350,556	16,845,578	-504,978	-67%
	Wells	23,076,956	23,076,956	0	0%
	Drains	36,667,716	38,084,656	1,416,940	187%
	River leakage	46,486,872	45,733,944	-752,928	-100%
	Head-dependent boundaries	81,961	62,260	-19,701	-3%
	Recharge	0	0	0	0%
	Total Out	123,664,064	123,803,392	139,328	

Table 8-6: Volumetric water budget comparison, increase in underflow.

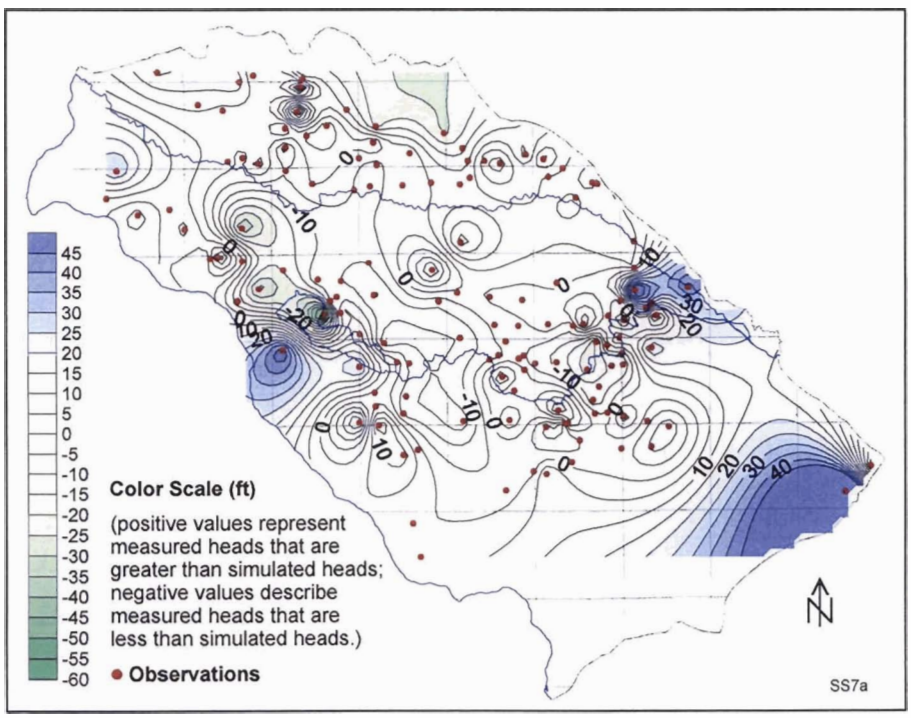

Figure 8-15: Increased underflow simulation residuals, layer 1.

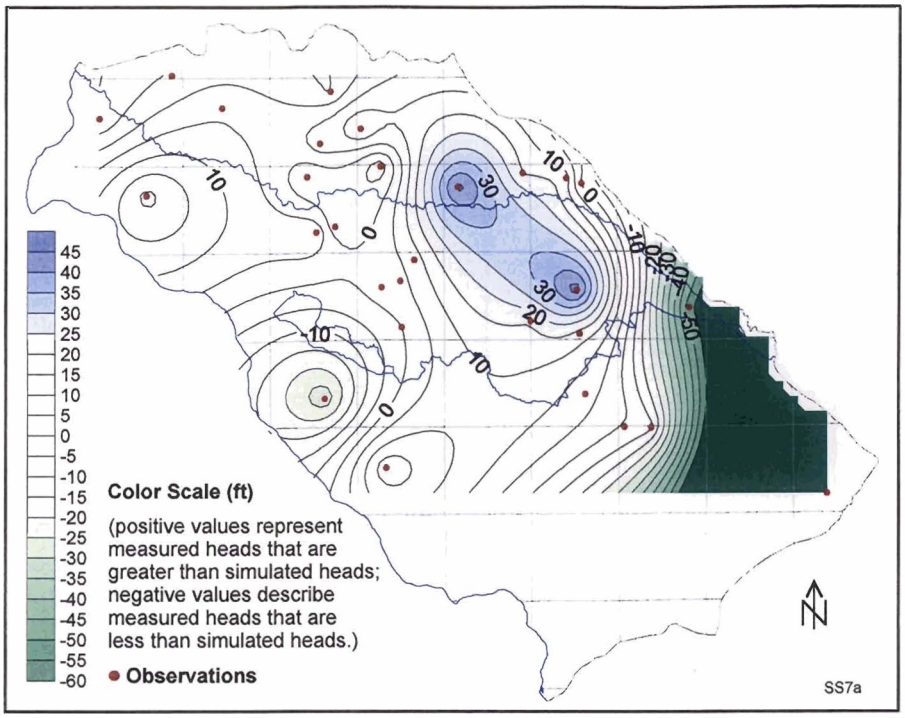

Figure 8-16: Increased underflow simulation residuals, layer 2.

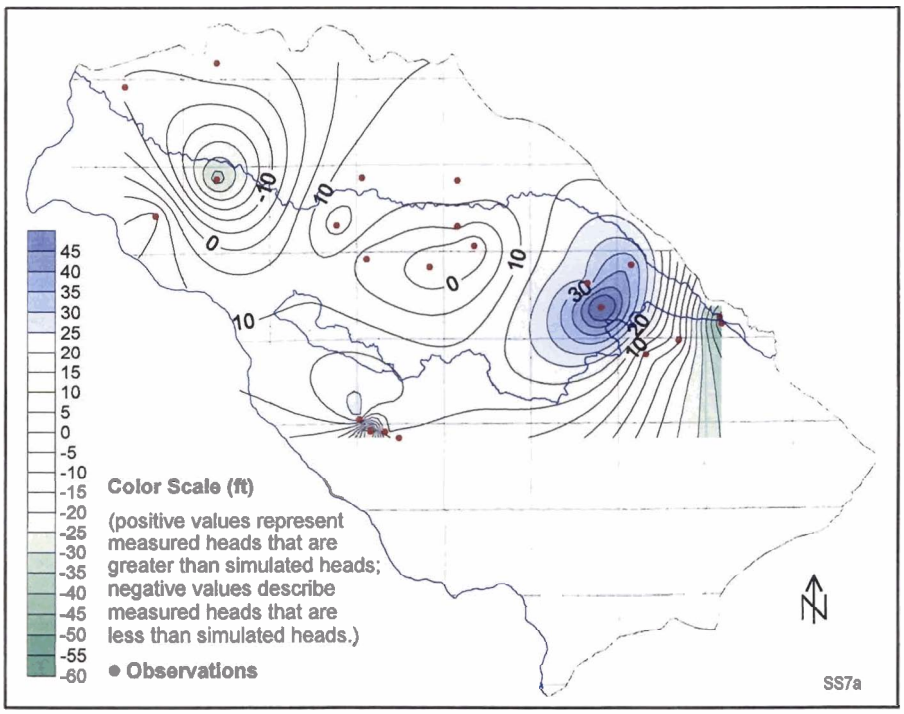

Figure 8-17: Increased underflow simulation residuals, layer 3.

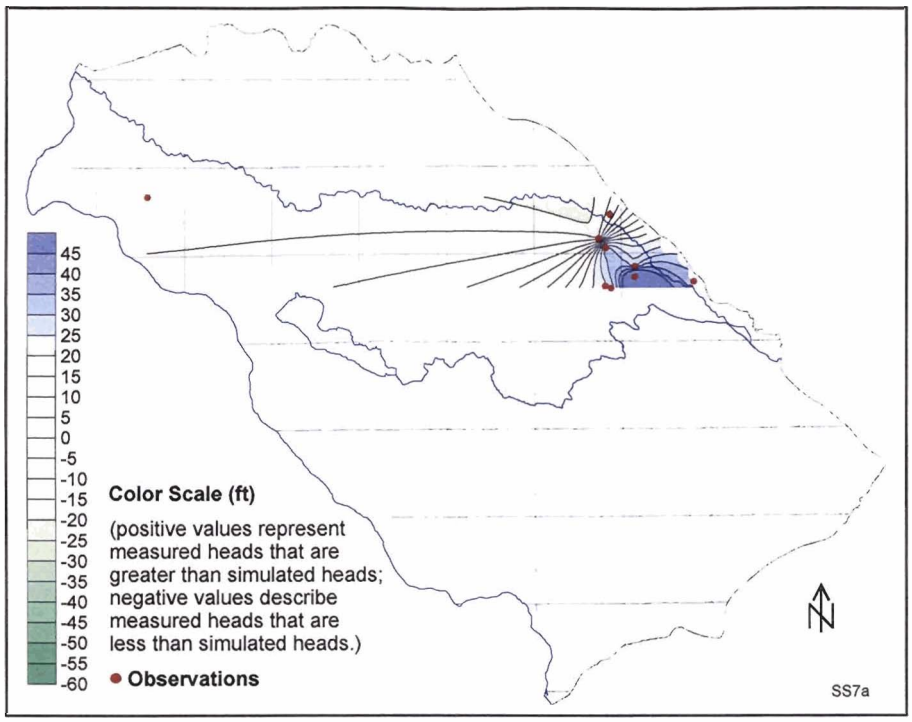

Figure 8-18: Increased underflow simulation residuals, layer 4.

9. PREDICTIVE ANALYSIS

9.1. Introduction

All calibrated ground water models have uncertainty associated with individual parameter values. The goal of predictive analysis is to find the worst (and best) possible outcomes within a set of calibrated model parameters.

In the predictive simulations, two scenarios (base simulation and predictive scenario) were run in succession until PEST found a set of parameter values that would both calibrate the model and provide the minimum (or maximum) water levels associated with the additional withdrawals. That is, PEST was asked to run two model scenarios in succession, while estimating parameters for the base simulation. For the predictive scenario, the model was provided with a set of inputs pertinent to the specific prediction that the model was required to make (e.g., increased withdrawals). PEST was asked to read that specific prediction from output files generated by the second model and then maximize or minimize that prediction. The parameter values required to maximize or minimize the prediction were constrained to the values that would calibrate the first model scenario (i.e., the base simulation).

To do this, it was necessary to define an objective function (i.e., sum of the squared residuals [Φ]) at which the base simulation would no longer be calibrated. This value was set slightly higher than the lowest objective function value achieved through normal calibration of the base simulation. The same regularization weight factor calculated by PEST for the base simulation was used to enforce parameter smoothness in the predictive simulations. Thus, parameters in the predictive simulations were forced to respect both the constraints imposed by the measurement data set and the smoothness attained during the base simulation. This prevented the predictive analysis process from introducing spurious and localized regions of parameter heterogeneity into the model domain, and thereby provided unduly pessimistic (or optimistic) estimates of predictive uncertainty.

Thus, smoothing constraints employed in the regularization process were maintained in the predictive analysis process. The prior information weights from the base simulation were multiplied by the optimized weight factor determined through regularized inversion. The calibration target ("PD0") for the predictive analysis was set slightly higher (Table 9-1) than the prior lowest calibration objective function value.

9.2. Predictive Points

Predictions of the impact from new aquifer stresses (e.g., ground water withdrawals) were calculated at one or more "prediction points" within the model domain. PEST attempted to maximize (or minimize) the average of head values at the selected

prediction points. Thus, the number of points, and the spatial and vertical distribution of the points, influences the simulation results. The predictive simulations were based on 12 points (Figure 9-1) in layers 1, 2, and 3 (36 points total). The prediction points were distributed spatially in the central portion of the valley (i.e., the area of greatest interest and the largest number of observations).

Step
Use PARREP.EXE to transfer optimized parameter values from the calibration run to the prediction PEST control file.
Use WTFACTOR.EXE to multiply regularization weights by the optimized regularization weight factor.
Run PEST once to ensure that the total objective function is the same as that achieved in the parameter estimation mode
Set PD0, PD1, and PD2 as indicated in the PEST documentation (Doherty, 2000).

Table 9-1: Selected steps in preparing a PEST control file for predictive simulations.

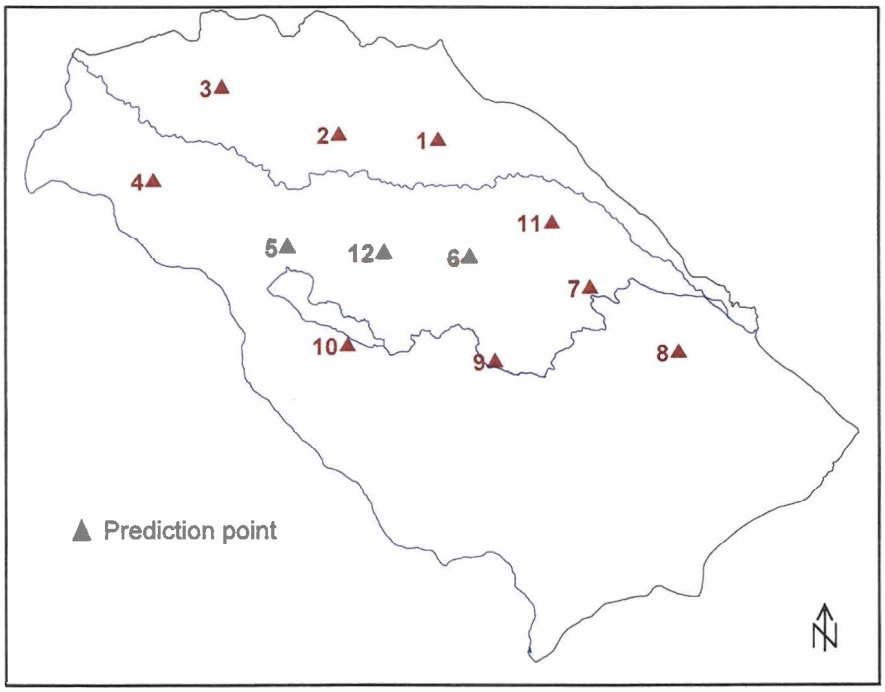

Figure 9-1: Prediction point locations.

9.3. Predictive Analysis Files

Files used for the predictive simulations are listed in Appendix F. These files are similar to those listed for model calibration (Appendix D) but also include files required for the predictive analysis. Output files from the predictive analysis are listed in Appendix G.

9.4. Processing Predictive Analysis Files

The process used for processing predictive analysis files was the same as that described in Section 5.11. In addition, changes in head (e.g., drawdown) were plotted for each predictive analysis simulation. The approach used for plotting changes in head for predictive simulations is outlined in Table 9-2.

	Process	File
1.	Review simulation results (Table 5-6)	
2.	Import hydraulic head file into GMS, and export from GMS as an ASCII *.dat* file. Subtract the predictive analysis head values from a calibration head file (in this case, simulation *SS2bc* was used).	**.hed* *HeadProcessor.xls* *active.bln* *pred-diffs.lvl* MODFLOW output file (**.out*)
3.	Separate head differences by layer in preparation for creating Surfer™ grid files. This can be done using *HeadProcessor.xls* (see instructions in *HeadProcessor.xls*). Save as	
4.	Create Surfer™ maps using default kriging parameters, using *active.bln* for blanking areas surrounding the model domain and using *pred-diffs.lvl* for plotting filled-contour maps.	*active.bln* *pred-diffs.lvl*

Table 9-2: Steps for processing predictive analysis results.

10. SCENARIOS

10.1. Introduction

Two scenarios were conducted using the PEST predictive analysis tools (Doherty, 2000). The results of one of the scenarios are reported here. Results from an additional scenario to simulate the potential impact on water levels from the aggregate withdrawals represented by Basin 63 unprocessed water right applications is reported under separate cover (Petrich, 2004a).

The initial parameters in these predictive simulations were the ending parameters of the base-case simulation (simulation *SS2bc*, Section 7.2). Base simulation results were summarized in Table 7-1). Use of these parameter values does not influence the predictive results; it simply leads to a faster predictive analysis run.

10.2. Scenario 1: 20% Increase in Withdrawals

10.2.1. Description

The purpose of this scenario was to explore potential effects of a 20% across-the-board withdrawal increase on current ground water levels in the lower Boise River basin. Scenario 1 (simulations *SS5e-min* and *SS5e-max*) consisted of an across-the-board ground water withdrawal increase of 20% over estimated 1996 withdrawals. The relative magnitude of the across-the-board increases in this scenario between model layers (Figure 10-1) were defined as being proportional to the estimated 1996 withdrawals by model layer (Urban and Petrich, 1998). A large portion of the assumed increased withdrawals in layer 1 (Figure 10-2) was in areas currently irrigated by ground water, such as the area south of the New York Canal. The largest hypothetical withdrawal increases in layers 2 (Figure 10-3) and 3 (Figure 10-4) were in the urban areas of Boise, Meridian, Nampa, and Caldwell.

The 20% increase is similar in total magnitude to that of the increase represented by the unprocessed, non-supplemental water right applications in the Treasure Valley (Petrich, 2004a). However, the horizontal and vertical distribution of the withdrawals represented by the unprocessed, non-supplemental water right applications is somewhat different than the 20% increase based on the 1996 withdrawal distribution (see Petrich, 2004a).

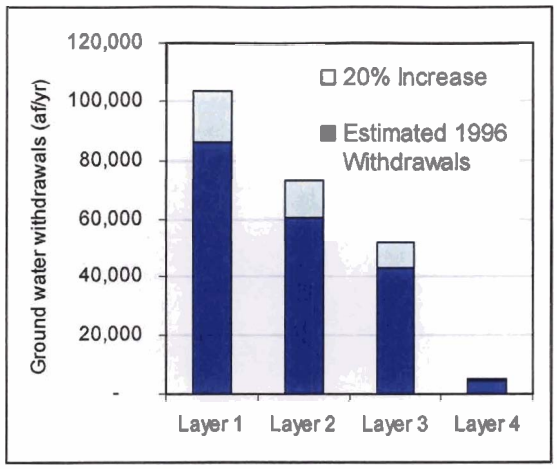

Figure 10-1: Estimated 1996 ground water withdrawals (Urban and Petrich, 1998) and hypothesized 20% increase, by model layer.

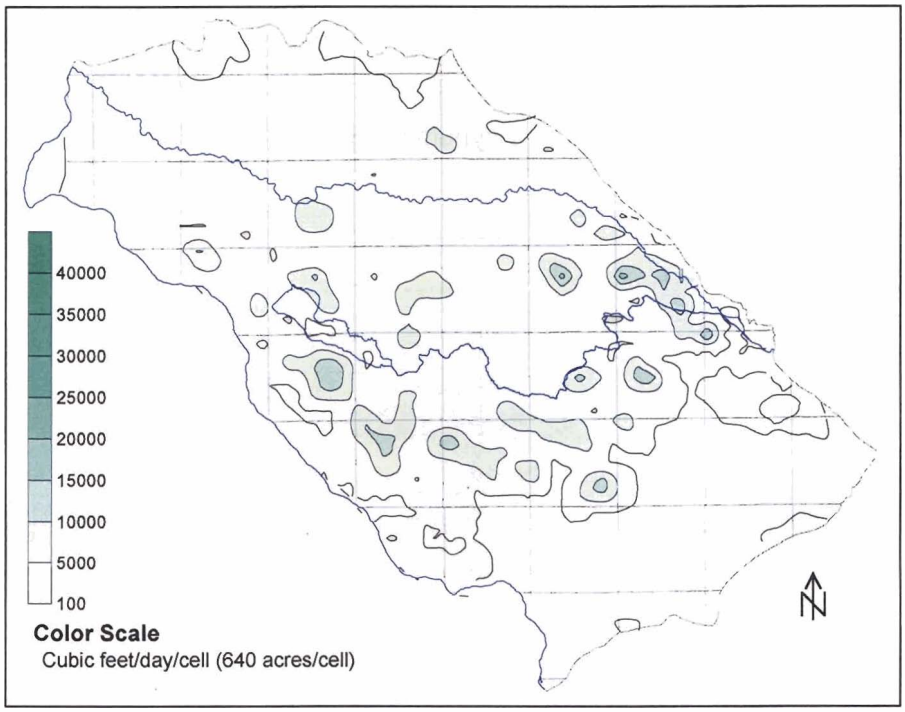

Figure 10-2: Distribution of hypothetical 20% increase in 1996 withdrawals, layer 1.

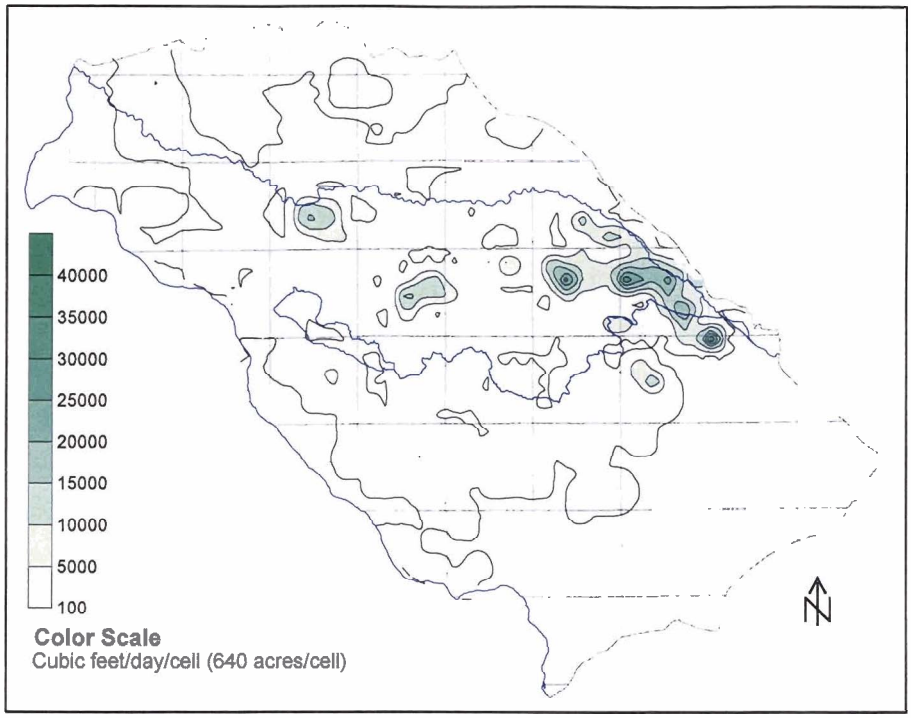

Figure 10-3: Distribution of hypothetical 20% increase in 1996 withdrawals, layer 2.

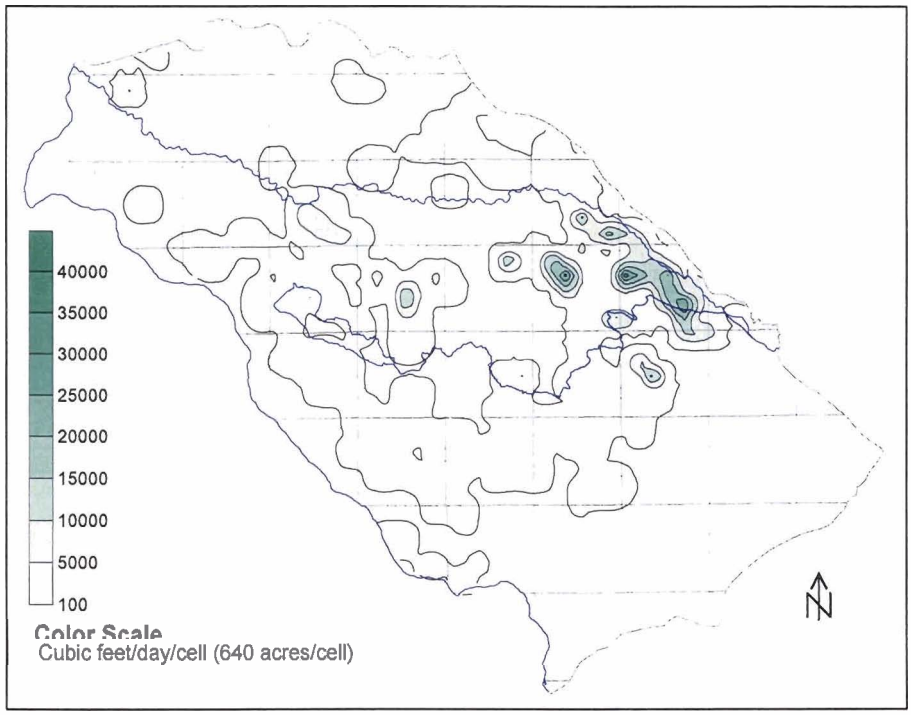

Figure 10-4: Distribution of hypothetical 20% increase in 1996 withdrawals, layer 3.

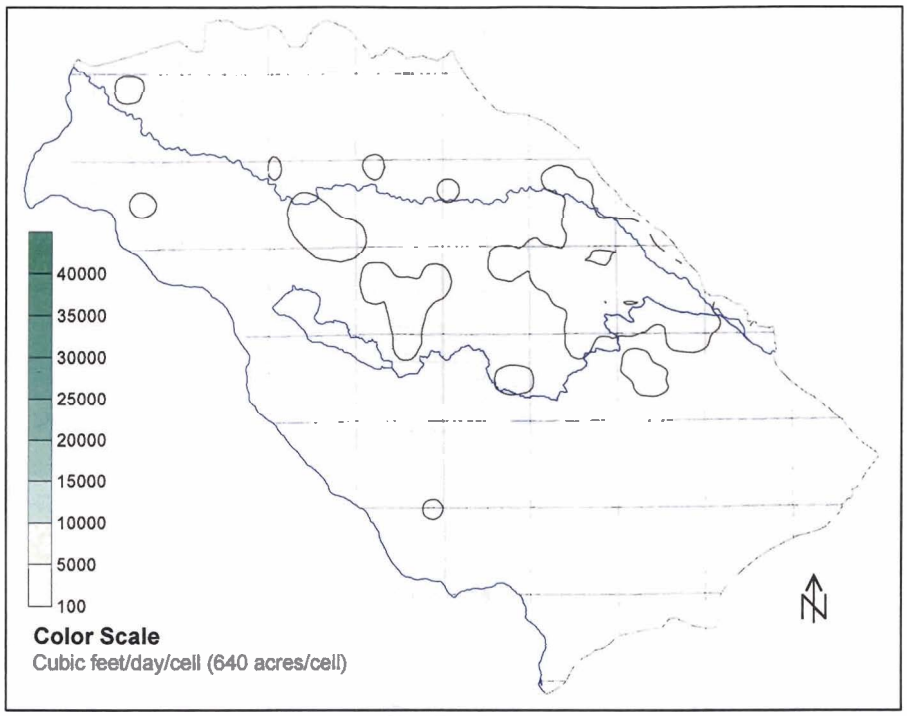

Figure 10-5: Distribution of hypothetical 20% increase in 1996 withdrawals, layer 4.

10.2.2. Results

This scenario simulation resulted in a minimum average simulated water level (based on 36 predictive point locations) of 2,484.7 feet (Table 10-1). This represents a decline of 6.5 feet over the starting average predictive point water level (2,491.3 feet). Residuals (Figure 10-6) were similar to those in the base calibration. The spatial distribution of simulated water level declines is shown in Figure 10-7 through Figure 10-10. The most substantial simulated declines (more than 30 feet) occurred south of Lake Lowell and the New York Canal in layers 2 and 3.

Residuals for the minimum head prediction are shown in Figure 10-11 through Figure 10-14. These are almost identical to the residuals for the base simulation (Figure 7-6 through Figure 7-9).

The K_h and K_v distributions that led to the minimum hydraulic heads are shown in Figure 10-15 through Figure 10-20. These are virtually identical to the K_h and K_v distributions in the base simulation (Figure 7-10 through Figure 7-15), with the exception of slight differences in the K_v distribution in layer 2 (Figure 7-14 and Figure 10-19).

Scenario 1 Simulation Results (*SS5d-min*) (based on observations with PEST weights greater than zero)				
Beginning prediction (ft)	2,491.3			
Ending prediction (ft)	2,484.7			
Initial objective function	6,427.2			
Initial contribution to Φ from heads	3,220.4			
Initial contribution to Φ from regularization	3,150.3			
Initial contribution to Φ from gradients	56.5			
Ending objective function (Φ)	6,565			
Ending contribution to Φ from heads	3,380			
Ending contribution to Φ from regularization	2,797			
Ending contribution to Φ from gradients	62.5			
Highest eigenvalue	1.247			
Lowest eigenvalue	1.76×10^{-7}			
Number of PEST iterations	3			
Number of MODFLOW runs	877			
Run Statistics (based on observations with weights > 0)				
	Total	**Layer 1**	**Layer 2**	**Layers 3 and 4**
Maximum positive residual	73.89	64.87	66.09	73.89
Minimum negative residual	-65.61	-65.61	-51.66	-43.72
Average absolute residual	14.98	12.10	18.47	24.72
Median absolute residual	11.03	8.14	13.28	21.80
Number of values	200	140	29	31

Table 10-1: Summary of results, Scenario 1, minimum head levels.

A summary of the simulation residuals and simulation results are presented in Figure 10-21 and Table 10-2, respectively. The maximum prediction of average heads at the predictive points was 2,500.1 feet (Table 10-2), about 8.8 feet above the starting average head of 2,491.3 feet.

The difference between the minimum and maximum heads (2,487.7 feet versus 2,500.1 feet) represents the uncertainty inherent in the model calibration. It is highly unlikely that average heads would increase in response to increased withdrawals. Thus, the finding of this predictive simulation is that heads (given the current model calibration) would decline no more than those indicated by the minimum head prediction in response to the increased withdrawals. This uncertainty inherent to the model calibration does not include or quantify the uncertainty inherent in model input variables or basic model construction.

A water budget for the increased withdrawal simulations is given in (Table 10-3). The largest impacts of the simulated increases (Figure 10-22) were decreased discharge to drains (62%) and increased (induced) leakage from the Boise River to the underlying aquifer (23%).

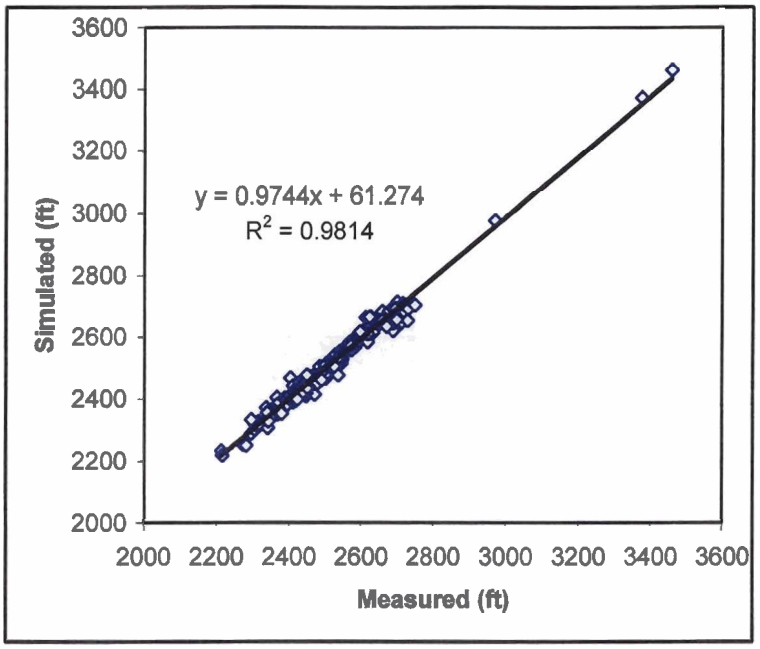

Figure 10-6: Simulated versus measured hydraulic head observations, steady-state hydraulic conditions (increased withdrawals simulation, minimum prediction).

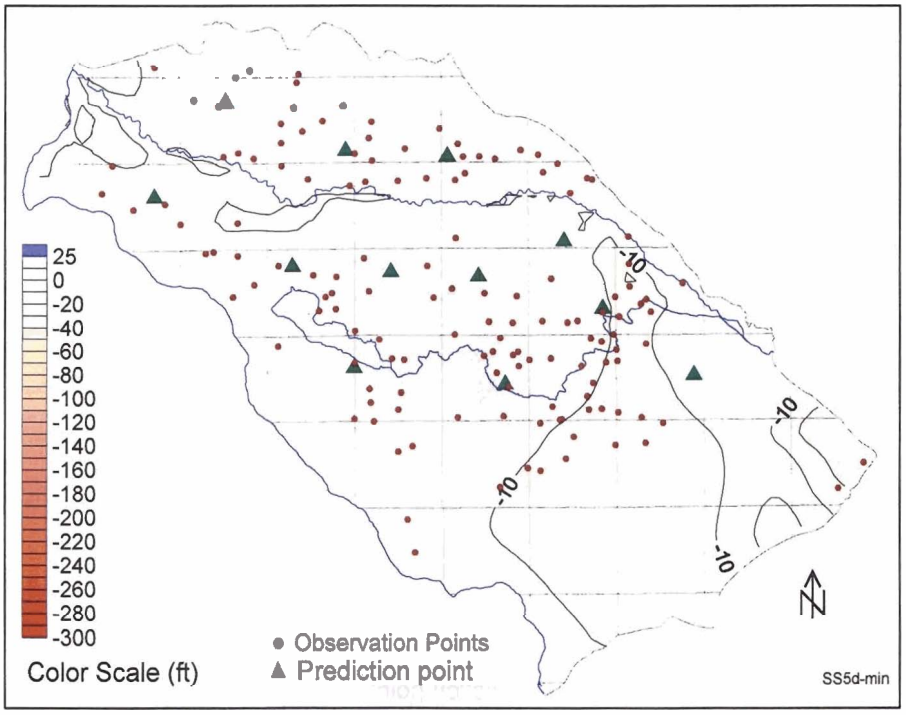

Figure 10-7: Head difference between base case and minimum predictive values, Scenario 1, layer 1.

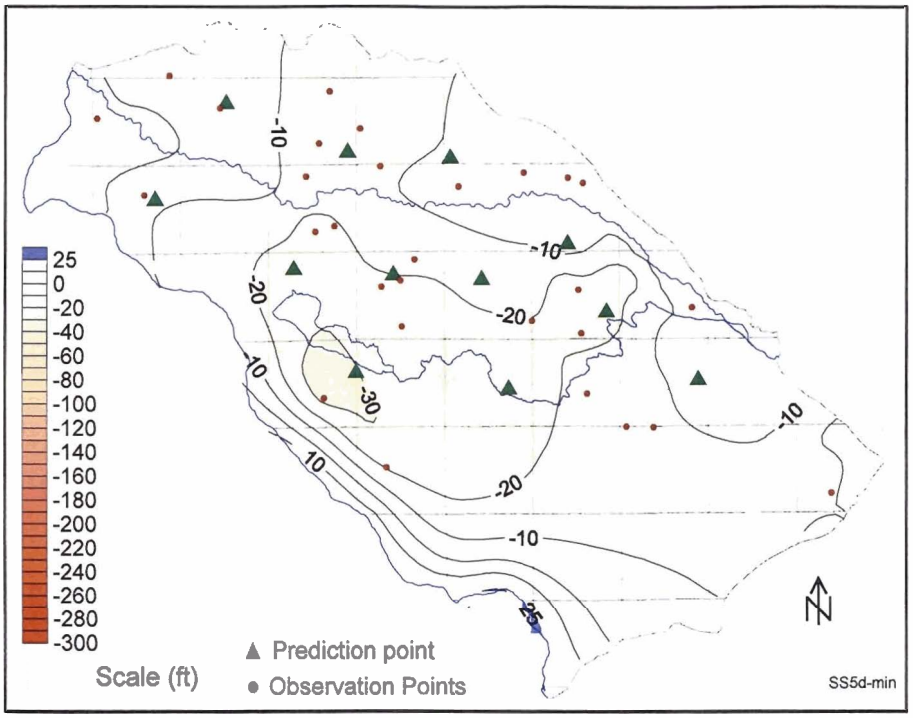

Figure 10-8: Head difference between base case and minimum predictive values, Scenario 1, layer 2.

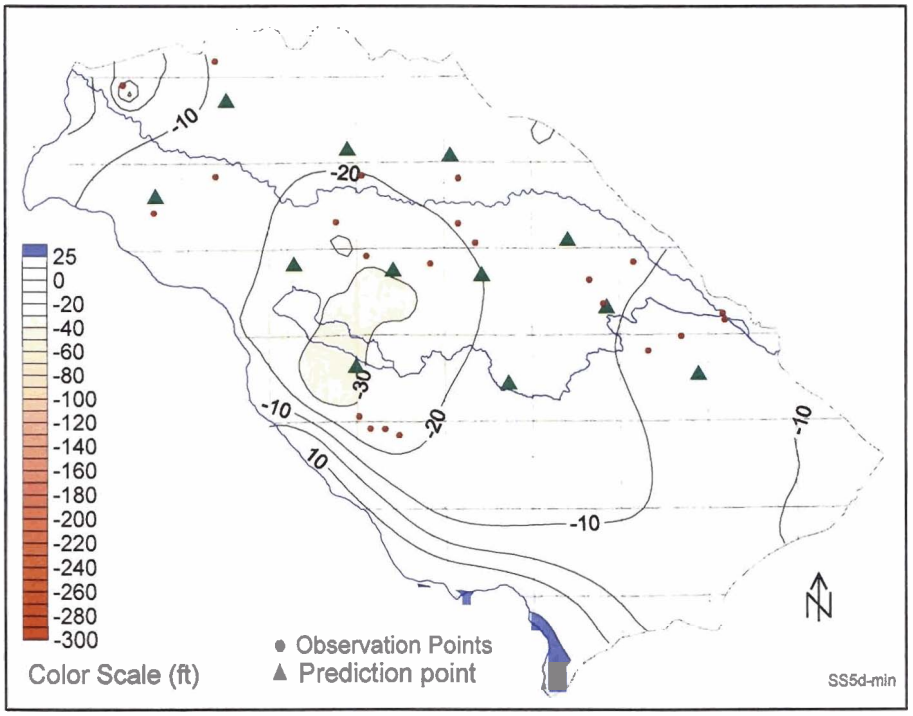

Figure 10-9: Head difference between base case and minimum predictive values, Scenario 1, layer 3.

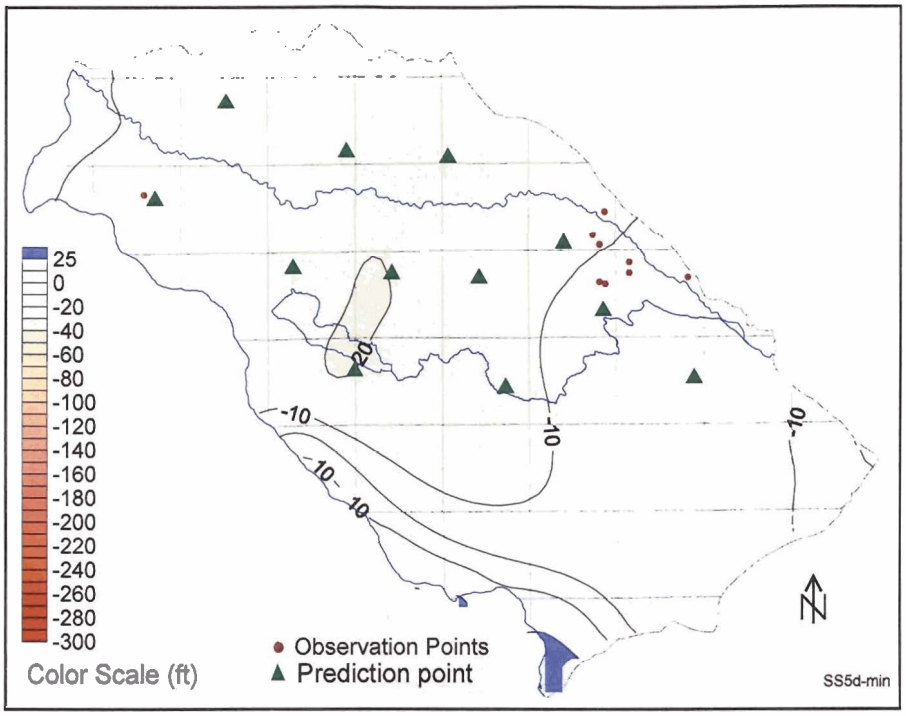

Figure 10-10: Head difference between base case and minimum predictive values, Scenario 1, layer 4.

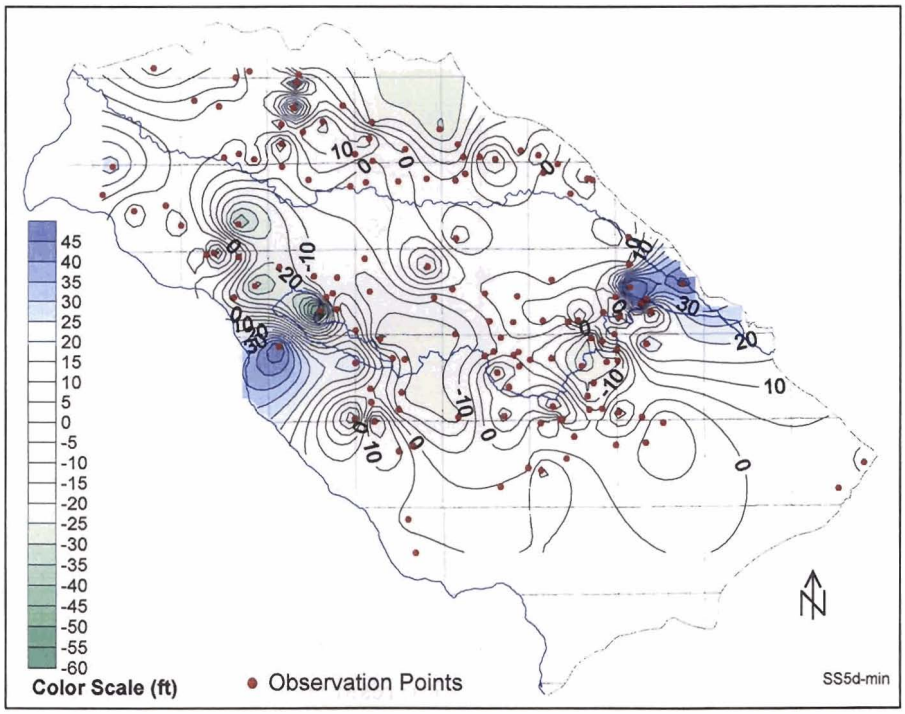

Figure 10-11: Scenario 1 simulation residuals, minimum heads, layer 1.

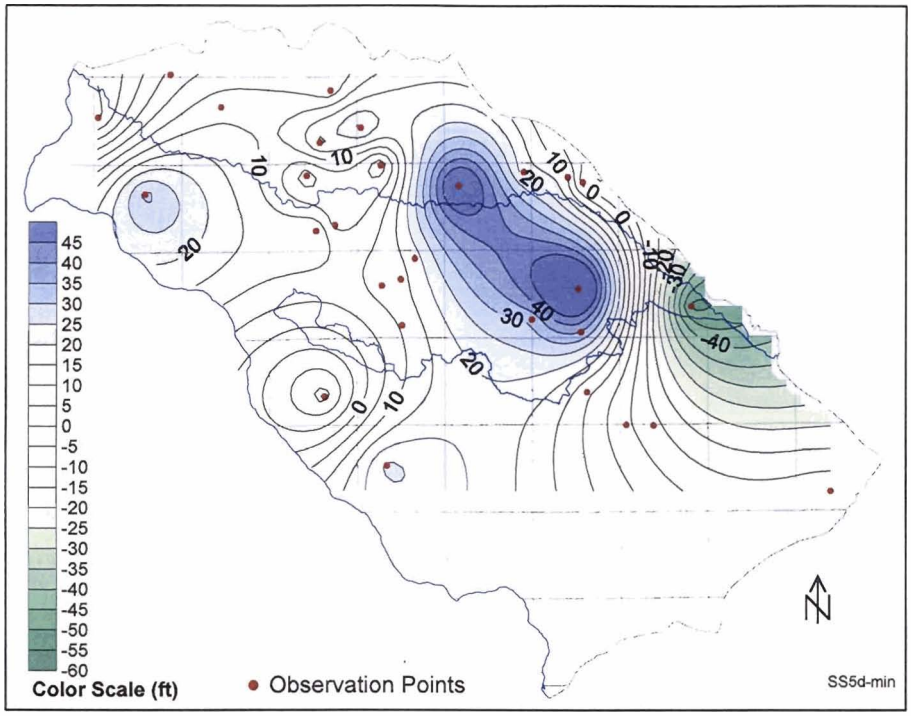

Figure 10-12: Scenario 1 simulation residuals, minimum heads, layer 2.

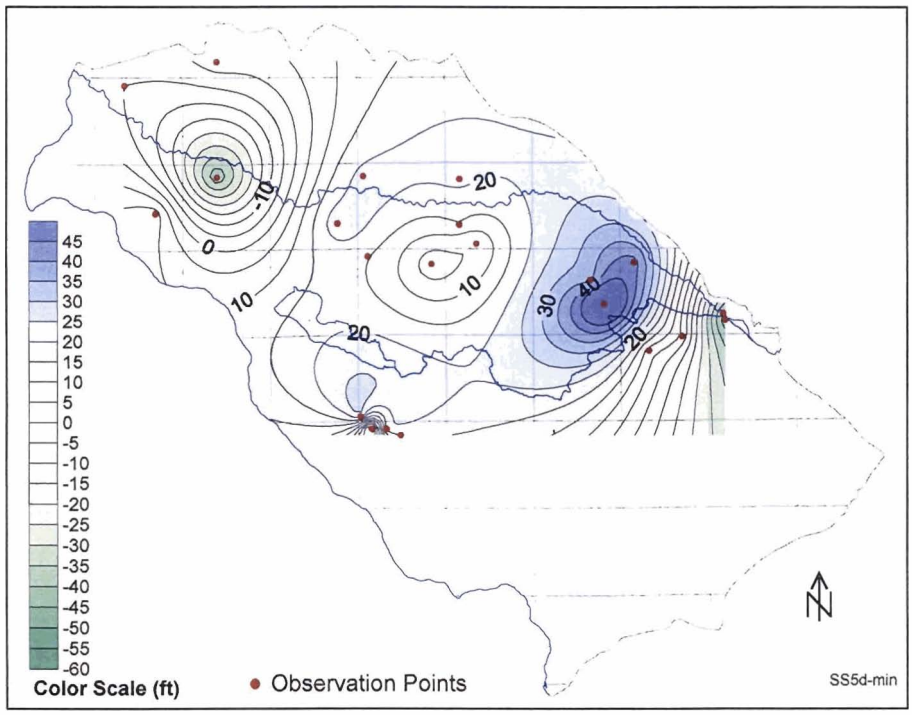

Figure 10-13: Scenario 1 simulation residuals, minimum heads, layer 3.

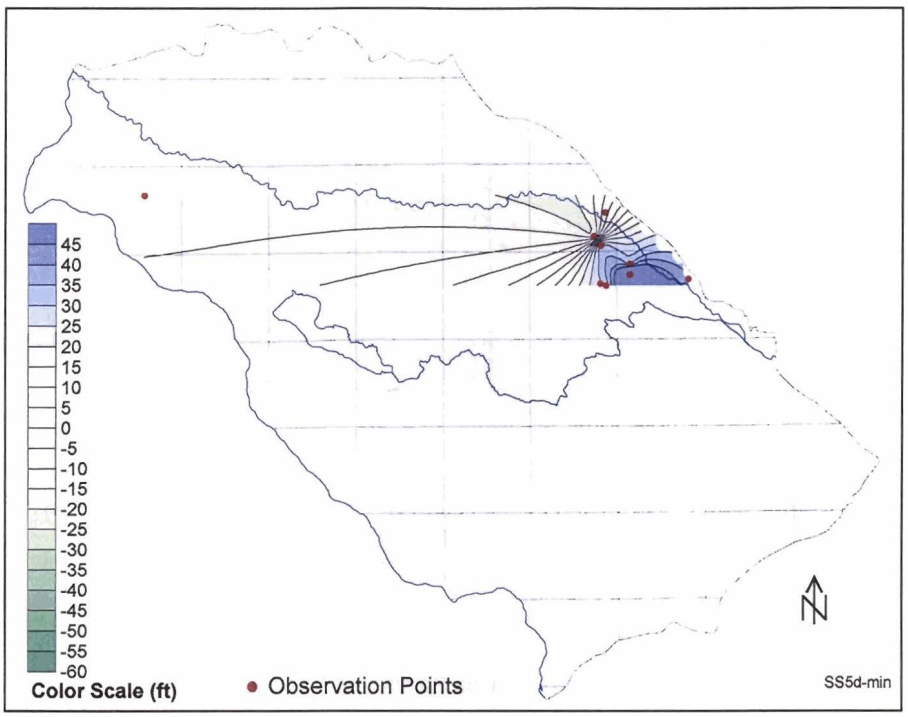

Figure 10-14: Scenario 1 simulation residuals, minimum heads, layer 4.

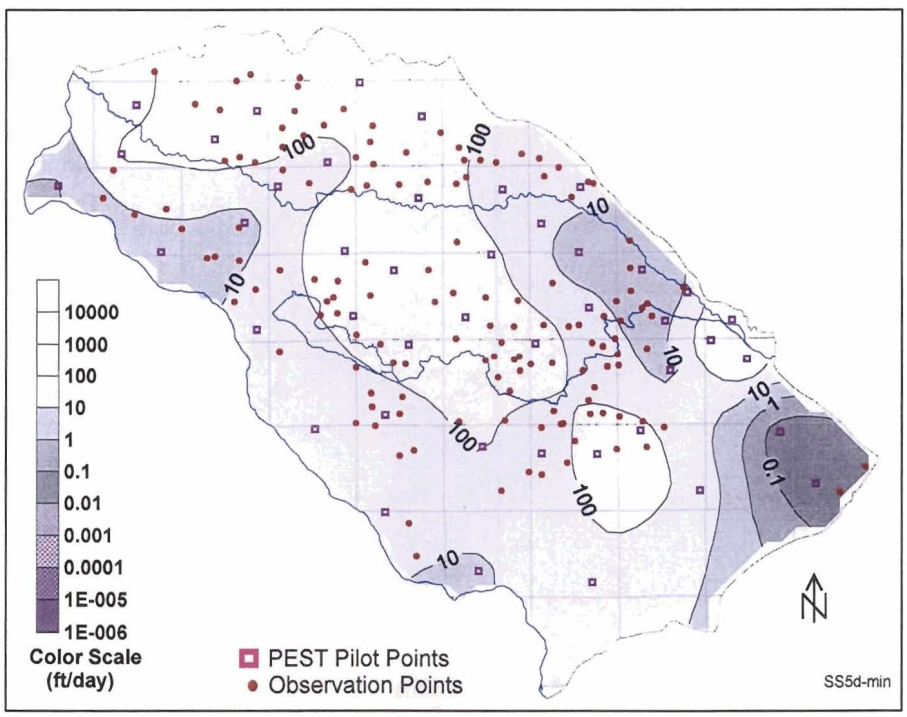

Figure 10-15: Simulated horizontal hydraulic conductivity distribution, Scenario1, layer 1.

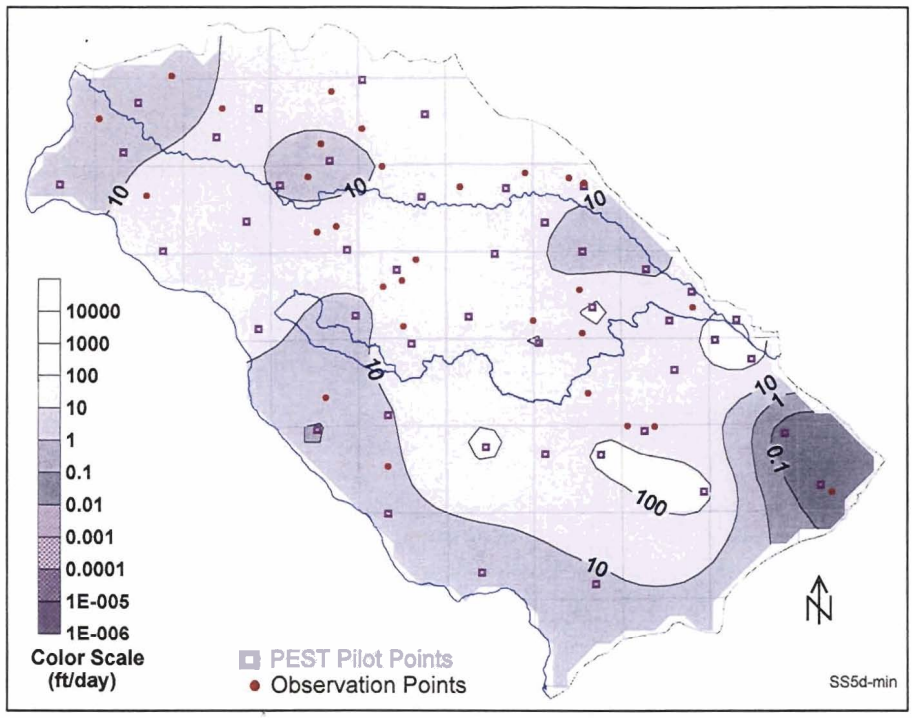

Figure 10-16: Simulated horizontal hydraulic conductivity distribution, Scenario1, layer 2.

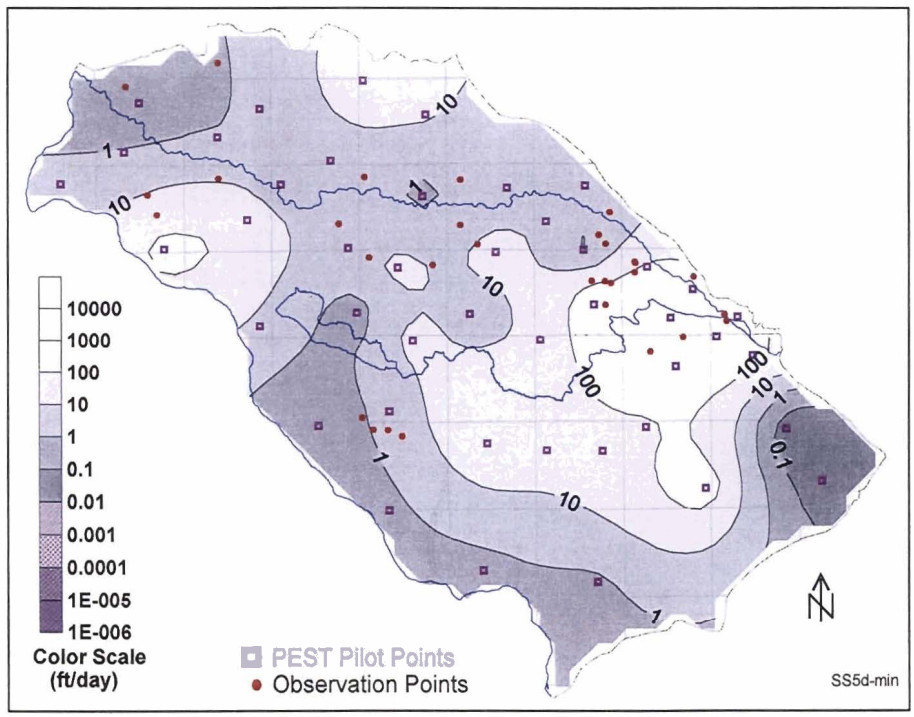

Figure 10-17: Simulated horizontal hydraulic conductivity distribution, Scenario1, layers 3 and 4.

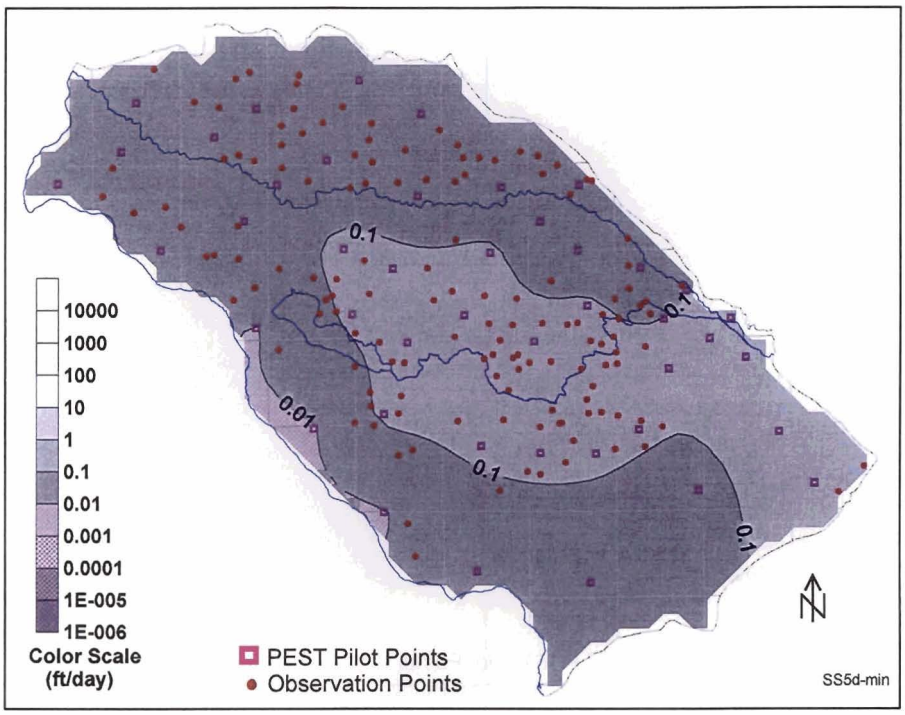

Figure 10-18: Simulated vertical hydraulic conductivity distribution, Scenario1, layer 1.

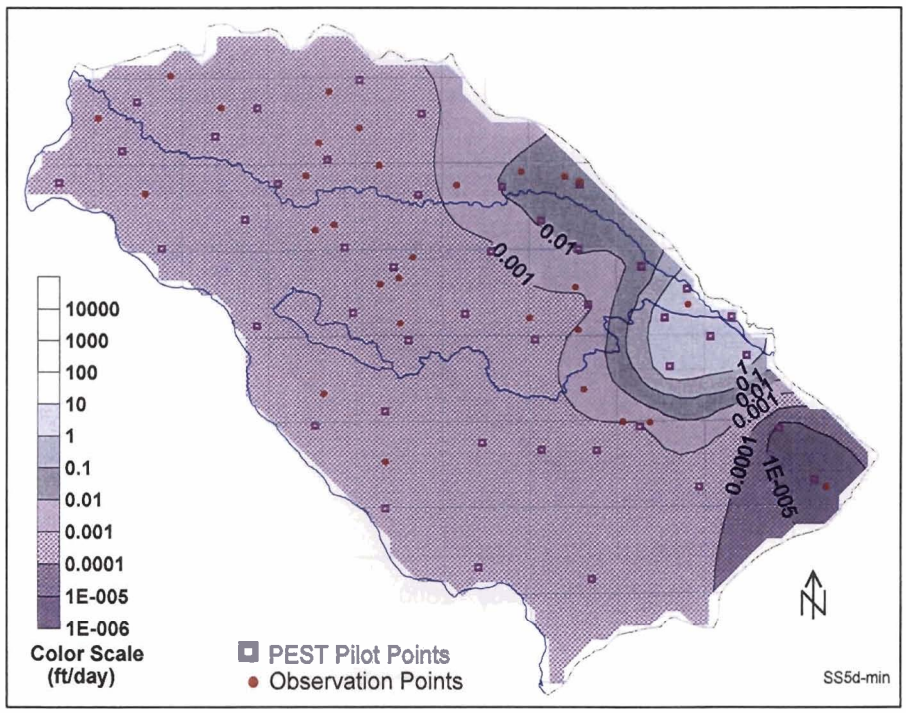

Figure 10-19: Simulated vertical hydraulic conductivity distribution, Scenario1, layer 2.

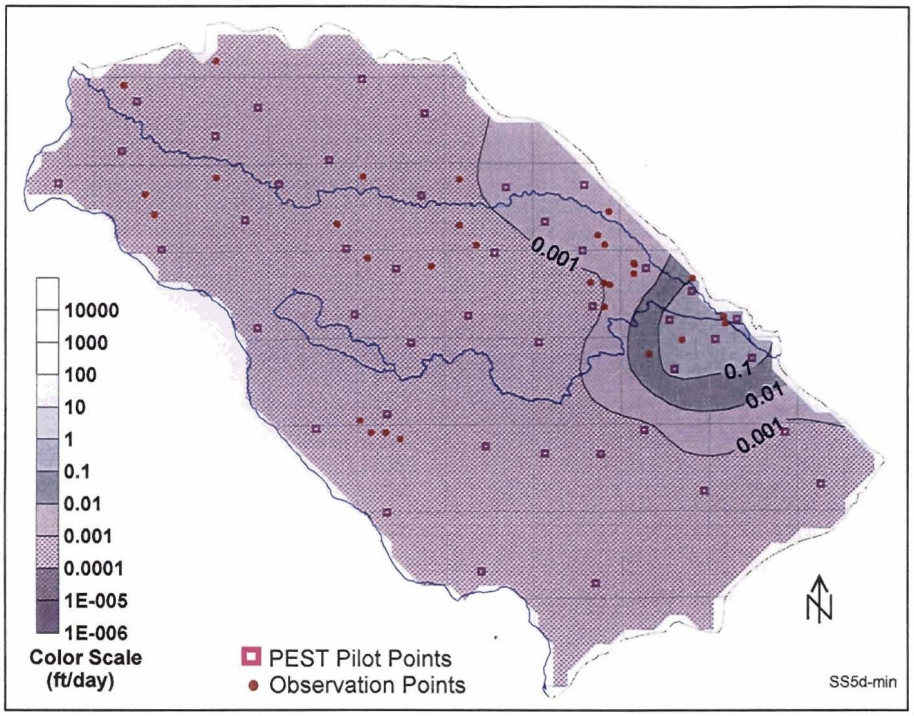

Figure 10-20: Simulated vertical hydraulic conductivity distribution, Scenario1, layers 3 and 4.

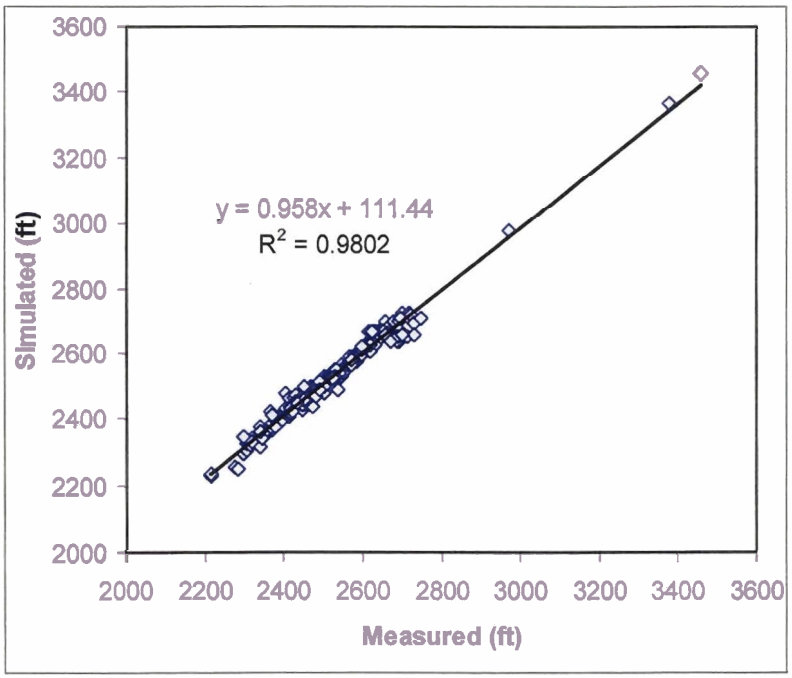

Figure 10-21: Simulated versus measured hydraulic head observations, steady-state hydraulic conditions (increased withdrawals simulation, maximum prediction).

Scenario 1 Simulation Results (*SS5b-max*) (based on observations with PEST weights greater than zero)				
Beginning prediction (ft)	2,491.3			
Ending prediction (ft)	2,500.1			
Initial objective function	6,427.2			
Initial contribution to Φ from heads	3,220.4			
Initial contribution to Φ from regularization	3,150.3			
Initial contribution to Φ from gradients	56.5			
Ending objective function (Φ)	7,020			
Ending contribution to Φ from heads	3,799			
Ending contribution to Φ from regularization	3,022			
Ending contribution to Φ from gradients	199			
Highest eigenvalue	1.41			
Lowest eigenvalue	2.69×10^{-7}			
Number of PEST iterations	3			
Number of MODFLOW runs	868			
Run Statistics (based on observations with weights > 0)				
	Total	**Layer 1**	**Layer 2**	**Layers 3 and 4**
Maximum positive residual	74.65	57.46	53.55	74.65
Minimum negative residual	-73.54	-73.54	-53.93	-51.52
Average absolute residual	16.59	15.19	16.34	23.12
Median absolute residual	11.63	11.20	12.26	19.84
Number of values	200	140	29	31

Table 10-2: Summary of results, Scenario 1, maximum head levels.

Simulation Volumetric Budget Comparison			
	Base Simulation (*SS2bc*)	**20% Increase in 1996 Withdrawal Rates (Minimum heads) (*SS5d-min*)**	**20% Increase in 1996 Withdrawal Rates (Maximum heads) (*SS5d-max*)**
Inflows			
Constant head	28,891	28,133	30,850
Wells	108,000	108,000	108,000
Drains	0	0	0
River leakage	5,784,137	6,827,901	7,270,731
Head-dependent boundaries	1,537,895	1,673,447	1,267,186
Recharge	116,205,088	116,205,088	116,205,088
Total In	123,664,008	124,842,568	124,881,856
Outflows:			
Constant head	17,350,556	16,939,652	16,091,218
Wells	23,076,956	27,692,348	27,692,348
Drains	36,667,716	33,778,404	38,858,980
River leakage	46,486,872	46,368,532	42,127,248
Head-dependent boundaries	81,961	63,698	112,129
Recharge	0	0	0
Summary			
Total	123,664,064	124,842,624	124,881,920
In - Out	-56	-56	-64
Percent discrepancy	0	0	0

Table 10-3: Simulation volumetric budget comparison (ft^3/day).

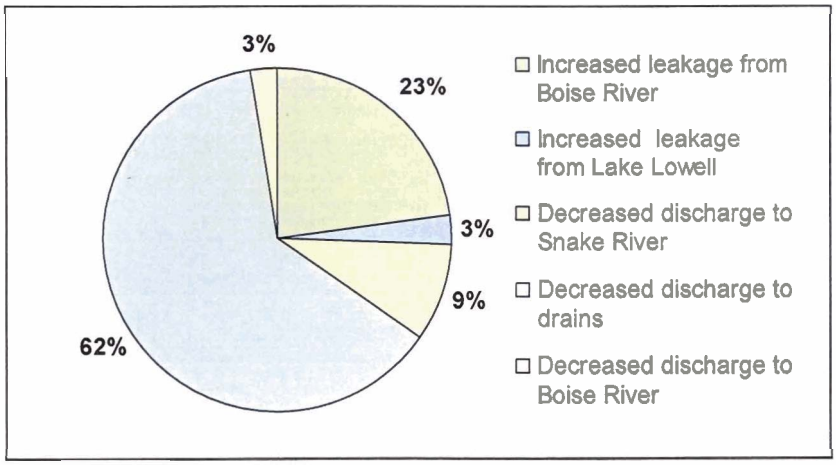

Figure 10-22: Sources of water for increased simulated withdrawals (*SS5d-min*).

11. SUMMARY AND DISCUSSION

A numerical model was constructed to simulate regional-scale ground water flow in the Treasure Valley of southwestern Idaho. The MODFLOW (McDonald and Harbaugh, 1996) model was calibrated to steady-state hydraulic conditions using the PEST automated parameter estimation code (Doherty, 2000).

Several sensitivity calibrations were conducted with the model to investigate potential variability in fixed model variables. In addition, one predictive (scenario) simulation was conducted for an across-the-board 20% increase in ground water withdrawals. This section provides a summary and discussion of results from these simulations. A second predictive simulation was performed to evaluate the potential effects on regional ground water levels associated with currently-unprocessed water right applications, which is described under separate cover (Petrich, 2004a).

As a regional-scale model, this model is appropriate for use in simulating regional-scale flow characteristics. It is not appropriate for simulating small-scale, local conditions or drawdowns in single wells. A regional-scale model can form the framework for constructing submodels or refined-grid models to simulate more detailed, local conditions. Model results from the calibration, sensitivity, and predictive simulations yielded several observations. These are discussed in the following sections.

11.1. Residuals Between Simulated and Observed Water Levels

Simulations generally resulted in reasonable agreement between simulated and observed water levels, with median absolute residuals ranging between about 8.5 and 9.5 feet. These magnitudes are probably within the error associated with some of the well elevations (well elevations were generally taken from USGS 7.5-minute quadrangle maps or by field-grade GPS devices).

The maximum absolute residuals, however, ranged to over 74 feet in the base simulation (Table 7-1) and over 165 feet in one of the sensitivity simulations (Table 8-3). Large residuals can occur for three general reasons: (1) observation data do not reflect local conditions, (2) well elevations are incorrect, or (3) local hydrologic conditions are incorrectly represented in the model. An observation may not reflect local conditions because the observation well was being pumped, influenced by pumping in a nearby well, completed in an aquifer zone other than that to which the well is attributed, or because of measurement errors. The average water levels (averaged between spring and fall measurements) may not reflect equilibrium water levels. Several observations were discarded upon review of specific local conditions in the context of abnormally large residuals. Several of the wells for which simulated water levels were substantially different than those measured (therefore resulting in a large residual) may not adequately reflect local conditions.

Two of the wells experiencing large residuals (Figure 8-8) in one of the simulations (10% decrease in recharge) are higher elevation wells in the eastern portion of the model domain. This entire portion of the model was problematic because of a lack of stratigraphic and water level data for this area. There is an apparent steep hydraulic gradient between this area and the remainder of the model domain. The hydraulic continuity of aquifer(s) in the far eastern portion of the model domain with the rest of the Treasure Valley aquifers is uncertain.

PEST could be forced to reduce model residuals by relaxing regularization constraints or by simply allowing the calibration to proceed through a greater number of iterations. Aquifer parameter values can be adjusted to meet individual observations more closely (resulting in decreased residuals), but the resulting distortion of aquifer parameter values is probably unjustified in most places, given (1) the potential for erroneous observations and (2) the relatively consistent regional-scale lacustrine/deltaic depositional environment that covers much of the model domain.

11.2. Mass Balance

The aquifer inflows and outflows reported in the base simulation mass balance (Section 7.2.1) are very similar to those estimated in the 1996 water budget (Urban and Petrich, 1998) because many of the simulated inflows and outflows are specified values. Flux rates through head-dependent model boundaries (e.g., drain, general head, and river cells) could be better constrained through the calibration of conductance parameters with better estimates of discharge to drains, canals, and rivers. There is a substantial effort underway to compile these data by the USBR, but the data were not available at the time of model calibration.

11.3. Potentiometric Surfaces

Comparisons of observed and simulated potentiometric surfaces in the base simulations were relatively close in areas of numerous observation data (i.e., the central portion of the basin). Areas of substantial discrepancy included the eastern, southeastern, and southern portions of the model domain. The discrepancies were attributed to inconsistent data, interpolation errors, and uncertain boundary conditions.

11.4. Boundary Conditions

Boundary conditions influenced the model simulations, especially in the vicinity of the Boise Front, the eastern model corner, and along the Snake River. For instance, the amount of underflow entering the northeastern boundary is highly uncertain, yet influences the estimation of aquifer parameter values in this area. Similarly, layer surfaces extend downward from the northern part of the model domain to the southern boundary along the Snake River. The stratigraphic nature of these sediments underlying the Snake River is unknown because there are few deep wells in this area.

The K_v of these sediments has substantial influence on the vertical movement of water from deeper aquifers upward toward the Snake River. Boundary conditions may be refined as more information becomes available.

11.5. A Discharge-Limited Flow System?

The conceptual model for ground water flow in the regional aquifer system (Section 2) outlines three possible reasons for the large ground water residence times (e.g., greater than 20,000 years) estimated from carbon-14 age-date analyses (Hutchings and Petrich, 2002a). Large residence times could be the result of (1) low aquifer transmissivity, (2) low recharge rates, and/or (3) low discharge rates.

It is unlikely that high residence times are the result of low transmissivity characteristics. Although there are abundant silt and clay layers with low hydraulic conductivity, productive sand layers are present throughout central portions of the valley. These sand zones are tapped by many irrigation and municipal wells. Thus, low aquifer transmissivity is probably not the sole cause of large ground water residence times.

More likely explanations for large residence times might be low discharge and/or recharge rates. Thick lacustrine clays throughout large portions of the basin limit vertical ground water flow. Thick clay layers at the distal end of the basin likely inhibit upward (discharge) flow, limiting the amount of water from deeper aquifers that can flow upward through the system. Numerous deep wells (and some relatively shallow wells) with artesian flow and/or substantial upward gradients in the western portion of the valley (e.g., TVHP#2 well, Figure 2-5) point to a system that is at least partially confined and discharge-limited by these clay aquitards. Similarly, the aggregate effects of lacustrine clays also limit recharge to the deep aquifer system over large portions of the basin (based on lithologic observations and water chemistry differences). The primary area of downward flow (e.g., TVHP#4 well,) is through alluvial/fluvial sediments in the far eastern portion of the basin.

Are the deep aquifers, particularly in the western portion of the basin, completely confined? If the deeper aquifers were completely confined, and if there were no withdrawals from the deeper aquifers, one would expect head differences between the bottom of deep wells and ground surface to be much greater than they currently are (possibly as much as 200 feet, based on elevation differences between recharge elevations and down-valley well elevations). However, artesian heads are often less; 40-foot head differences between screen and ground surface are more common (E. Squires, per. comm., 2000), such as those indicated in the TVHP Caldwell monitoring well (Figure 2-5). The difference between the theoretical and observed vertical head differences could be attributed to (1) leaky confining conditions and/or (2) the effects of current levels of withdrawals.

The simulations reflected the aggregate effects of fine-grained silt and clay layers that are present in much of the basin. The simulations indicated a relatively small amount of vertical flux between model layers (Table 7-4) compared to the magnitude of total flux into and out of the aquifer system (Table 7-3). The difference between downward and upward simulated flux rates in the lower model layers was accounted for primarily by simulated aquifer withdrawals.

It is unclear from these simulations to what extent the deep, regional Treasure Valley flow system is discharge- or recharge-limited. The implication of a discharge-limited flow system is that additional withdrawals could induce greater recharge from the eastern portion of the model area (e.g., Boise area) where downward flux occurs. At some point, recharge rates and/or aquifer transmissivities would limit the amount of water that can be withdrawn without substantial ground water level declines. Additional data collection and simulations with greater withdrawal levels are warranted to estimate the extraction levels at which discharge might exceed recharge and substantial water level declines occur.

11.6. Impact of Variations in Total Recharge

Results from model simulations with increased and decreased total recharge (Sections 8.2 and 8.3) indicated small water level differences. It appears that the ground water levels in the shallow system are not very sensitive to this amount of variation (e.g., ± 10%) in recharge. There are two probable reasons for this.

First, shallow ground water levels are close to ground surface in many portions of the central basin, especially in flood-irrigated areas. Shallow ground water levels are controlled by the elevations of canals and ditches, a portion of which were installed solely to collect shallow ground water. These surface channels (Boise River, Snake River, and drains) appear to prevent ground water level rises in response to a 10% increase in recharge. Similarly, a decrease in recharge results in a decrease in discharge to surface channels. Second, relatively high PEST-calibrated K_h values (Figure 7-10, Figure 8-7, and Figure 8-13) facilitate effective movement of excess shallow recharge.

The implication of this is that increased recharge in areas drained by surface channels (e.g., drains, canals, and rivers) would lead to more surface water discharge. Decreased recharge (i.e., resulting from changing land use) would lead to decreasing surface water discharge, as long as local aquifer levels remain above those of the surface channels. Shallow ground water levels could decrease rapidly on a local basis if recharge decreased to the point where shallow ground water levels were below that of the surface channels. Additional simulations based on more detailed local data might help identify the amount of decrease necessary for this to occur.

The prime areas of recharge to the deeper flow system in the central portion of the valley include underflow from basin margins, the upper reaches of the lower Boise

River (e.g., below Barber Dam and upstream of Capital Street Bridge), and areas underlain by alluvial fan sediments in the eastern portion of the basin. The latter two areas experience downward hydraulic gradients (e.g., Boise Municipal Park well, Figure 2-5). These areas would not appear to be substantially impacted by decreases in recharge to the shallow system in central portions of the valley.

11.7. Role of Basin Underflow

The rate and spatial and vertical distribution of underflow into the valley and into the model domain is highly uncertain. The amount of underflow estimated in the 1996 water budget (Urban and Petrich, 1998) was based on the difference between precipitation falling in the Boise Foothills, runoff, and evapotranspiration. However, even if the total volume is correct, it is highly unlikely that the underflow is equally distributed with depth or along the Boise Foothills. Both of these conditions were assumed in the model for lack of better information.

The amount of underflow is relatively small compared to other water budget components but is large (Section 8.3.1) compared to downward simulated fluxes into lower model layers (Table 7-4). The amount of underflow affects both K_h and K_v parameter estimates in areas near the northeastern model boundary. Additional simulations with various combinations and distributions of underflow values may provide insight into actual underflow conditions.

11.8. Impact of Increased Ground Water Withdrawals

Ground water levels appear to be relatively sensitive to regional increases in ground water withdrawals from the regional flow system. This was seen in areas of maximum simulated ground water level declines in response to the 20% increase in withdrawals (Section 10.2 and Figure 10-7 through Figure 10-10). Areas of predicted shallow aquifer declines developed in the Boise area and south of Boise, east of the New York Canal[19]. The greatest regional simulated declines began to develop in deeper aquifers near and south of Lake Lowell.

Several factors may have contributed to these simulated declines. First, the simulated declines are partly the result of increased withdrawals and partly the result of parameter uncertainty. Second, more water may be leaking from Lake Lowell, at least into shallow zones, than was described in the model because of uncertainty regarding the conductance values used in the Lake Lowell general head boundary. More leakage would mitigate the simulated declines. Third, simulated K_h values may have been lower in this area because the model attempted to calibrate to current declines in this area. Fourth, because of the current declines, it is unlikely that substantial increases in

[19] Areas of decline extending south to the model boundary are unsubstantiable because of a lack of withdrawals and observations in this area.

withdrawals would be permitted in this area. Finally, simulated K_v values in this area may be too low, preventing simulated vertical downward movement of water that might help mitigate some of the deeper declines.

Part of the simulated declines can be attributed to parameter uncertainty. The predictive simulations found a combination of parameter values that minimized (or maximized) simulated heads and minimized the residuals between simulated and measured observations in the base simulation. The resulting head values were compared to head values from the pre-predictive analysis simulations, which are not optimized for a minimum (or maximum) outcome. Thus, a comparison between the two represents changes in the calibration and hydraulic stress. This also applies to the base balance comparisons between the base simulation and predictive scenario (e.g., Figure 10-22). The changes in mass balance reflect both increased withdrawals and parameter uncertainty.

An alternative approach to evaluating potential head declines would have been to first run predictive analyses using the base simulation. Heads (or mass balance terms) could be minimized (or maximized) with no changes in model stresses (e.g., increase in withdrawals). The resulting head distribution from these simulations would then form the basis for the comparison between base simulation and predictive scenarios.

Another approach would have been to simulate the maximum or minimum change in water levels (instead of simulating minimum or maximum heads) in the predictive analyses with increased withdrawals. This approach would have eliminated some of the parameter uncertainty inherent to the base simulation. In other words, one might not be able to determine the precise head level at a given point in the base simulation (because of parameter uncertainty), but one would be able to predict the maximum head decrease at that point in response to additional simulated withdrawals. This approach also would have eliminated the interpolation error that arose in comparing two surfaces.

What do these results from increased withdrawal simulations mean for a water manager? Predicted regional declines in some areas based on model simulations should not necessarily preclude additional ground water development in these areas. First, additional simulations (see recommendations in Section 12) may allow improved predictions regarding possible declines. Second, managers might consider enhanced water level monitoring in these areas to detect possible changes should increased withdrawals occur.

Model predictions for some areas (i.e., some shallow aquifers) indicate that additional withdrawals are probably possible without changing water levels. However, additional extractions in these areas may increase losses from, or decrease discharge to, surface water channels. Such interaction between ground and surface water is of increasing interest to water users and water managers in the Treasure Valley. One approach to better evaluate the current (or future) effects of ground water withdrawals on surface

flows would be through the development of response functions. Response functions have been developed in the ESRP to better define the impact of ground water withdrawals on specific reaches of the Snake River (Johnson and Cosgrove, 1999). The precision of such simulations could be enhanced using a more refined grid than, and/or submodels of, the current model.

11.9. Transient Flow Simulations

Model results for a steady-state simulation describe equilibrium conditions. The time required to reach equilibrium is not estimated in a steady-state simulation. A transient model can be constructed to simulate temporal conditions and estimate the time required to reach a steady-state equilibrium. However, a transient model was not developed as part of this project. Construction of a transient model for the regional Treasure Valley domain faces two challenges.

First, transient simulations require more detailed temporal flux data than were available during the course of this project. The USBR and IDWR are currently compiling more detailed irrigation diversion and return data for the valley, which would be essential for transient simulations (especially those focusing on shallow aquifer conditions). However, these data were not available at the time of model construction and simulation.

Second, a transient simulation requires the estimation of aquifer storativity values[20]. Often storativity is correlated with hydraulic conductivity. Temporal water level change data are required to help calibrate the storativity parameters. Transient simulations with temporal data can be conducted over short or long periods of time, depending on data availability. With several exceptions, Treasure Valley water levels have remained relatively steady over the last several decades, and therefore may not provide adequate long-term changes that could be used to calibrate a transient model. Exceptions include an area south of Lake Lowell and southeast Boise, but these two areas are probably not extensive enough to provide a sufficient basis for a regional transient model calibration. Seasonal water levels do fluctuate (see hydrographs in Petrich and Urban, 2004); fluctuations are dominated by two general patterns. Water levels in wells are influenced either by water level rises corresponding with irrigation applications or by summer irrigation withdrawals, or both. However, many of the seasonal water level fluctuations are within median residual ranges (e.g., ± 10-15 feet) or within the error range associated with well elevations[21] (also about ± 10-15 feet). These seasonal water level fluctuations may be insufficient for a solid seasonal transient calibration for a model covering the entire Treasure Valley area.

---

[20] Aquifer storativity is assumed to be zero during a steady-state simulation, because water levels do not change with time in a steady-state simulation.

[21] Many of the water levels used for calibration come from wells for which elevations have been estimated from USGS quad map contours or from field-grade GPS devices.

However, transient calibrations may be feasible for local ground water flow models within the Treasure Valley or submodels of the regional model. These calibrations would be possible (depending on the specific type of question to be answered by the model) given the availability of detailed local water level and surface recharge/ discharge data.

11.10. Parameter Uncertainty and Model Limitations

The range of predicted head values for Scenario 1 (Section 10.2.2) reflects uncertainty associated with the model calibration. The minimum and maximum water levels that are possible with virtually the same distribution of K_h and K_v values is a quantification of uncertainty in these estimated parameter values. The uncertainty stems from parameter insensitivity (insufficient observations to constrain estimated parameter values) and parameter correlation (simultaneous changes in two parameter values yield the same outcome). The underlying cause of the uncertainty is a lack of observation data, insufficient information about aquifer stratigraphy and characteristics, including structural controls, and possible error in input data and/or model construction. A more detailed discussion of model limitations and factors contributing to model uncertainty is included in Section 6.

12. CONCLUSIONS AND RECOMMENDATIONS

A numerical model was constructed to simulate regional-scale, steady-state, ground water flow in the Treasure Valley of southwestern Idaho. Conclusions from simulations using this model consist of the following:

1. PEST-calibrated parameter values indicate relatively higher K_h values in the uppermost aquifer zones, corresponding with known areas of coarser-grained sediments. PEST-calibrated parameter values also indicate relatively higher K_h and K_v values in areas of the eastern and central portion of the valley associated with fluvial deltaic deposition.
2. Simulated fluxes between model layers in the base calibration indicates a relatively small amount of water moving vertically between model layers, especially in the lower layers. Based on simulation results, most recharge occurring in shallow aquifer zones does not reach lower zones.
3. A 10% increase or decrease in recharge led to minimal changes in water levels or parameter value estimates. This is because shallow ground water levels in central portions of the basin are controlled, in part, by elevations of surface water channels. Decreased or increased recharge resulted in changes in the rates of water discharging to model drain, general head boundary (Lake Lowell), constant head (Snake River), and river (Boise River) cells.
4. Underflow does not appear to be consistently distributed along the Boise Front. The model experienced difficulty in applying rates as high as 8,000 ft^3/day/cell (similar to water budget estimates) in some model areas, especially in the far eastern portions of the model domain.
5. Simulated minimum water levels (maximum impact) indicated that some ground water level declines might occur with a 20% increase over 1996 levels. Simulated modest declines were observed in the Boise area in layers 1 and 2. Greater simulated declines were observed in the central portion of the valley (especially in the Lake Lowell area) in layers 3 and 4. Simulated water level declines and/or changes in mass balance components reflect a combination of parameter uncertainty and response to a changed hydraulic stress.
6. The simulated 20% increase in ground water withdrawals resulted in increased losses from the Boise River (23%), decreased discharge to agricultural drains (62%), and decreased discharge to the Snake River (9%). Again, simulated water level declines and/or changes in mass balance components reflect a combination of parameter uncertainty and response to a changed hydraulic stress.
7. Uncertainty in the model calibration limits a more precise description of responses to changes in recharge and/or withdrawals.
8. Changes in land use that lead to decreases in shallow-aquifer recharge may not have a substantial effect on shallow ground water levels until the water table elevations remain below those of nearby surface channels.

Additional simulations should be considered to better define aquifer system characteristics or scenario predictions. These include the following:

1. Maximum and minimum hydraulic head predictions with no changes in model stresses from the base simulation. Use the results from these simulations for comparisons in scenario predictions.
2. Increases and decreases of 30% (over 1996 levels) in aquifer recharge.
3. Across-the-board withdrawal increases and decreases in aquifer withdrawals over 1996 levels.
4. Increased local withdrawals in various locations in the valley to test responses in water levels and in recharge rates to lower model layers.
5. Simulations with reductions in recharge and increases in withdrawals to estimate at what point shallow ground water levels drop below drain elevations in the central portion of the valley.
6. Horizontal and vertical variations in underflow along the Boise Front.
7. Conduct additional simulations to refine the understanding of ground and surface water interaction in the Boise River corridor using a more refined grid than, and/or submodel of, the current model .
8. Develop response ratios for the interaction between ground water extractions and seepage from or discharge to surface channels.

Additional recommendations include the following:

1. Expand monitoring in areas showing recent ground water level declines.
2. Consider incorporating new monitoring data into the model as they become available.
3. Better define discharge rates to surface water channels to allow more constraint on simulated discharge.
4. Better define temporal diversion and return rates for transient simulations.
5. Refine model based on newly compiled diversion and return data.
6. Install additional multi-completion monitoring wells to expand vertical gradient data.
7. Search for opportunities to enhance ground water level monitoring in portions of the valley with relatively few current data.

13. REFERENCES

Anderson, M.P. and Woessner, W.W., 1992. Applied Groundwater Modeling - Simulation of Flow and Advective Transport. Academic Press, 381 pp.

Brigham Young University, 2002. Groundwater Modeling System (GMS). Brigham Young University (supported by Environmental Modeling Systems, Inc. www.ems-i.com).

Brockway, C.E. and Brockway, C.G., 1999. Southeast Boise Aquifer Simulation and Aquifer Recharge and Recovery Evaluation. Brockway Engineering, prepared for Micron Technology, Inc.

Chiang, W.-H. and Kinzelbach, W., 2001. 3-D Groundwater Modeling with PMWIN. Springer-Verlag, Berlin Heilelberg New York.

Christensen, S. and Cooley, R.L., 2002. Experience gained in testing a theory for modelling groundwater flow in heterogeneous media, ModelCARE 2002. IAHS Publ no.277, Prague, Czech Republic.

de Sonneville, J.L.J., 1972. Development of a mathematical ground water model. M.S. thesis Thesis, University of Idaho.

Doherty, J., 1998. PEST - Model Independent Parameter Estimation. Watermark Computing, Australia.

Doherty, J., 2000. PEST - Model Independent Parameter Estimation. Watermark Computing, Australia.

Doherty, J., 2003. *written report comments.*

Freeze, R.A. and Cherry, J.A., 1979. Groundwater. Prentice-Hall, Englewood Cliffs, NJ, 604 pp.

Harbaugh, A.W., Banta, E.R., Hill, M.C. and McDonald, M.G., 2000. MODFLOW-2000, the U.S. Geological Survey modular ground water model—user guide to modularization concepts and ground-water flow process. U.S. Geological Survey, Open-File Report 00-92.

Harbaugh, A.W., Banta, E.R., Hill, M.C., and McDonald, M.G., 2000. MODFLOW-2000, the U.S. Geological Survey modular ground-water model--user guide to modularization concepts and the ground-water flow process. U.S. Geological Survey Open-File Report 00-92.

Hill, M.C., 1992. A computer program (MODFLOWP) for estimating parameters of a transient, three dimensional, ground-water flow model using nonlinear regression. U.S. Geological Survey Open-File Report 91-484.

Hill, M.C., Banta, E.R., Harbaugh, A.W. and Anderman, E.R., 2000. MODFLOW-2000, the U.S. Geological Survey modular ground-water model -- user guide to the observation, sensitivity, and parameter-estimation processes and three post-processing programs. U.S. Geological Survey Open- File Report 00-184.

Hutchings, J. and Petrich, C., 2002a. Ground water recharge and flow in the regional Treasure Valley aquifer system - geochemistry and isotope study. Idaho Water Resources Research Institute, Research Report IWRRI-2002-08.

Hutchings, J. and Petrich, C., 2002b. Influence of canal seepage on aquifer recharge near the New York Canal. Idaho Water Resources Research Institute, Research Report IWRRI-2002-09.

Johnson, G.S. and Cosgrove, D.M., 1999. Application of Steady-State Response Ratios to the Snake River Plain Aquifer. Idaho Water Resource Research Institute Research Report.

Lindgren, J.E., 1982. Application of a ground water model to the Boise Valley Aquifer in Idaho. M.S. Thesis, University of Idaho.

McDonald, M.G. and Harbaugh, A.W., 1988. A modular three-dimensional finite difference ground-water flow model. Techniques of Water-Resources Investigation of the United States Geological Survey. Book 6: Modeling Techniques.

McDonald, M.G. and Harbaugh, A.W., 1996. User's Documentation for MODFLOW-96, and update to the U.S. Geological Survey Modular Finite-Difference Ground-Water Flow Model. U.S. Geological Survey, Open-File Report 96-485.

Newton, G.D., 1991. Geohydrology of the regional aquifer system, Western Snake River Plain, Southwestern Idaho. U.S. Geological Survey Professional Paper 1408-G.

Nolet, G., Montelli, R. and Virieux, J., 1999. Explicit, approximate expressions for the resolution and a posteriori covariance of massive tomographic systems. Geophys. J. Int, 138: 36-44.

Petrich, C. and Urban, S., 2004. Characterization of Ground Water Flow in the Lower Boise River Basin. Idaho Water Resources Research Institute and the Idaho Department of Water Resources, Research Report IWRRI-2004-01.

Petrich, C.R., 2004a. Simulation of Increased Ground Water Withdrawals in the Treasure Valley Associated with Unprocessed Well Applications. Idaho Water Resources Research Institute, Research Report IWRRI-2004-03.

Petrich, C.R., 2004b. Treasure Valley Hydrologic Project - Executive Summary. Idaho Water Resources Research Institute, Research Report IWRRI-2004-04.

Poeter, E.P. and Hill, M.C., 1998. Documentation of UCODE a computer code for universal inverse modeling. U.S. Geological Survey, Water Resource Investigations Report 98-4080.

Squires, E. and Wood, S.H., 2001. Stratigraphic Studies of the Boise (Idaho) Aquifer System using Borehole Geophysical logs with Emphasis on Facies Identification of Sand Aquifers, prepared for the Treasure Valley Hydrologic Study, Idaho Department of Water Resources.

Squires, E., Wood, S.H. and Osiensky, J.L., 1992. Hydrogeologic Framework of the Boise Aquifer System, Ada County, Idaho. Research Technical Completion Report, Idaho Water Resources Research Institute, University of Idaho. 114 pp.

Urban, S.M. and Petrich, C.R., 1998. 1996 Water Budget for the Treasure Valley Aquifer System. Idaho Department of Water Resources Research Report.

Wood, S.H., 1997. Hydrogeologic Framework of the Boise Valley of Southwest Idaho. Dept. of Geosciences, Boise State University.

Wood, S.H. and Clemens, D.M., *in press*. Geologic and tectonic history of the western Snake River Plain, Idaho and Oregon. In: B. Bonnichsen, C.M. White and M. McCurry (Editors), Tectonic and Magmatic Evolution of the Snake River Plain Volcanic Province. Idaho Geologic Survey.

Appendix A: Conversion Factors

Volume

1 cubic foot of water = 7.4805 gallons = 62.37 pounds of water

1 acre-foot (af) = enough water to cover 1 acre of land 1 foot deep

1 acre-foot (af) = 43,560 cubic feet

1 acre-foot (af) = 325,850 gallons

1 million gallons = 3.0689 acre-feet

Flow Rates

1 cubic foot per second (cfs) = 448.83 gallons per minute (gpm) = 26,930 gallons per hour

1 cubic foot per second (cfs) = 646,635 gallons per day = 1.935 acre-feet per day

1 cubic foot per second (cfs) for 30 days = 59.502 acre-feet

1 cubic foot per second (cfs) for 1 year = 723.94 acre-feet

1 cubic meter per second (cms) = 25.31 cubic feet per second

1 cubic meter per second (cms) = 15,850 gallons per minute

1 million gallons per day (mgd) = 1,120.147 acre-feet per year

1 miner's inch = 9 gallons per minute

1 miner's inch = 0.02 cubic feet per second

Hydraulic Conductivity

1 gallon per day per foot^2 (gal/day/ft^2) = 0.134 foot/day = 0.0408 meters/day

Economic

$0.10 per 1,000 gallons = $32.59 per acre-foot

Appendix B: Listing of Model Files

Extension	Code	Description	Reference
.bas	MODFLOW	Basic package	(Harbaugh et al., 2000)
.bcf	MODFLOW	Block-centered flow package	(Harbaugh et al., 2000)
.wel	MODFLOW	Well package	(Harbaugh et al., 2000)
.drn	MODFLOW	Drain package	(Harbaugh et al., 2000)
0.ghb	MODFLOW	General head boundary package	(Harbaugh et al., 2000)
.oc	MODFLOW	Output control package	(Harbaugh et al., 2000)
.pcg	MODFLOW	Solver	(Harbaugh et al., 2000)
.rch	MODFLOW	Recharge package	(Harbaugh et al., 2000)
.2dg	GMS	2-D grid file	GMS Documentation
.ba6	GMS	Basic package	GMS Documentation
.bc6	GMS	Block-centered flow package	GMS Documentation
.dis	GMS		GMS Documentation
.dxf	GMS	DXF file	GMS Documentation
.gpr	GMS	GMS project file	GMS Documentation
.hed		Simulated hydraulic head values	GMS Documentation
.hob	GMS		GMS Documentation
.img	GMS	Identifies background image, lists registration points	GMS Documentation
.ini	GMS	Initialization file	GMS Documentation
.lmt	GMS		GMS Documentation
.mfn	GMS	MODFLOW name file	GMS Documentation
.mfr	GMS		GMS Documentation
.mfs	GMS	MODFLOW super file	GMS Documentation
.mst	GMS		GMS Documentation
.obs	GMS	Observation file	GMS Documentation
.xy	GMS		GMS Documentation
*2g.dat	GMS		GMS Documentation
*2s.dat	GMS		GMS Documentation
*3g.dat	GMS		GMS Documentation
.map	GMS	Map file	GMS Documentation

Table B-1: Listing of model files.

Appendix C: Steady-State Observation Data

GMS & PEST ID	WELL_NUMBER	Easting (ft)	Northing (ft)	Layer	Spring Water Level (ft)	Fall Water level (ft)	Average Water Level (ft)	Initial PEST Weight	Group
1_1	05N06W-26CAA1	1634246	15888187	1	2103	2102	2102.5	0.196	head
2_1	05N06W-11AAD1	1637331	15905899	1	2188	2190	2189	0.000	head
3_1	05N05W-20CCD1	1649875	15891124	1	2236	2241	2238.5	0.000	head
4_1	05N06W-35CAC1	1634612	15882114	1	2248	2256	2252	0.000	head
5_1	04N05W-07DCD1	1646212	15870172	1	2273	2272	2272.5	0.196	head
6_1	05N05W-04BCC1	1653386	15909343	1	2270	2274	2272	0.000	head
7_1	05N05W-32CDC1	1649953	15880396	1	2280	2283	2281.5	0.196	head
8_1	05N05W-13CBC1	1669236	15897821	1	2288	2290	2289	0.000	head
9_1	05N04W-34BCB1	1690172	15883790	1	2294	2296	2295	0.196	head
10_1	04N05W-21AAB2	1657600	15864207	1	2305	2305	2305	0.196	head
11_1	06N05W-35BAC1	1664741	15916539	1	2307	2305	2306	0.196	head
12_1	05N04W-35BBB1	1695527	15885118	1	2312	2318	2315	0.196	head
13_1	03N04W-15DCC1	1693674	15832283	1	2314	2318	2316	0.196	head
14_1	05N04W-08BCC1	1679420	15904617	1	2332	2333	2332.5	0.196	head
15_1	04N04W-22DDD1	1695298	15859411	1	2339	2335	2337	0.196	head
16_1	05N04W-36BCC1	1701110	15883109	1	2335	2338	2336.5	0.196	head
17_1	04N03W-16DDDC1	1721289	15864855	1	2348	2347	2347.5	0.000	head
18_1	01S02W-14CCC2	1760025	15738521	1	2347	2352	2349.5	0.196	head
19_1	04N03W-30ADA1	1711174	15857837	1	2353	2353	2353	0.000	head
20_1	05N04W-09DCA1	1688370	15902510	1	2353	2354	2353.5	0.196	head
21_1	04N04W-25BDD3	1702874	15856800	1	2356	2354	2355	0.000	head
22_1	04N03W-06AAA1	1711175	15880407	1	2360	2364	2362	0.196	head
23_1	05N03W-08DDC1	1715505	15901979	1	2366	2366	2366	0.196	head
24_1	06N04W-34DDB1	1694357	15913050	1	2368	2366	2367	0.196	head
25_1	04N03W-13BAA1	1734710	15870172	1	2374	2374	2374	0.000	head
26_1	04N03W-27CBAD1	1722863	15856461	1	2374	2376	2375	0.000	head
27_1	04N03W-04DDCD1	1720809	15875582	1	2376	2378	2377	0.196	head
28_1	04N03W-12ACDD1	1736018	15873214	1	2377	2378	2377.5	0.196	head
29_1	01S02W-03DBC1	1757302	15750550	1	2386	2390	2388	0.196	head
30_1	05N03W-30ADD1	1711074	15888807	1	2391	2385	2388	0.196	head
31_1	04N02W-07AAC1	1741740	15874656	1	2391	2391	2391	0.196	head
32_1	04N03W-24ACB1	1735179	15863494	1	2392	2392	2392	0.000	head
33_1	06N04W-35ADC1	1699408	15915391	1	2394	2393	2393.5	0.196	head
34_1	03N03W-27ABB1	1724960	15827320	1	2408	2399	2403.5	0.196	head
35_1	06N03W-33CBA1	1717369	15914131	1	2403	2402	2402.5	0.196	head
36_1	03N04W-13BBC1	1701386	15836756	1	2418	2405	2411.5	0.196	head
37_1	05N03W-19AAD1	1710978	15895891	1	2410	2411	2410.5	0.196	head
38_1	04N05W-14DAD1	1669057	15866243	1	2411	2412	2411.5	0.196	head
39_1	06N03W-30DCC1	1708709	15917645	1	2411	2412	2411.5	0.000	head
40_1	04N03W-25DAA3	1737559	15856926	1	2410	2414	2412	0.000	head
41_1	04N02W-21CBB1	1748187	15862542	1	2414	2416	2415	0.000	head
42_1	04N02W-10BBCB1	1753560	15875018	1	2423	2422	2422.5	0.196	head
43_1	04N04W-21CAA2	1687357	15861720	1	2418	2423	2420.5	0.000	head
44_1	03N02W-06ACD1	1741283	15846620	1	2422	2425	2423.5	0.196	head
45_1	05N03W-21CAD1	1718764	15893084	1	2423	2425	2424	0.196	head
46_1	05N02W-20BBA1	1743912	15896630	1	2424	2426	2425	0.196	head

GMS & PEST ID	WELL_NUMBER	Easting (ft)	Northing (ft)	Layer	Spring Water Level (ft)	Fall Water level (ft)	Average Water Level (ft)	Initial PEST Weight	Group
47_1	05N02W-24DAB1	1768647	15894129	1	2433	2427	2430	0.196	head
48_1	04N02W-31AAA1	1742863	15854217	1	2425	2428	2426.5	0.000	head
49_1	05N02W-32CBD1	1744199	15882461	1	2426	2428	2427	0.196	head
50_1	05N03W-12CCA1	1733322	15902756	1	2430	2429	2429.5	0.196	head
51_1	03N03W-11DAC1	1731237	15839794	1	2430	2433	2431.5	0.196	head
52_1	03N03W-10CBA3	1722777	15840368	1	2441	2435	2438	0.196	head
53_1	03N02W-08BCCC1	1743293	15841365	1	2436	2439	2437.5	0.000	head
54_1	04N02W-02DDD1	1763908	15875985	1	2441	2441	2441	0.196	head
55_1	05N02W-31BBC1	1737802	15884962	1	2435	2441	2438	0.196	head
56_1	05N02W-27DCC1	1756141	15886772	1	2442	2440	2441	0.196	head
57_1	04N02W-33ABC1	1751025	15853447	1	2439	2442	2440.5	0.000	head
58_1	04N04W-28ACB1	1687733	15857773	1	2434	2443	2438.5	0.000	head
59_1	03N03W-23DCD1	1731065	15827952	1	2451	2452	2451.5	0.196	head
60_1	03N02W-17CCB2	1743114	15834481	1	2442	2444	2443	0.196	head
61_1	03N03W-06DDC1	1710190	15843765	1	2452	2451	2451.5	0.196	head
62_1	02N03W-36DAD1	1737866	15787497	1	2460	2446	2453	0.196	head
63_1	05N03W-15DDC1	1726086	15896856	1	2442	2447	2444.5	0.196	head
64_1	05N03W-04BCB1	1716647	15911092	1	2448	2447	2447.5	0.196	head
65_1	03N03W-14CDA1	1729643	15833816	1	2446	2448	2447	0.196	head
66_1	03N04W-05AAB1	1683784	15848252	1	2460	2443	2451.5	0.196	head
67_1	05N01W-29CBA1	1775355	15888601	1	2457	2446	2451.5	0.196	head
68_1	03N03W-23BBC1	1727294	15832390	1	2453	2452	2452.5	0.196	head
69_1	04N04W-30BBB2	1674652	15858964	1	2451	2456	2453.5	0.196	head
70_1	05N02W-29BBC2	1742986	15890654	1	2454	2456	2455	0.196	head
71_1	03N02W-10ACC1	1756318	15841430	1	2455	2456	2455.5	0.000	head
72_1	04N02W-24CCC1	1764217	15860299	1	2454	2457	2455.5	0.000	head
73_1	03N02W-29BCD1	1744399	15825681	1	2459	2461	2460	0.000	head
74_1	04N02W-26CAD1	1761374	15856133	1	2461	2462	2461.5	0.000	head
75_1	04N01W-07AAAD1	1774411	15875340	1	2464	2466	2465	0.196	head
76_1	04N01W-19DADA1	1774422	15861980	1	2461	2467	2464	0.000	head
77_1	03N02W-15DCDA1	1757364	15834047	1	2468	2467	2467.5	0.000	head
78_1	05N01W-32ACC1	1777285	15883959	1	2469	2468	2468.5	0.196	head
79_1	02N03W-06DBA1	1710064	15814111	1	2470	2470	2470	0.196	head
80_1	03N04W-03AAD1	1695402	15847367	1	2468	2471	2469.5	0.196	head
81_1	04N01W-05DBD1	1777994	15877789	1	2479	2476	2477.5	0.196	head
82_1	02N02W-05ABA1	1746866	15816788	1	2487	2481	2484	0.196	head
83_1	03N04W-11ADA1	1700785	15841308	1	2480	2483	2481.5	0.000	head
84_1	03N02W-12BBB1	1764300	15843802	1	2480	2483	2481.5	0.196	head
85_1	04N01W-16CAAA1	1782320	15867797	1	2481	2483	2482	0.000	head
86_1	03N02W-26BAA1	1761740	15828098	1	2482	2486	2484	0.000	head
87_1	04N01W-30ADAA2	1774367	15858639	1	2482	2488	2485	0.000	head
88_1	03N02W-31BCC1	1738014	15820086	1	2500	2492	2496	0.196	head
89_1	04N01W-22DBB1	1788154	15862675	1	2501	2502	2501.5	0.000	head
90_1	04N01W-32BBBC1	1774688	15854085	1	2500	2504	2502	0.196	head
91_1	03N02W-24BAD2	1766644	15832174	1	2496	2504	2500	0.196	head
92_1	04N01W-03CDDA1	1787622	15876334	1	2501	2503	2502	0.000	head
93_1	04N04W-33CDC2	1686650	15848764	1	2497	2505	2501	0.196	head
94_1	03N02W-35DBAC1	1762609	15819804	1	2502	2505	2503.5	0.000	head
95_1	05N01W-33ACD1	1783231	15883997	1	2508	2507	2507.5	0.196	head
96_1	02N02W-10CAA2	1755960	15809345	1	2518	2514	2516	0.196	head

GMS & PEST ID	WELL_NUMBER	Easting (ft)	Northing (ft)	Layer	Spring Water Level (ft)	Fall Water level (ft)	Average Water Level (ft)	Initial PEST Weight	Group
97_1	03N01W-08BDAC1	1777852	15841858	1	2514	2516	2515	0.000	head
98_1	02N02W-02CACC1	1760797	15813722	1	2516	2518	2517	0.000	head
99_1	02N02W-09ACC1	1751540	15809727	1	2524	2518	2521	0.196	head
100_1	03N01W-18DAC1	1773331	15835454	1	2517	2521	2519	0.196	head
101_1	02N02W-29BCC1	1743809	15793496	1	2530	2528	2529	0.196	head
102_1	04N01W-33ADAD1	1784987	15852735	1	2526	2528	2527	0.000	head
103_1	02N02W-20CBB1	1743417	15798554	1	2531	2527	2529	0.196	head
104_1	03N01W-31DDA1	1774316	15818760	1	2527	2530	2528.5	0.196	head
105_1	04N01W-28ADD1	1785102	15857594	1	2526	2531	2528.5	0.000	head
106_1	02N02W-07CBC1	1737923	15808043	1	2535	2531	2533	0.196	head
107_1	03N01W-09AACB1	1784314	15843215	1	2528	2532	2530	0.000	head
108_1	04N01W-13DDB1	1799663	15866296	1	2531	2532	2531.5	0.000	head
109_1	05N01W-34DBAD1	1788971	15883124	1	2539	2536	2537.5	0.196	head
110_1	02N01W-07BBC1	1769722	15811142	1	2534	2538	2536	0.000	head
111_1	01N02W-09DDD2	1753851	15775530	1	2538	2538	2538	0.196	head
112_1	02N02W-22CCA1	1754845	15797194	1	2540	2539	2539.5	0.196	head
113_1	02N02W-32CDB1	1744948	15786518	1	2546	2543	2544.5	0.196	head
114_1	05N01W-36ABB1	1798277	15886327	1	2542	2545	2543.5	0.196	head
115_1	02N02W-28DDD1	1753846	15790914	1	2545	2546	2545.5	0.196	head
116_1	01N01W-27ADD1	1790967	15762594	1	2551	2547	2549	0.196	head
117_1	04N01E-21DCCC1	1814182	15860334	1	2548	2550	2549	0.000	head
118_1	04N01E-17CDDD1	1808556	15865755	1	2553	2554	2553.5	0.000	head
119_1	03N01W-16DDD1	1785185	15833808	1	2554	2557	2555.5	0.196	head
120_1	01N02W-10DAA1	1759078	15777481	1	2551	2562	2556.5	0.196	head
121_1	04N01E-16AAA1	1816378	15870574	1	2561	2562	2561.5	0.196	head
122_1	04N01E-05CBBD1	1806478	15878189	1	2566	2564	2565	0.196	head
123_1	03N01W-11BDCC1	1791973	15841647	1	2561	2565	2563	0.000	head
124_1	04N01W-35AAA1	1795557	15854528	1	2561	2566	2563.5	0.000	head
125_1	01N01W-24AAA1	1801028	15769548	1	2562	2569	2565.5	0.196	head
126_1	03N01W-27CDCB1	1786873	15823496	1	2568	2572	2570	0.196	head
127_1	05N01E-31ACA1	1804668	15884653	1	2572	2572	2572	0.196	head
128_1	02N01W-32CBB1	1775534	15788101	1	2562	2573	2567.5	0.196	head
129_1	04N01E-11BBB1	1822502	15876090	1	2582	2574	2578	0.196	head
130_1	05N01E-33CCCD1	1811740	15881367	1	2572	2575	2573.5	0.196	head
131_1	02N02E-12AAC1	1864868	15811601	1	2583	2577	2580	0.000	head
132_1	01N01E-19ADB1	1805684	15768570	1	2584	2581	2582.5	0.196	head
133_1	01N02E-08ADA2	1843812	15778806	1	2591	2581	2586	0.196	head
134_1	02N01W-09ADA1	1785116	15810731	1	2572	2585	2578.5	0.196	head
135_1	01N01E-16ACC1	1814946	15772993	1	2589	2585	2587	0.196	head
136_1	03N01E-06BBAB1	1801771	15849409	1	2583	2586	2584.5	0.000	head
137_1	03N01W-12CBBB1	1796166	15841474	1	2587	2588	2587.5	0.000	head
138_1	02N01W-10ABB1	1788273	15812270	1	2577	2589	2583	0.196	head
139_1	01N01E-12DAA1	1832904	15778000	1	2595	2592	2593.5	0.196	head
140_1	02N02E-34CCD1	1850160	15786153	1	2593	2592	2592.5	0.196	head
141_1	03N01W-26DDDC1	1795486	15823150	1	2593	2594	2593.5	0.196	head
142_1	04N01E-29CCCD1	1806728	15855013	1	2584	2593	2588.5	0.000	head
143_1	04N01E-11BAA1	1824342	15875599	1	2597	2590	2593.5	0.196	head
144_1	01N01E-03CCC1	1817759	15781011	1	2599	2596	2597.5	0.196	head
145_1	02N02E-32DBA1	1842401	15788206	1	2599	2596	2597.5	0.196	head
146_1	02N01W-02BBA1	1790962	15817450	1	2585	2597	2591	0.196	head

GMS & PEST ID	WELL_NUMBER	Easting (ft)	Northing (ft)	Layer	Spring Water Level (ft)	Fall Water level (ft)	Water Level (ft)	Initial PEST Weight	Group
147_1	03N01W-24BBDA1	1796964	15832775	1	2592	2599	2595.5	0.196	head
148_1	04N01E-24BCA1	1828483	15863691	1	2599	2599	2599	0.000	head
149_1	03N01E-06DDD1	1805775	15844884	1	2600	2602	2601	0.000	head
150_1	02N01E-26BBC1	1822651	15795929	1	2612	2602	2607	0.196	head
151_1	02N01E-35BBC1	1823281	15790975	1	2606	2604	2605	0.196	head
152_1	02N01E-36BBB1	1827923	15791317	1	2606	2604	2605	0.196	head
153_1	03N01E-17BBB1	1806326	15838512	1	2601	2605	2603	0.000	head
154_1	02N01E-33CCA2	1812684	15787247	1	2606	2605	2605.5	0.196	head
155_1	02N01E-31DDC1	1805554	15785977	1	2607	2609	2608	0.196	head
156_1	02N01W-11ADA1	1795645	15811107	1	2599	2610	2604.5	0.196	head
157_1	04N01E-33AADC1	1816219	15853771	1	2606	2612	2609	0.000	head
158_1	02N01W-23ACC1	1794033	15799254	1	2604	2616	2610	0.196	head
159_1	02N01W-12BAA1	1797478	15812233	1	2604	2616	2610	0.196	head
160_1	03N01E-08DCDC1	1809498	15839145	1	2613	2616	2614.5	0.196	head
161_1	02N01E-23BAD1	1824821	15800805	1	2623	2616	2619.5	0.196	head
162_1	04N01E-21DDDC1	1816385	15860554	1	2614	2618	2616	0.000	head
163_1	02N02E-31BCA1	1833905	15790053	1	2620	2618	2619	0.196	head
164_1	02N01W-35BDC1	1792266	15788513	1	2611	2619	2615	0.196	head
165_1	02N01E-07CBBC1	1801623	15809328	1	2607	2620	2613.5	0.196	head
166_1	02N01W-15ADC1	1789715	15804488	1	2615	2623	2619	0.196	head
167_1	04N02E-30ACDB1	1836178	15858393	1	2623	2624	2623.5	0.000	head
168_1	02N01E-05CBDC1	1807113	15813822	1	2624	2627	2625.5	0.000	head
169_1	02N01W-13BAB1	1797736	15806972	1	2608	2626	2617	0.196	head
170_1	04N02E-31ACAB1	1836142	15853434	1	2630	2626	2628	0.000	head
171_1	04N02E-31AAB2	1837534	15854661	1	2627	2624	2625.5	0.196	head
172_1	02N01E-08ACC1	1809427	15809791	1	2625	2627	2626	0.196	head
173_1	02N01E-15ABA1	1820570	15807045	1	2630	2630	2630	0.196	head
174_1	04N01E-26CDD1	1824440	15855154	1	2632	2636	2634	0.000	head
175_1	03N01E-30DDD1	1806306	15823736	1	2632	2637	2634.5	0.196	head
176_1	04N01E-35DAA1	1826968	15851734	1	2646	2640	2643	0.000	head
177_1	03N01E-10BDA1	1819400	15842462	1	2638	2642	2640	0.000	head
178_1	04N01E-35CCA1	1823227	15850792	1	2639	2643	2641	0.000	head
179_1	02N02E-07CBC1	1833591	15808977	1	2643	2644	2643.5	0.196	head
180_1	04N02E-29ACC1	1840654	15857825	1	2642	2646	2644	0.000	head
181_1	02N01E-12CDB1	1829470	15808537	1	2646	2647	2646.5	0.196	head
182_1	02N01E-33CAC1	1813431	15787454	1	2608	2656	2632	0.196	head
183_1	03N01E-15CBD1	1817920	15835666	1	2648	2659	2653.5	0.000	head
184_1	03N03E-32BBA1	1870712	15823302	1	2661	2659	2660	0.000	head
185_1	02N01E-02BACB1	1823947	15817296	1	2656	2660	2658	0.196	head
186_1	03N02E-04DAB1	1847903	15846557	1	2663	2662	2662.5	0.000	head
187_1	03N01E-28DCDD2	1815424	15823198	1	2653	2663	2658	0.196	head
188_1	03N01E-27CDDB1	1819101	15823836	1	2665	2675	2670	0.196	head
189_1	03N01E-15AAD1	1821873	15838026	1	2664	2666	2665	0.000	head
190_1	02N02E-04CBB1	1843919	15815244	1	2671	2670	2670.5	0.196	head
191_1	03N02E-15BDB2	1850559	15837272	1	2674	2667	2670.5	0.000	head
192_1	03N02E-06DDD2	1837755	15844642	1	2676	2664	2670	0.196	head
193_1	03N02E-06DDD1	1837836	15844543	1	2675	2676	2675.5	0.000	head
194_1	03N02E-28BDB1	1845649	15827103	1	2684	2676	2680	0.196	head
195_1	02N02E-06CCC2	1833265	15813123	1	2676	2678	2677	0.196	head
196_1	03N02E-03BAAD2	1851238	15849423	1	2677	2678	2677.5	0.000	head

GMS & PEST ID	WELL_NUMBER	Easting (ft)	Northing (ft)	Layer	Spring Water Level (ft)	Fall Water level (ft)	Average Water Level (ft)	Initial PEST Weight	Group
197_1	03N01E-12BCD1	1828512	15842032	1	2679	2681	2680	0.000	head
198_1	03N01E-13BDB1	1828845	15837177	1	2684	2685	2684.5	0.000	head
199_1	03N01E-24ADA1	1832727	15832554	1	2690	2689	2689.5	0.196	head
200_1	02N01E-29DCA1	1810005	15792083	1	2690	2695	2692.5	0.196	head
201_1	03N02E-18DAA1	1837988	15836343	1	2691	2694	2692.5	0.196	head
202_1	03N02E-30CAC1	1834247	15825280	1	2700	2699	2699.5	0.196	head
203_1	02N01E-01BCBC1	1827859	15816114	1	2688	2701	2694.5	0.196	head
204_1	03N02E-15DDDD1	1854110	15834268	1	2705	2704	2704.5	0.000	head
205_1	03N02E-14ACB2	1857177	15837536	1	2706	2703	2704.5	0.196	head
206_1	03N01E-25BCB1	1828218	15826947	1	2709	2720	2714.5	0.196	head
207_1	03N01E-36DDB1	1832263	15818783	1	2713	2726	2719.5	0.196	head
208_1	03N02E-21BCC1	1843988	15831642	1	2728	2733	2730.5	0.196	head
209_1	03N03E-30BCBD1	1865301	15826890	1	2733	2739	2736	0.000	head
210_1	03N02E-25AAC1	1864112	15827585	1	2737	2745	2741	0.000	head
211_1	03N03E-30DAAD2	1869950	15825723	1	2745	2745	2745	0.000	head
212_1	03N02E-20DBD1	1842092	15830005	1	2734	2762	2748	0.196	head
213_1	03N03E-29ADD2	1874947	15826484	1	2768	2769	2768.5	0.000	head
214_1	02N03E-11ACC1	1888740	15810845	1	2826	2824	2825	0.000	head
215_1	01N04E-27CBD1	1914095	15762154	1	3377	3374	3375.5	0.196	head
216_1	01N04E-13CCCB1	1923419	15771584	1	3458	3457	3457.5	0.196	head
217_1	01N04E-28CAC1	1909385	15762696	2	2970	2970	2970	0.196	head
218_1	02N03E-02CDD1	1888439	15814175	2	2998	2926	2962	0.196	head
219_1	02N03E-18BAC1	1866563	15807159	2	2705	2703	2704	0.000	head
220_1	03N01E-15CDA1	1818012	15836472	2	2686	2689	2687.5	0.196	head
221_1	03N01E-34CAA1	1819077	15820670	2	2672	2678	2675	0.196	head
222_1	03N01W-25DAD1	1801236	15825210	2	2615	2619	2617	0.196	head
223_1	02N01E-22DCA1	1821181	15798742	2	2620	2615	2617.5	0.196	head
224_1	02N01W-27BCC1	1786308	15795224	2	2589	2602	2595.5	0.000	head
225_1	01N02E-04BBA1	1845243	15786606	2	2600	2599	2599.5	0.196	head
226_1	01N02E-06BAA1	1835434	15786820	2	2599	2597	2598	0.196	head
227_1	03N02E-23DDBC2	1858980	15830108	2	2629	2595	2612	0.196	head
228_1	04N01E-04DCC1	1814148	15877031	2	2571	2574	2572.5	0.196	head
229_1	04N01E-10ACB2	1819598	15875151	2	2569	2573	2571	0.196	head
230_1	03N02E-36CDD1	1862177	15819361	2	2614	2566	2590	0.000	head
231_1	04N01W-01CAA1	1798201	15878834	2	2545	2549	2547	0.196	head
232_1	04N01W-13AACC1	1774589	15873818	2	2536	2535	2535.5	0.196	head
233_1	03N02W-34BBCB1	1754151	15822991	2	2482	2484	2483	0.196	head
234_1	03N02W-03DAA1	1758711	15847309	2	2468	2469	2468.5	0.196	head
235_1	03N02W-09DDDD1	1753615	15839694	2	2458	2459	2458.5	0.196	head
236_1	01N02W-17DDA1	1748651	15771853	2	2500	2458	2479	0.196	head
237_1	03N02W-04ADD1	1752978	15848144	2	2453	2454	2453.5	0.000	head
238_1	05N02W-19CBA1	1739024	15894784	2	2445	2450	2447.5	0.196	head
239_1	03N02W-17ACDB1	1746794	15837430	2	2448	2449	2448.5	0.196	head
240_1	05N02W-25BCD1	1765464	15889959	2	2443	2443	2443	0.000	head
241_1	05N02W-22CAD1	1755977	15893754	2	2426	2421	2423.5	0.000	head
242_1	05N03W-27CAA1	1724224	15889357	2	2417	2418	2417.5	0.196	head
243_1	04N02W-05ABB1	1746345	15881114	2	2417	2414	2415.5	0.196	head
244_1	05N03W-02CCD1	1728038	15908198	2	2416	2412	2414	0.196	head
245_1	04N03W-27AACD1	1729851	15859318	2	2372	2372	2372	0.196	head
246_1	04N03W-28ADDD1	1722951	15857266	2	2369	2369	2369	0.196	head

GMS & PEST ID	WELL_NUMBER	Easting (ft)	Northing (ft)	Layer	Spring Water Level (ft)	Fall Water level (ft)	Average Water Level (ft)	Initial PEST Weight	Group
247_1	02N03W-22DDC1	1726125	15796956	2	2369	2365	2367	0.196	head
248_1	04N03W-04DCB1	1719571	15877294	2	2359	2361	2360	0.196	head
249_1	05N04W-16ABA1	1688605	15902205	2	2342	2344	2343	0.196	head
250_1	04N05W-10CDD1	1661279	15870583	2	2340	2342	2341	0.196	head
251_1	06N05W-36CDB1	1670327	15913913	2	2318	2316	2317	0.196	head
252_1	05N05W-18CAC1	1644161	15898408	2	2213	2214	2213.5	0.196	head
253_1	03N01E-23DDD1	1826984	15830010	3	2706	2717	2711.5	0.196	head
254_1	03N02E-07DAAC1	1837857	15845448	3	2690	2687	2688.5	0.196	head
255_1	03N01E-15ADD1	1821966	15838831	3	2677	2673	2675	0.196	head
256_1	02N02E-02BBC1	1855118	15818123	3	2660	2658	2659	0.196	head
257_1	02N02E-08AAD1	1843197	15812727	3	2665	2649	2657	0.196	head
258_1	03N03E-30DDAA1	1870045	15826528	3	2639	2613	2626	0.196	head
259_1	03N03E-32CDD1	1870806	15824105	3	2636	2609	2622.5	0.196	head
260_1	01N02W-04DDC1	1753250	15781492	3	2549	2533	2541	0.196	head
261_1	04N01W-33CBB1	1780662	15852263	3	2535	2533	2534	0.196	head
262_1	04N01W-31AAA1	1774457	15859444	3	2527	2524	2525.5	0.196	head
263_1	01N02W-05ADD1	1748150	15783795	3	2544	2506	2525	0.196	head
264_1	04N01W-07DAAA1	1774502	15876146	3	2503	2498	2500.5	0.196	head
265_1	03N02W-14DBA1	1764399	15844608	3	2486	2488	2487	0.196	head
266_1	02N02W-31CBA1	1738779	15788335	3	2496	2484	2490	0.196	head
267_1	03N02W-06DCC1	1741369	15847425	3	2434	2431	2432.5	0.196	head
268_1	04N02W-06CDD1	1739682	15877084	3	2424	2421	2422.5	0.196	head
269_1	01N02W-06ADD1	1742841	15783869	3	2485	2413	2449	0.196	head
270_1	04N03W-26ABCC1	1730456	15859795	3	2381	2377	2379	0.196	head
271_1	06N04W-28CDC1	1686724	15918933	3	2347	2347	2347	0.196	head
272_1	04N05W-23BCC1	1664646	15863156	3	2342	2345	2343.5	0.196	head
273_1	04N04W-04CDC1	1686895	15876555	3	2297	2295	2296	0.196	head
274_1	05N05W-04DCD1	1653470	15910153	3	2218	2213	2215.5	0.196	head
275_1	03N01E-14AAC2	1828938	15837981	4	2683		2683	0.196	head
276_1	03N01E-14AAC3	1826815	15838670	4	2683		2683	0.196	head
277_1	03N02E-06DDC1	1837580	15845923	4	2685		2685	0.196	head
278_1	04N01E-36BAC1	1827060	15852540	4	2670		2670	0.196	head
279_1	04N01E-24DABB1	1828576	15864497	4	2606		2606	0.196	head
280_1	03N02E-11BABD1	1837594	15842005	4	2720	2736	2728	0.196	head
281_1	03N02E-13BABA1	1858867	15840383	4	2700	2696	2698	0.196	head
282_1	04N02E-30ACAC1	1836190	15859214	4	2618	2611	2614.5	0.000	head
283_1	04N01E-27AADA1	1824532	15855960	4	2619	2574	2596.5	0.196	head
284_1	04N05W-14CCC2	1661284	15870583	4	2340	2340	2340	0.196	head

Taken from "SS Obs Pts" in "Final 1996 Obs Data.xls"

Vertical Gradient Observations

PEST-ID		Easting (ft)	Northing (ft)				Estimated Value	Weight	Group
grad1		1666612	15870975				40	25	grad
grad2		1665066	15902407				40	25	grad
grad3		1717624	15862215				40	25	grad
grad4		1793886	15854486				30	25	grad
grad5		1765546	15876128				30	25	grad
grad6		1865510	15817901				-30	25	grad

Appendix D: Model Calibration Input Files

Program or File	Calls these Files	Requires these files	Creates these files
pest.exe	*.pst *PEST control file*	Model3.bat	
		pph1.tpl	pph1.dat
		pph2.tpl	pph2.dat
		pph3.tpl	pph3.dat
		ppv1.tpl	ppv1.dat
		ppv2.tpl	ppv2.dat
		ppv3.tpl	ppv3.dat
		structh1.tpl	structh1.dat
		structh2.tpl	structh2.dat
		structh3.tpl	structh3.dat
		structv1.tpl	structv1.dat
		structv2.tpl	structv2.dat
		structv3.tpl	structv3.dat
		sswel.tpl	ss.wel
		ssmoo.ins	ss.moo
		modvgrad.ins	modvgrad.out

Table D-1: Treasure Valley model calibration files.

File	Process	Requires these files		Requires these files	Additional required files and/or Comments	
Model3.bat *Prepares files for each MODFLOW run, initates MODFLOW run, deletes intermediate files*	*The *.ref files (a remainder of the previous run) are deleted*	kh1.ref	kv1.ref			
		kh2.ref	kv2.ref			
		kh3.ref	kv3.ref			
		kh1s.ref	kh2s.ref			
		kh3s.ref	kv1s.ref			
		kv2s.ref	kv3s.ref			
	Delete head file from previous run	*.hed				
	Build hydraulic property arrays with fac2real.exe	frh1.in		fach1.dat pph1.dat kh1.ref	Produces "kh1.ref"	
		frh2.in		fach2.dat pph2.dat kh2.ref	Produces "kh2.ref"	
		frh3.in		fach3.dat pph3.dat kh3.ref	Produces "kh3.ref"	
		frv1.in		facv1.dat ppv1.dat kv1.ref	Produces "kv1.ref"	
		frv2.in		facv2.dat ppv2.dat kv2.ref	Produces "kv2.ref"	
		frv3.in		facv3.dat ppv3.dat kv3.ref	Produces "kv3.ref"	
	strips headers from the array files with striphead.exe	sh1.in		kh1.ref		
		sh2.in		kh2.ref		
		sh3.in		kh3.ref		
		sv1.in		kv1.ref		
		sv2.in		kv2.ref		
		sv3.in		kv3.ref		
	Run model with MODFLOWs.exe ("MODFLOWs.exe" is a modified MODFLOW code provided with GMS)	modflows.in → *.mfs *"modflows.in" is the input file for modflows.exe; gives GMS super file name). The *.mfs file should not have any quotes surrounding the file names (quotes around units are OK).*		*.mfn (MODFLOW super file, which lists files for MODFLOW packages)	*.out *.bas *.bcf *.oc *.hed *.drw *40.ccf *50.ccf *.pcg *.riv *.wel *.drn *.ghb *.rch *.hff	*These files are described in Table B-1*
				*.lyr	?	
	Calculate the *vertical hydraulic head difference for specified well pairs (e.g., multi-completed piezometers)* with modvgrad.exe	modvgrad.in		tvm.spc *grid specification file*		
				vgradpairs.lst *ID number for each completion fo the vertical gradient pairs*		
				vgradpairs.dat *x-y locations of vertical gradient wells*		
				Modvgrad.out		

Table D-2: Treasure Valley model calibration files.

Appendix E: Model Calibration Output Files

File	Description
*.ccf	Cell to cell flow terms
*.fnn	Flag file that indicates PEST run is complete
*.hed	MODFLOW head file
*.hld	Parameter hold file
*.jac	Jacobian matrix from the current optimization iteration (for a possible restart)
*.jco	Jacobian matrix pertaining to the best parameters for access by the JACWRIT utility
*.jst	Jacobian matrix from the previous optimization iteration
*.moo	MODFLOW output file for PEST
*.mtt	Parameter statistical matrices (PEST)
*.out	MODFLOW output file
*.par	Best parameter values achieved
*.rec	Run record file
*.res	Tabulated observation residuals
*.rst	Restart information stored at the beginning of each optimization iteration
*.sen	Parameter sensitivities
*.seo	Observation sensitivities
*.wel	Well file (produced with calibration if underflow is a calibration parameter)
Kh1.ref	Hydraulic conductivity arrays
Kh2.ref	
Kh3.ref	
Kv1.ref	
Kv2.ref	
Kv3.ref	
Kh1s.ref	Hydraulic conductivity arrays with stripped headers
Kh2s.ref	
Kh3s.ref	
Kv1s.ref	
Kv2s.ref	
Kv3s.ref	
modvgrad.out	Interpolated simulated vertical gradient data
pph1.dat	Pilot point parameter values (layer 1 K_h)
pph2.dat	Pilot point parameter values (layer 2 K_h)
pph3.dat	Pilot point parameter values (layer 3-4 K_h)
ppv1.dat	Pilot point parameter values (layer 1 K_v)
ppv2.dat	Pilot point parameter values (layer 2 K_v)
ppv3.dat	Pilot point parameter values (layer 3-4 K_v)
structh1.dat	Variogram structure data for K_h, layer 1
structh2.dat	Variogram structure data for K_h, layer 2
structh3.dat	Variogram structure data for K_h, layer 3-4
structv1.dat	Variogram structure data for K_v, layer 1
structv2.dat	Variogram structure data for K_v, layer 2
structv3.dat	Variogram structure data for K_v, layer 3-4

Table E-1: Files produced during a Treasure Valley model calibration.

Appendix F: Predictive Analysis Input Files

Program or File	Calls these Files	Requires these files	Creates these files	Notes
pest.exe	*.pst *PEST control file* *Specifies predicitive analysis mode*	Model4.bat *(see also Table F-2)*		
		pph1.tpl	pph1.dat	
		pph2.tpl	pph2.dat	
		pph3.tpl	pph3.dat	
		ppv1.tpl	ppv1.dat	
		ppv2.tpl	ppv2.dat	
		ppv3.tpl	ppv3.dat	
		structh1.tpl	structh1.dat	
		structh2.tpl	structh2.dat	
		structh3.tpl	structh3.dat	
		structv1.tpl	structv1.dat	
		structv2.tpl	structv2.dat	
		structv3.tpl	structv3.dat	
		sswel.tpl	ss.wel	
		ssmoo.ins	ss.cow	
		modvgrad.ins	modvgrad.out	
		modave.ins	modave.out	

Table F-1: Files required for PEST predictive simulations.

File	Process	Requires these files		these files	Additional required files and/or Comments
Model4.bat *Prepares files for each MODFLOW run, initates MODFLOW run, deletes intermediate files*	*The *.ref files (a remainder of the previous run) are deleted*	kh1.ref	kv1.ref		
		kh2.ref	kv2.ref		
		kh3.ref	kv3.ref		
		kh1s.ref	kh2s.ref		
		kh3s.ref	kv1s.ref		
		kv2s.ref	kv3s.ref		
	Delete head file from previous run	*.hed			
	Build hydraulic property arrays with fac2real.exe	frh1.in		fach1.dat pph1.dat kh1.ref	Produces "kh1.ref"
		frh2.in		fach2.dat pph2.dat kh2.ref	Produces "kh2.ref"
		frh3.in		fach3.dat pph3.dat kh3.ref	Produces "kh3.ref"
		frv1.in		facv1.dat ppv1.dat kv1.ref	Produces "kv1.ref"
		frv2.in		facv2.dat ppv2.dat kv2.ref	Produces "kv2.ref"
		frv3.in		facv3.dat ppv3.dat kv3.ref	Produces "kv3.ref"
	strips headers from the array files with striphead.exe	sh1.in		kh1.ref	
		sh2.in		kh2.ref	
		sh3.in		kh3.ref	
		sv1.in		kv1.ref	
		sv2.in		kv2.ref	
		sv3.in		kv3.ref	
	Copy calibration pumping values to well file	sscal.wel		ss.wel	
	Run MODFLOW under calibration conditions with modflows.exe	modflows.in → *.mfs *"modflows.in" is the input file for modflows.exe; gives GMS super file name). The *.mfs file should not have any quotes surrounding the file names (quotes around units are OK).*		*.mfn (MODFLOW super file, which lists files for MODFLOW packages)	*.out *.bas *.bcf *.oc *.hed *.drw *40.ccf *50.ccf *.lyr *.pcg *.riv *.wel *.drn *.ghb *.rch *.hff

Continued on next page

Table F-2: Predictive analysis files.

Continued from previous page				
File	**Process**	**Requires these files**	**Requires these files**	**Requires these files or Comments**
Model4.bat (*continued*)	Calculate the *vertical hydraulic head difference for specified well pairs (e.g., multi-completed piezometers) with* modvgrad.exe	modvgrad.in	tvm.spc *grid specification file*	
			vgradpairs.lst *ID number for each completion fo the vertical gradient pairs*	
			vgradpairs.dat *x-y locations of vertical gradient wells*	
			Modvgrad.out	
	Copy scenario well file to model well file	ssinq.wel	ss.wel	
	Run MODFLOW under predicitive analysis conditons	modflows.in → *.mfs *"modflows.in" is the input file for modflows.exe; gives GMS super file name).*	*.mfn (MODFLOW super file, which lists files for MODFLOW packages)	*.out *.bas *.bcf *.oc *.hed *.drw *40.ccf *50.ccf *.pcg *.riv *.wel *.drn *.ghb *.rch *.hff
	Average head values at prediction points with modave.exe	modave.in (creates modave.out)	tvm.spc	Grid specification file
			Predpoints.lst	Prediction point locations
			Predpoints.dat	Prediction point locations
			ss.hed	MODFLOW head file

Table F-3: Treasure Valley model predictive analysis files (*continuation from Table F-2*).

Appendix G: Predictive Analysis Output Files

File	Description
*.ccf	Cell to cell flow terms
*.fnn	A file containing a flag indicating that a PEST calibration is complete
*.hed	MODFLOW head file
*.hld	Parameter hold file
*.jac	Jacobian matrix from the current optimization iteration (for a possible restart)
*.jco	Jacobian matrix pertaining to the best parameters for access by the JACWRIT utility
*.jst	Jacobian matrix from the previous optimization iteration
*.moo	MODFLOW output file for PEST
*.mtt	Parameter statistical matrices (PEST)
*.out	MODFLOW output file
*.par	Best parameter values achieved
*.rec	Run record file
*.res	Tabulated observation residuals
*.rst	Restart information stored at the beginning of each optimization iteration
*.sen	Parameter sensitivities
*.seo	Observation sensitivities
*.wel	Well file (produced with calibration if underflow is a calibration parameter)
Kh1.ref	Hydraulic conductivity arrays
Kh2.ref	
Kh3.ref	
Kv1.ref	
Kv2.ref	
Kv3.ref	
Kh1s.ref	Hydraulic conductivity arrays with stripped headers
Kh2s.ref	
Kh3s.ref	
Kv1s.ref	
Kv2s.ref	
Kv3s.ref	
modvgrad.out	Interpolated simulated vertical gradient data
pph1.dat	Pilot point parameter values (layer 1 K_h)
pph2.dat	Pilot point parameter values (layer 2 K_h)
pph3.dat	Pilot point parameter values (layer 3-4 K_h)
ppv1.dat	Pilot point parameter values (layer 1 K_v)
ppv2.dat	Pilot point parameter values (layer 2 K_v)
ppv3.dat	Pilot point parameter values (layer 3-4 K_v)
structh1.dat	Variogram structure data for K_h, layer 1
structh2.dat	Variogram structure data for K_h, layer 2
structh3.dat	Variogram structure data for K_h, layer 3-4
structv1.dat	Variogram structure data for K_v, layer 1
structv2.dat	Variogram structure data for K_v, layer 2
structv3.dat	Variogram structure data for K_v, layer 3-4

Table G-1: Files produced during a predictive analysis simulation.

Costs associated with this publication are available from the Idaho Department of Water Resources in accordance with Section 60-202, *Idaho Code*. IDWR-21000-20-03/2004.